# Natural Product Biosynthesis; Mechanistic and Enzymatic studies

Claire Leadbeater

PhD

The University of Edinburgh

1999

## Declaration

I Claire Leadbeater, hereby certify that this thesis has been composed by myself, that it is a record of my own work, and that it has not been accepted in partial or complete fulfilment of any other degree of professional qualification.

University of Edinburgh

August 1999

## Acknowledgements

I would like thank my supervisor Robert Baxter for all the help and encouragement for the last three years. I would also like to thank Andrew Munro, Dominic Campopiano and Lisa McIver for all their invaluable guidance and help. There are many other people to thank who I have worked with and have helped me, including Scott Webster, Lisa Mullan, Janet Dyker, Steve Chapman, Gareth Roberts, Nicola Preston, Andrew Cronshaw, Emma Beatty, Dominikus Lysek.

Thank you to my family & friends for all the support and encouragement of the last three years. A special thank you to Simon for everything.

## Dedication

To Simon, Charlotte, Jack & Megan.

## Abstract

The gene encoding the *E. coli* flavodoxin $NADP^+$ oxidoreductase (FLDR) has been overexpressed in *E. coli* and the enzyme was purified to homogeneity. The molecular mass of FLDR apoprotein was determined as 27648 Da. The midpoint reduction potentials of the oxidised/semiquinone and semiquinone/hydroquinone couples of FLDR (-308mV and -268mV, respectively) were measured using redox potentiometry. FLDR was fully characterised kinetically both by steady state and pre-steady state techniques. Arginines (R144, R174 and R184) in the proposed NADPH binding site of *E. coli* flavodoxin $NADP^+$ oxidoreductase (FLDR) were replaced by alanines and the mutant enzymes fully characterised and studied by pre-steady-state and steady-state kinetics. From our studies R174 and R184 appear to interact with the adenosine ribose 2′ phosphate, while R144 is more likely to stabilise NADPH binding by interaction with the nicotinamide ribose 5′ phosphate. R174A and R184A are more efficient enzymes than wild-type or R144A with NADH as substrate, consistent with the proposed phosphate-binding roles for these residues. Arginine residues R237 and R238 in the proposed binding site for FLDR redox partner flavodoxin, have been mutated to alanine. These mutant enzymes have been characterised by pre-steady-state and steady-state kinetics, UV-Vis spectrophotometry, CD and fluorescence. These mutants are less efficient electron transfer proteins.

In a separate project it was attempted to identify genes associated with the antibiotic biosynthetic pathway of aristeromycin from *Streptomyces citricolor*. An aristeromycin-induced protein was isolated from *S. citricolor* purified to homogeneity and an N-terminal sequence was determined. From this an oligonucleotide was designed and used to probe *S. citricolor* chromosomal DNA. A 1000bp fragment of DNA was isolated and sequenced, and the presence of part of an ORF identified.

## Abbreviations

AdoHcy – *S*-Adenosyl-L-homocysteine

AdoMet – *S*-Adenosyl-L-methionine

AIP – Aristeromycin induced proteins

AMP – Adenine monophosphate

ATP – Adenine triphosphate

C-ATP – carbocyclic analogue of aristeromycin triphosphate

C-Guo-carbocyclic analogue of guanosine

C-GMP – carbocyclic analogue monophosphate f guanosine

C-GTP – Triphosphate of carbocyclic analogue of guanosine

C-IMP – carbocyclic analogue of inosine

C-Ino – carbocyclic analogue of inosine

CPR - Cytochrome P-450 reductase

ESMS – Electrospray Mass Spectrometry

FAD – Flavin adenine dinucleotide

FLD - *E. coli* Flavodoxin

FLDR - *E. coli* Flavodoxin $NADP^+$ oxidoreductase

*fldr* – *E. coli* flavodoxin reductase gene

FMN- Flavin mononucleotide

H(G)PRT – Hypoxanthine (guanine) phosphoribosyl transferase

hq – Hydroquinone

HSQC – Heteronuclear single quantum coherence

IPTG - Isopropyl - β, D – thiogalactopyranoside

OD - Optical density

ox - Oxidised

P-450 - Cytochrome P-450 monooxygenase

PCR – polymerase chain reaction

PDR – Phthalate dioxygenase reductase

PFL – Pyruvate formate lyase

PRPP - 5-phosphoribosyl-α-1-pyrophosphate

sq – Semiquinone

wt- wild type

# Contents



## Part 1 FLDR

# Chapter 1 (FLDR)

## Introduction

The enzyme which is the subject of this study is the *E. coli* flavodoxin $NADP^+$ reductase, a flavin containing electron transfer enzyme, it is involved in many important systems in *E. coli*. A deeper comprehension of electron transfer is required before a full understanding of the enzyme can be gained.

## Electron transfer

Electron transfer is a key process in all living organisms and is involved in many essential pathways. For example, mitochondrial respiration is a series of electron transfer steps, which are coupled with chemical reactions through membrane bound multi-subunit proteins. It is an energetically favourable process, in which the redox reactions pump ions and metabolites across the membrane, driving the synthesis of ATP. Electron transfer is also a key process in the capture of light energy in photosynthesis, and in many anabolic and catabolic reactions. Electron transfer has been the subject of many reviews as it is such an essential process (McLendon 1988, McLendon & Hake 1991, McLendon 1992, Moser 1992, Chapman & Mount 1995, Moser *et al.* 1995, Larsson 1998).

There are some fundamental factors that control electron transfer, which need to be appreciated before it can be fully understood. Assuming the reaction involves the interaction of two species, then an encounter complex is formed and the exchange of electrons follows. There is no energy change in electron transfer, as the process is radiationless. The combined energy of the system must remain constant; therefore the redistribution of electrons is isoenergetic. The 'Frank-Condon principle' also applies to these reactions (Kauzmann 1957). In other words electron transfer is so rapid that the reactants do not have time to change their nuclear configuration during the reaction. If the reactant and product have different structures, the common isoenergetic configuration is most likely, which is the intermediate between the reactant and the product. This intermediate will be of higher energy than both. The higher the energy, the slower the rate of electron transfer. These factors have been

developed into a quantitative theory by Marcus, "The Marcus Theory" (Marcus1956, Marcus 1964, Marcus 1965).

In order to understand how electron transfer occurs in proteins, it is necessary to understand how electrons can travel through them. There are thought to be various mechanisms by which this process occurs. One, which has been demonstrated, is through space electron transfer between biological redox centres (Moser *et al.* 1992). This involves an electron in an orbital of one redox centre being transferred to a vacant orbital of another. The electron tunnels through the medium, the efficiency of this process depending on the extent of the overlap of the electronic wave functions. As the process is non-adiabatic, the electron transfer rate is best described by 'Fermi's golden rule' (Devault 1980). "The electron transfer rate is proportional to the square of the coupling of the reactant and the product electronic wavefunctions, which is proportional to the overlap of the donor and acceptor molecules across the space". The greater the overlap the better the electron transfer rate, and therefore the rate decreases exponentially with increased distance between redox centres.

This system obviously does not explain how electron transfer occurs over larger distances. A system is needed where the electronic wavefunction does not decrease rapidly with distance. One way, in which it would occur is if the energy of the intervening medium is lowered, therefore the nature of the medium is important. If the medium is homogenous, the protein can be thought of as organic glass, which would provide a good medium for electrons to travel through (Moser *et al.* 1992). An example of this is a photosynthetic reaction centre.

Alternative mechanisms need to be considered, as not all proteins can be thought of as organic glasses. Electron transfer can also occur by electron tunnelling, where the electron is transferred *via* covalent bonds, hydrogen bonds, and small space jumps through a specific pathway in the medium. A controversial mechanism which has been proposed involves electron transfer *via* $\pi$ orbitals of conjugated molecules (aromatic residues), which in principle provide an alternative low energy pathway (Beratan & Onuchic1989, Beratran *et al.* 1991). As there are many mechanisms by

which electron transfer can occur, this leads to complications when considering along which pathway electron transfer occurs. Another complication when considering electron transfer is that a longer pathway between redox centres in proteins may lead to the greatest stabilisation of electronic wavefunctions, in turn leading to faster electron transfer rates than the shortest electron transfer route.

There are two basic types of electron transfer proteins, those that simply shuttle electrons, and oxido-reductases that combine electron transfer with a net chemical transformation. Electron transfer proteins include redox active prosthetic groups such as haem, Cu, iron-sulphur, chlorophyll and flavins.

## Flavin and Flavoproteins

Flavoproteins contain a prosthetic group. The flavin's structure is based on riboflavin a 7,8-dimethlyisoazoxalline ring. There are two types of flavin found in proteins, FAD and FMN, see fig 1.1.

**Fig 1.1 Structure of FAD and FMN**

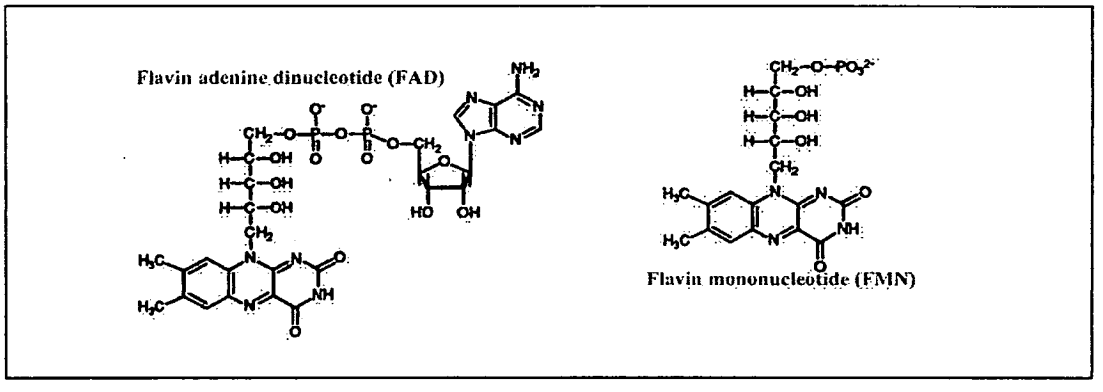


Side chains such as adenine in FAD serves to anchor the prosthetic group to its host protein structure (Gishla & Massey1989). In most cases the flavin protein interaction exists as a tightly bound non-covalent complex. However, there are a small number of examples of enzymes where the flavin is covalently attached (Mewies *et al.* 1997). Flavin chemistry usually involves oxidation and reduction, and is centred on the isoazoxalline ring. The pyrimidine nucleus of the isoalloxanine ring is an electron

deficient group, which acts as an electron sink during oxidation of the substrate (Gishla & Massey1989), see fig 1.2.

**Fig 1.2 Electron transfer reaction of FAD and FMN**

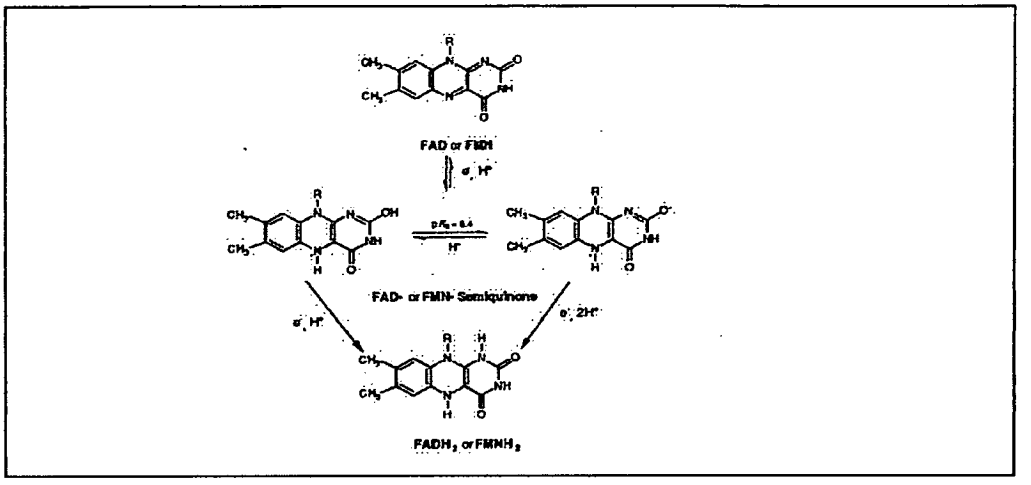

Since flavoproteins take part in a number of very different types of catalysis, the chemistry underlying these events can be quite different in the various reactions. The specific properties of the flavin results from interaction with the surrounding protein structure. Several hundred flavoproteins have been discovered to date. Flavoproteins are very versatile enzymes, and play an important role in a variety of processes, involving the transfer of either one or two electrons. Flavoproteins are involved in processes as diverse as photochemistry, DNA damage repair, light emission, and dehydrogenation. Flavoproteins also fill a unique niche due to the fact that they can mediate electron transfer between a two electron donor and one electron acceptor. In the process of the reaction the flavin is reduced. The oxidized form of flavin is regenerated, at the expense of the reduction of an electron acceptor. In many cases the acceptor molecule is molecular oxygen, or another redox protein. Flavoproteins reduce molecular oxygen in a variety of ways including the production of the superoxide ion ($O_2^-$), direct two electron reduction of $O_2$ to $H_2O_2$, and also the insertion of one atom of $O_2$ into the substrate and with the other forming $H_2O$. These characteristics have formed the basis of the classification system of flavoproteins (Massey & Hemmerich1980).

**Class 1 Transdehydrogenases.**

These dehydrogenate saturated double bonds of the type C-C, C-S, C-N and N-N, an example of C-N transdehydrogenase is D-lactate dehydrogenase from *Megasphera elsdenii* (Olson & Massey 1979).

**Class 2. Dehydrogenases/oxidases**

These enzymes combine the dehydrogenation of one substrate with the reduction of molecular oxygen, to generate $H_2O_2$. An example is L-lactate oxidase from *Mycobacterium smegmatis* (Massey *et al.* 1969).

**Class 3 Dehydrogenases/oxygenases**

This class differs from the previous one in the fate of oxygen as the substrate. Peroxide is not liberated, but instead all four equivalents of $O_2$ are consumed, two for water formation and two for incorporation into another substrate of the enzyme (AH→ AOH), an example of this type of enzyme is *p*-hydroxy-benzoate hydroxylase from *Pseudomonas fluorescens* (Entsch *et al.* 1979).

**Class 4 Dehydrogenases/electron trasnferases**

These enzymes carry out the transformation of two electron transfer into one electron transfer, sometimes the reverse reaction. These enzymes are important in all known biological redox chains, as no redox transfer occurs between strictly two electron nicotinamide nucleotides and strictly one electron reacting haem proteins and iron sulfur proteins without the aid of a flavoprotein. An example of this class is liver microsomal NADPH-cytochrome *P*-450 reductase (Vermillion & Coon 1978).

**Class 5 Pure electron transferases**

These do not catalyse dehydrogenation reactions but only take part in the electron transfer process. These electron transfers may occur from other flavoproteins with one or two electrons to a number of other acceptors. An example of this is spinach ferredoxin NADP reductase (Massey *et al.* 1969).

## Flavodoxin $NADP^+$ Reductase (FLDR)

FLDR is an electron transfer enzyme containing the flavin FAD as a prosthetic group, see fig 1.1. FLDR's main redox partner is flavodoxin (FLD), which contains FMN as its prosthetic group, see fig 1.1. However, although FLDR can also pass electrons to ferredoxin, there is no known function for this redox partnership. In the reaction NADPH transfers two electrons to FLDR and FAD is converted to its hydroquinone. An electron is then transferred to flavodoxin and a stable semiquinone is formed. FLDR is a member of a large family of flavin dependent oxidoreductases known as the FNR family. The members of the family are electron transfer proteins mainly containing FAD as a prosthetic group and are NADPH or NADH specific. The only member of the family to contain FMN as a prosthetic group is phthalate dioxygenase reductase. A pattern of conserved residues, proposed by Karplus and co-workers (Karplus *et al.* 1991), is reported to be the sequence signature characteristic of the family, see fig1.3. The ordering of these binding sequences along the chain is important in discriminating FNR proteins from other families. The structural motif is that that the members of the family are expected to be a two-domain module, one domain binding the flavin the other binding the pyridine nucleotide.

**Fig 1.3 Conserved sequences that characterise the FNR family**

Conserved fingerprint region in *E. coli* FLDR (Ingleman *et al.* 1997), *Pseudomonas cepacia* PDR, phthalate dioxygenase reductase (Correll *et al.* 1992) and spinach FNR ferredoxin $NADP^+$ reductases (Karplus *et al.* 1991) are aligned in lines 1,2 and 3. Characters in blue represent residues that are implicated in the binding of flavin or pyridine nucleotide. Line 4 represents an approximate consensus for the whole family. Here the pink letters represent the absolutely conserved residues, and the red represent semi-conserved residues. The first two sequences bind the isoalloxanine and phosphate group of the flavin, respectively. The consensus for segment 2 distinguishes FAD and FMN binding. The third and fourth sequences are involved in the binding and differentiation of $NAD^+/NADP^+$. The conserved C in the fifth sequence may be involved in the binding of the nicotinamide group. The final aromatic group of the sixth sequence is stacked against the flavin ring.

| | 1 | 2 | 3 | 4 | 5 | 6 |
|---|---|---|---|---|---|---|
| FLDR | $^{50}$RAYS | $^{73}$GKLS | $^{115}$GTAIGP | $^{173}$TR | $^{217}$MLCGN | $^{245}$EHY |
| PDR | $^{53}$RTYS | $^{80}$RGGS | $^{120}$GIGITP | $^{173}$DH | $^{197}$YCCGP | $^{223}$ESF |
| FNR | $^{93}$RLYS | $^{130}$GVCS | $^{171}$GTGIAP | $^{234}$SR | $^{270}$YMCGL | $^{312}$EVY |
| Consensus | RxYS | GxxS (FAD) RGGS (FMN) | GtGixp | sr (NADP) de (NAD) | yxcGp | exf |

FLDR and FLD are involved in a number of important systems in *E. coli*, including various aerobic and anaerobic processes, such as methionine synthase, anaerobic ribonucleotide reductase, pyruvate formate lyase and biotin synthase a number of these systems are described.

The flavoprotein system of FLDR and FLD supports methionine synthase, which is an important *E. coli* enzyme in aerobic growth conditions. It is a key enzyme in the one-carbon metabolism of mammals, and micro-organisms. Impairment of this enzyme results in megablastic anaemia and spinal cord degeneration in humans. Methionine synthase catalyses two separate methylation reactions. The primary reaction involves the transfer of a methyl group from methyltetrahydrofolate to the

cob(I)alamin form of the co-factor, to form methylcobalamin and tetrahydrofolate. The methyl group is then transferred to homocystiene forming methionine and regenerating the cob(I)alamin form of the enzyme. The regeneration methylation reaction of methionine synthase, occurs when the enzyme undergoes oxidation and forms its inactive cob(II)alamin form. The enzyme along with FLDR and FLD catalyses its reactivation to the active cob(I)alamin form. Electron transfer via FLDR and FLD to cob(II)alamin is thought to generate the cob(I)alamin form, which is then trapped by methyl transfer from adenosylmethionine to the cobalt, forming the active form of the enzyme, see fig 1.4 (Jarrett *et al.* 1998, Jarrett *et al.* 1997, Fuji & Huennekens 1974).

**Fig 1.4 Scheme for the primary turnover and reactivation cycles of methionine synthase (Jarrett *et al.* 1998).**

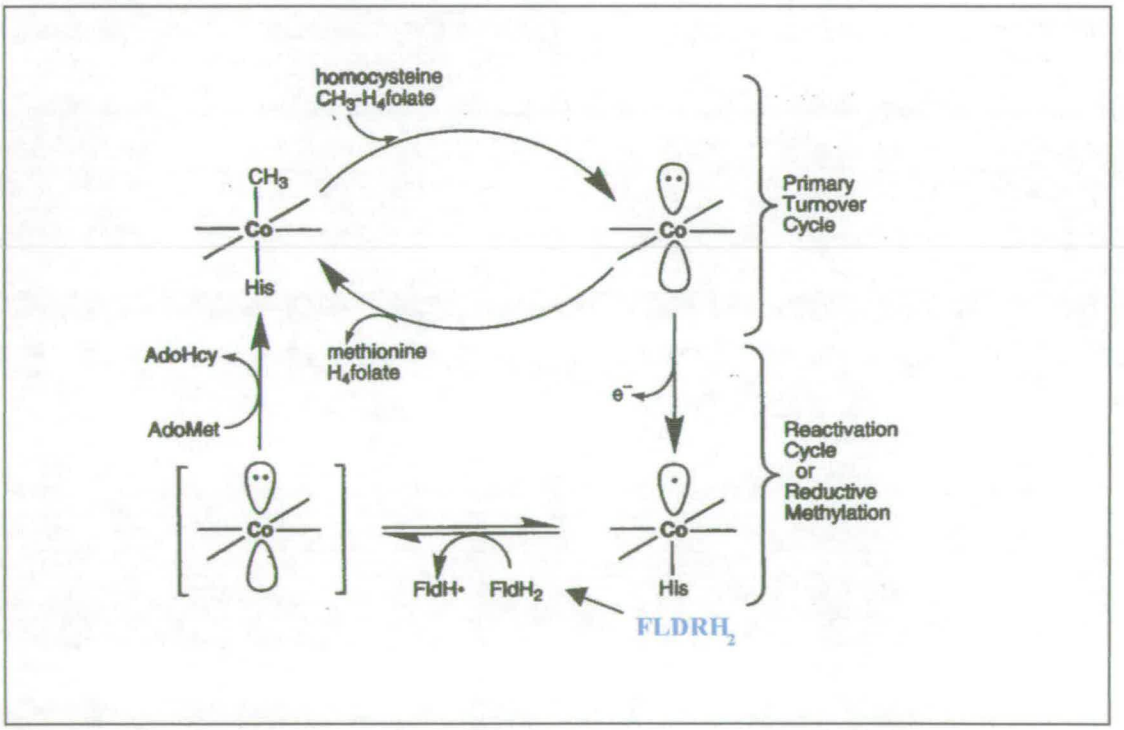


Methionine synthase is made up of four subunits each responsible for the binding the three substrates and cobalamin cofactor. Repositioning of these units allow the enzyme to control which substrate has access to the cofactor, and therefore which

methylation reaction is carried out. It has been proposed that methionine synthase exists in two separate conformations that interconvert in the cob(II)alamin state, thus enabling the enzyme to perform two separate methylation reactions, its primary turnover and its own reactivation. In its primary turnover reaction it is active towards homocysteine and methyltetrahydrofolate, but is unreactive to FLD and adenosylmethionine, in its other conformation it is active to FLD and adenosylmethionine and unreactive to homocysteine and methyltetrahydrofolate (Jarrett *et al.* 1998).

Pyruvate formate lyase is an important enzyme in anaerobic glycolysis of *E. coli*, it catalyses the CoA-dependent non-oxidative cleavage of pyruvate to acetyl-CoA and formate. The mechanism is proposed to be a homolytic process, since the enzyme in the active form has an organic free radical at the active site (gly734). However, the enzyme also exists in an inactive form where there is no free radical. An iron-dependent converter enzyme, pyruvate formate lyase activase, which requires FLD and adenosylmethionine (AdoMet), is thought to regenerate the free radical. (Blaschkowski *et al.* 1982, Knappe & Sawers 1990). Here, FLD is reduced by FLDR which converts NADPH to $NADP^+$, or by pyruvate:flavodoxin (ferredoxin) oxidoreductase which catalyses the conversion of pyruvate and CoA to acetyl-CoA + $CO_2$, see fig 1.5

**Fig 1.5 Interconversion of pyruvate formate lyase between radical and non radical forms (Knappe & Sawers 1990).**

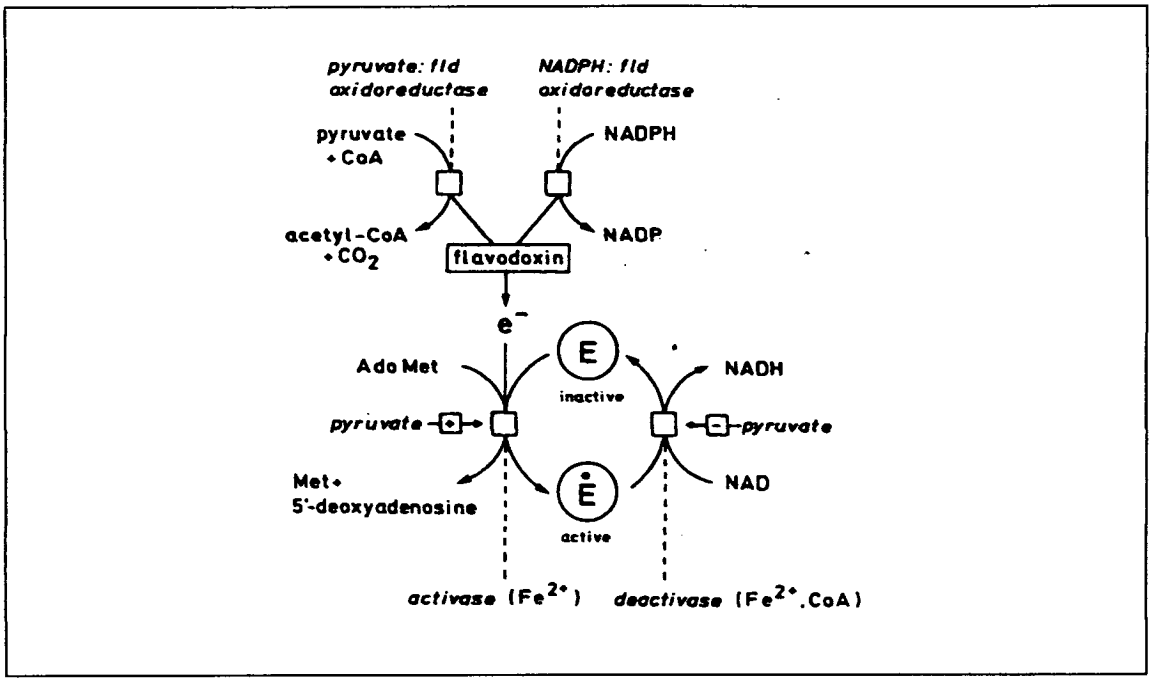


There are similarities between pyruvate formate lyase and methionine synthase systems, as both require flavodoxin and adenosylmethionine to reactivate the enzyme. However, they have different modes of processing these substrates. Pyruvate formate lyase needs an activator enzyme to utilise the co-factors, flavodoxin and adenosylmethionine, whereas methionine synthase appears to interact directly with them. Additionally, in pyruvate formate lyase the hydroquinone form of FLD acts as an electron donor, whereas in methionine synthase it is the semiquinone of flavodoxin which is the electron donor (Knappe & Sawers 1990).

Ribonucleotide reductase is another enzyme, which is similar to pyruvate formate lyase, as both enzymes contain a radical and requires adenosylmethionine (AdoMet) and the reducing flavodoxin system for activation. Ribonucleotide reductase is essential in anaerobic growth, where it catalyses the formation of deoxyribonucleotide triphosphates needed for DNA replication, from ribonucleoside di- or triphosphate. Ribonucleotide reductase catalyses the replacement of the hydroxyl group at C-2′ of the ribose ring by a hydrogen, using a number of small redox proteins in their reduced forms as electron donors e.g. thioredoxin. The

reaction is thought to proceeds by a radical mechanism (Ollagnier *et al.* 1996). In its active form the enzyme contains a glycyl radical (Gly-681) which is stable in anaerobic conditions, but not in the presence of oxygen. To regenerate the radical the enzyme uses the FLDR and FLD electron donating system (Bianchi *et al.* 1993b). An appreciation of the structure of ribonucleotide reductase is necessary, to understand how FLDR and FLD interact with the enzyme. It has a $\alpha_2\beta_2$ structure, where the $\alpha_2$ unit is a large homodimer containing the gylcyl radical, and the $\beta_2$ unit is a smaller homodimer containing a 4Fe-4S centre (Reichard 1993). The first step in radical generation is the reduction of the iron centre of the $\beta_2$ subunit by the flavoprotein system (FLDR and FLD). AdoMet then binds to the reduced enzyme, and is thought to give rise to the transient 5′-deoxyadenosyl radical, which is then involved in generation of the stable glycyl radical in the $\alpha_2$ protein. The enzyme is similar to pyruvate formate lyase (PFL) in a number of ways as it contains a glycyl radical which is produced by FLDR, FLD andAdoMet. However, the two reductase proteins in ribonucleotide reductase are tightly bound in the $\alpha_2\beta_2$ structure whereas the binding of the PFL activase to PFL is relatively weak (Knappe & Sawers 1990).

In constrast to pyruvate formate lyase and methionine synthase which are strictly anaerobic processes, is biotin biosynthesis an important aerobic process; FLDR is involved in the final step where dethiobiotin is converted to biotin by the insertion of sulphur, see fig 1.6.

**Fig 1.6 Conversion of dethiobiotin to biotin**

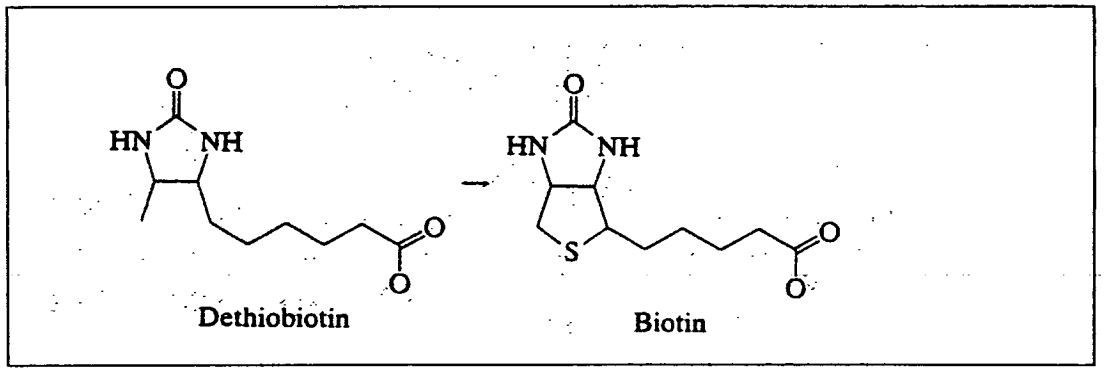

In this reaction a sulphur atom is inserted between methyl and methylene carbon atoms adjacent to the imidazolinone ring. The reaction is catalysed by the *bioB* gene product. It needs a variety of co-factors, $Fe^{2+}$, adenosyl methionine, NADPH and KCl. It was also shown that FLD is required for the conversion of dethiobiotin to biotin (Ifuku *et al.*1994). Another protein in addition to *bioB* gene product and FLD is required. It has been assumed that this is FLDR (Ifuku *et al.*1994), as this is FLD's main redox partner. The conversion of dethiobiotin to biotin shares similarity to the anaerobic ribonucleotide reductase and pyruvate formate lyase. All require FLD and FLDR redox system and adenosyl methionine as a radical intiator. In the PFL and anerobic ribonucleotide reductase systems there is a formation of a radical. While it has been proposed that radical chemistry is also involved in the mechanism of biotin synthase, the fact that this enzyme functions in air is anomalous. Additionally, PFL and anaerobic ribonucleotide reductase both require an activating enzyme. It could be that biotin synthase requires an activating enzyme, which has not yet been identified (Flint & Allen 1997).

In addition to their role as activation systems in *E. coli* for the three enzymes discussed above, the redox system of FLDR and FLD appears to be able to support microsomal cytochrome P450s (Jenkins & Waterman 1998). This is unexpected, as *E. coli* does not contain indigenous P450s. However, it has been observed that FLDR and FLD are structurally similar to the functional domains of NADPH-cytochrome P450-reductases. Consequently it has been proposed that cytochrome P450 reductases may have arisen from the fusion of a flavodoxin and a ferredoxin reductase (Porter & Kasper1986). Though there are some differences between the FLDR and FLD system and NADPH-cytochrome P450-reductase, it is the stable semiquinone of FMN in FLD that is the electron donor to cytochrome P450. Whereas in P450 reductase it is proposed to be the hydroquinone of FMN which is the electron donor, to cytochrome P450 (Jenkins & Waterman 1998). There are however major structural differences between the systems. Specifically P450 reductase possesses an N-terminal anchor domain, which links it to the membrane, where as FLDR and FLD, are not linked to the membrane and therefore are both soluble. FLDR and FLD are not connected by a bridging polypeptide, unlike P450

reductase. This factor may go some way to explaining why FLDR and FLD support cytochrome P450 at a reduced rate, (Jenkins & Waterman 1998).

FLDR has a role in the cellular defence against oxidative damage in *E. coli*. This is caused by species such as hydrogen peroxide ($H_2O_2$), superoxide ($O_2^{\cdot-}$) and hydroxyl radicals ($^{\cdot}OH$), which in their combined form give rise to the phenomenon of "oxidative stress". To deal with oxidative stress aerobic organisms have developed an antioxidant defence system, composed of both enzymatic and non-enzymatic constituents. In *E. coli* FLDR has been hypothesised to be involved in the cell defence system against oxidative damage. Evidence that this may be the case is provided by the finding that FLDR expression is regulated by the *sox*RS regulon (Liochev *et al.* 1994), which is activated by an increase in superoxide stress. The response is now understood to be regulated by a two stage control system. Firstly *sox*R, an iron-sulphur protein which senses oxidative stress, activates the transcription of the *sox*S gene. The product of the *sox*S gene then activates the expression of various proteins, including FLDR, which in turn regulates the amount of superoxide in the cell, fig 1.7 (Demple 1996). FLDR may play a general role in the oxidative stress response by regulating the NADPH/$NADP^+$ ratios within the cell, and this seems to be logical since it has been shown that a transient accumulation of NADPH can lead to the formation of hydroxyl radical ($^{\cdot}OH$) (fig1.7) (Krapp *et al.* 1997).

**Fig 1.7 A schematic model representing possible role of FLDR in the oxidative stress response, and a representation of the two stage transcriptional induction in the *sox*RS regulon (Krapp 1997 *et al.*, Demple 1996).**

A canonical Haber-Weiss cycle is shown in the central pathway (with $O_2^-$ acting as the metal ion reductant. The exsisting Sox R protein is activated by an intracellular redox signal caused by excess superoxide or nitric oxide. The activated SoxR stimulates the transcription at the *soxS* promotor, and the increased levels of the SoxS protein activates regulon genes inculding *fldr*. A role is proposed for NADPH in the reduction of free or DNA-bound $Fe^{3+}$ to $Fe^{2+}$, which will then react with $H_2O_2$. The resulting hydroxyl, ferryl and other radicals attack the adjacent DNA.

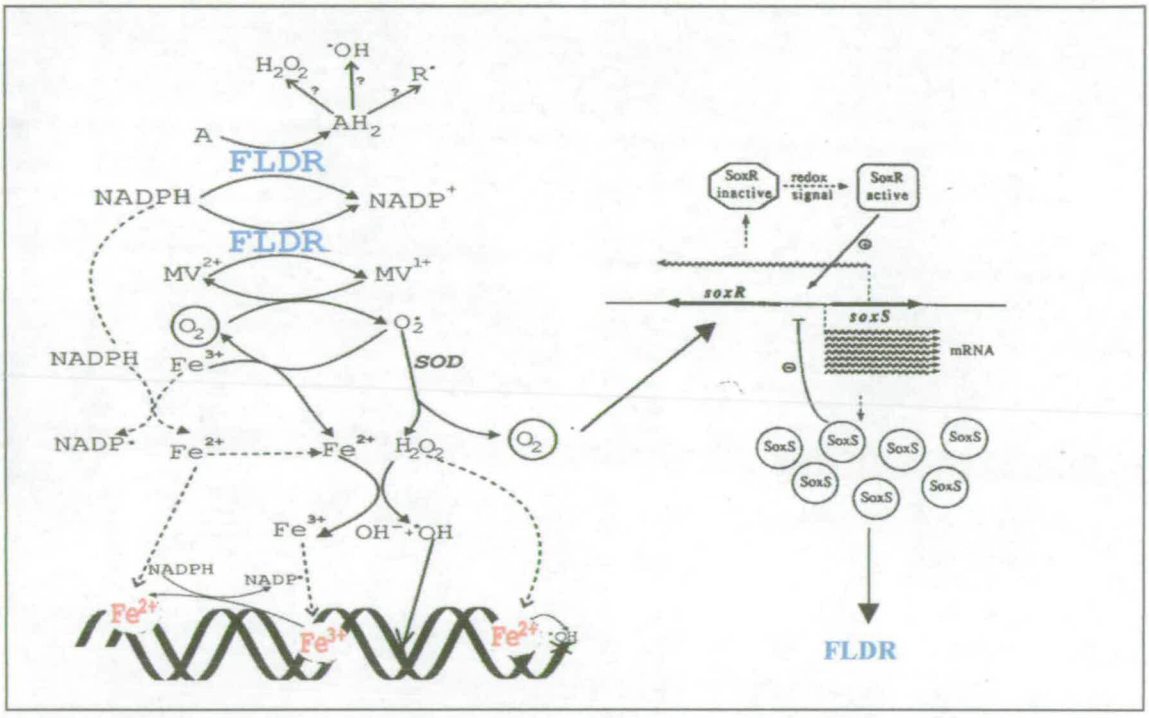


***E. coli* flavodoxin $NADP^+$ reductase structure**

FLDR is an important enzyme in *E. coli* and a full understanding of the enzyme is necessary to gain insight into the metabolic pathways in which it participates in. The gene encoding FLDR has been cloned from *E. coli* (Bianchi *et al.* 1993 a) and was found to encode a protein containing 248 amino acids and to have a molecular weight of 27 648Da. The crystal structure of FLDR has been solved (Ingleman *et al.*1997), and indicates that the enzyme has two distinct domains. One these is

involved in the binding of FAD and the other in the binding of NADPH. The FAD domain has structural similarity to other members of the ferredoxin reductase super family *e.g.* spinach ferredoxin reductase (Karplus *et al.* 1991), having a flattened cylindrical β-domain with a double sandwich with six strands. The cylinder is open, which makes space for the isoalloxazine and ribityl moieties of the FAD, to which direct and water mediated hydrogen bonds are formed from the edges of the strands (Ingleman *et al.* 1997).

In the FLDR family a total of seven crystal structures have been solved, see fig 1.8. These include spinach ferredoxin $NADP^+$ reductase (Karplus *et al.* 1991, Bruns & Karplus 1995), *Anabaena* (Serre *et al.* 1996), corn nitrate reductase (Lu *et al.* 1994), *Pseudomonas cepacia* phthalate dioxygenase reductase (PDR) (Correll *et al.* 1992), *Azotobacter vinelandii* NADPH:ferredoxin reductase (Prasad *et al.* 1998) and, of course, *E. coli* FLDR (Ingleman *et al.* 1997), see fig1.8. All the structures show a FAD or FMN binding domain, comprising a six stranded β-barrel with a capping α-helix. The $NADP^+$ or $NAD^+$ binding domain contains a parallel β-sheet nucleotide binding fold.

**Fig 1.8 Comparison of the properties of the solved crystal structures of members of the FNR family.**

| Protein | Cofactor | Substrate | Bound | Target | Source |
|---|---|---|---|---|---|
| FLDR | FAD | NADP | - | FLD | *Escherichia coli* |
| FPR | FAD | NADP | - | 7FeFd | *Azotobacter vinelandii* |
| FNR | FAD | NADP | 2',5'ADP | 2FeFd | Spinach |
| FNR | FAD | NADP | NADP | 2FeFd | *Anabaena* |
| NiR | FAD | NAD | ADP | Cytb5 | Corn (domain of NiR) |
| PDR | FMN | NAD | NAD | 2FeFd | *Pseudomonas cepacia* |

Structural studies have defined the FAD and FMN binding sites (Karplus *et al.* 1991, Bruns & Karplus 1995, Serre *et al.* 1996, Correll *et al.* 1992). The $NADP^+$ or $NAD^+$ binding sites of some enzymes have been demonstrated by co-crystallisation with $NADP^+$ or $NAD^+$, or with ADP, which is a good analogue of $NADP^+$. This led to structure/sequence alignment studies of theses six enzymes and, as a result, a number of specific residues have been implicated in the binding of $NADP^+$ or $NAD^+$, see fig 1.9.

**Fig 1.9 Sequence alignment analysis**

Structure alignment of *E. coli* FLDR (Ingleman *et al.* 1997) with five homologous oxioreductases whose structure are known, NADPH:flavodoxin reductase *Azobacter vinelandii* (Prasad 1998), flavodoxin reductase from spinach (Karplus *et al.* 1991, Bruns & Karplus 1995), flavodoxin reductase from *Anabaena* (Serre *et al.* 1996), corn nitrate reductase (Lu *et al.* 1994) PDR from *Pseudomonas cepacia* (Correll *et al.* 1992). Motifs are indicated by the coloured text. * represent conserved residues.

```
FNR_E.coli       ----------------MAD-WVTGKVTKVQNWTD------ALFSLTVHA----PVLPFTA 33
FDR_Azobzcotor   ----------------MSN-LNVERVLSVHHWND------TLFSFKTTR---NPSLRFEN 34
FNR_Spinach      HSKKMEEGITVNKFKPKTP-YVGRCLLNTKITGDDAPGETWHMVFSHEG-EIPYREGQSV 58
FNR_Anabaena     QAKAKHADVPVNLYRPNAP-FIGKVISNEPLVKEGGIGIVQHIKFDLTGGNLKYIEGQSI 59
NiR_Corn         ----VRAPALSN---PREK-IHCRLVGKKELSRD-----VRLFRFSLPS--PDQVLGLPI 45
PDR_Pseudomonas ------------TTPQEDGFLRLKIASKEKIAR------NIWSFELTNPQGAPLPPFEA 41
                                        : .           :

                                FAD
FNR_E.coli       GQFTKLGLEIDGERVQRAYSYVNSP----DNPDLEFYLVTVP--------------DGKL 75
FDR_Azobzcotor   GQFVMIGLEVDGRPLMRAYSIASPN----YEEHLEFFSIKVQ--------------NGPL 76
FNR_Spinach      GVIPDGEDKNGKPHKLRLYSIASSA--LGDFGDAKSVSLCVKRLIYTN--DAGETIKGVC 114
FNR_Anabaena     GIIPPGVDKNGKPEKLRLYSIASTR--HGDDVDDKTISLCVRQLEYKHP-ESGETVYGVC 116
NiR_Corn         GKHIFVCASIEGKLCMRAYTPTSMVDEIGHFDLLVKVYFKNEHPKFPNGGLMTQYLDSLP 105
PDR_Pseudomonas GANLTVAVPNGSR---RTYSLCNES----SERDRYTIAVKRD-----------SNGRGGS 83
                *                * *:  .                .                .

                                                    NADP
FNR_E.coli       SPRLAALK-PGDEVQVVSEAAGFFVLDEVPHCETLWMLATGTAIGPYLSILQ-L------ 127
FDR_Azobzcotor   TSRLQHLK-EGDELMVSRKPTGTLVTSDLLPGKHLYMLSTGTGLAPFMSLIQ-------- 127
FNR_Spinach      SNFLCDLK-PGAEVKLTGPV-GKEMLMPKDPNATIIMLGTGTGLAPFRSFLWKM------ 166
FNR_Anabaena     STYLTHIE-PGSEVKITGPV-GKEMLLPDDPEANVIMLATGTGIAPMRTYLWRM------ 168
NiR_Corn         VGSYIDVKGPLGHVEYTGRG-SFVINGKQRHASRLAMICGGSGITPMYQIIQAV------ 158
PDR_Pseudomonas ISFIDDTS-EGDAVEVSLPR-NEFPLDKR--AKSFILVAGGIGITPMLSMARQLRAEGLR 139
                       .     :       .             . ::  * .: *

FNR_E.coli       -------GKDLD-----------RFKNLVLVHAAR---YAADLSYLPLMQE--LEKRYE- 163
FDR_Azobzcotor   ---------DPE--------VYERFEKVVLIHGVR---QVNELAYQQFITEHLPQSEYFG 167
FNR_Spinach      -------FFEKH----------DDYKFNGLAWLFLGVPTSSSLLYKEEFEK--MKEKAP- 206
FNR_Anabaena     -------FKDAER------AANPEYQFKGFSWLVFGVPTTPNILYKEELEE--IQQKYP- 212
NiR_Corn         -------LRDQP----------EDHTEMHLVYANR---TEDDILLRDELDR--WAAEYP- 195
PDR_Pseudomonas SFRLYYLTRDPEGTAFFDELTSDEWQSDVKIHHDHG-DPTKAFDFWSVFEKSKPAQHVYC 198
                       :                                 :     : .     .

                                      2'P
FNR_E.coli       -----------GKLRIQT--VVSRETA--AGSLTGRIPALIESGELESTIGL-PMNKETS 207
FDR_Azobzcotor   E-------AVKEKLIYYP--TVTRESF--H--NQGRLTDLMRSGKLFEDIGLPPINPQDD 214
FNR_Spinach      -----------DNFRLDF--AVSREQT--N-EKGEKMYIQTRMAQYAVELWE-MLKKDNT 249
FNR_Anabaena     -----------DNFRLTY--AISREQK--N-PQGGRMYIQDRVAEHADELWQ-LIKNQKT 255
NiR_Corn         -----------DRLKVWY--VIDQVKR--P-EEGWKYSVGFVTEAVLREHVP-EG-GDDT 237
PDR_Pseudomonas CGPQALMDTVRDMTGHWPSGTVHFESFGGAAAAAAANTADTVRDARSGTSFEIPANRSIN 258
                              .:                                        .

FNR_E.coli       HVM--------------LCGNP-----QMVRDTQQLLKETRQMTKHLRRRPGHMTAEHYW 248
FDR_Azobzcotor   RAM--------------ICGSP-----SMLDESCEVLDGFGLKISPRMGEPGDYLIERAF 255
FNR_Spinach      YFY--------------MCGLKGM---EKGIDDIMVSLAAAEGIDWIEYKRQLKKAEQWN 292
FNR_Anabaena     HTY--------------ICGLRGM---EEGIDAALSAAAAKEGVTWSDYQKDLKKAGRWH 298
NiR_Corn         LAL--------------ACGPP-----P------MIQFAISPNLEKMKYDMANSFVVF-- 270
PDR_Pseudomonas QVLRDANVRVPSSCESGTCGSCKTGLCSGAADHRDDVLAAAAKGTQIMVCVSRAKSAELV 318
                                 **

FNR_E.coli       ----
FDR_Azobzcotor   VEK- 258
FNR_Spinach      VEVY 296
FNR_Anabaena     VETY 302
NiR_Corn         ----
PDR_Pseudomonas LDL- 321
```

However, the NADPH binding domain in *E. coli* FLDR is not fully understood, as the enzyme has never been co-crystallised with NADPH or one of its analogues. Citrate present in the crystallisation buffer is incorporated in the proposed NADPH binding site (Ingleman *et al.* 1997). The citrate molecule interacts with three arginine residues Arg144, Arg174 and Arg184, which are proposed to be involved in NADPH binding. Arg 174 is conserved in spinach and *Anabaena* and has been proposed to be involved in the binding of the 2′ phosphate group of NADPH. This 2′ phosphate group is what discriminates between NADPH and NADH, see fig 1.10. From fig1.11 it is clear that these residues form a positive area, which would be an attractive docking site for NADPH (Ingleman *et al.* 1997).

**Fig 1.10 Structure of NADPH and NADH**

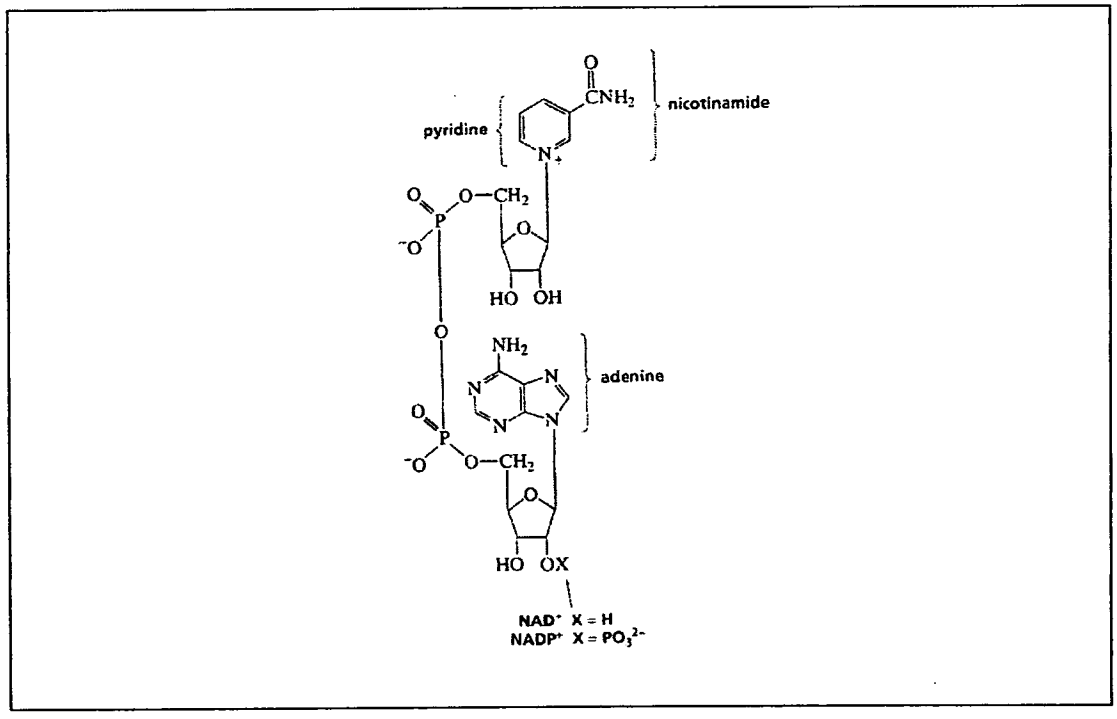


The binding of FLDR's redox partner, flavodoxin (FLD), is also not understood. There is a distinct bowl-shaped depression in the FLDR molecule, close to FAD that involves both domains. In this depression there are three surface arginine residues, Arg236, Arg237 and Arg238, which form a large positive patch in the putative

**Fig 1.11 Potential Map of FLDR**
Scale -5eV(red) to+5eV (blue)

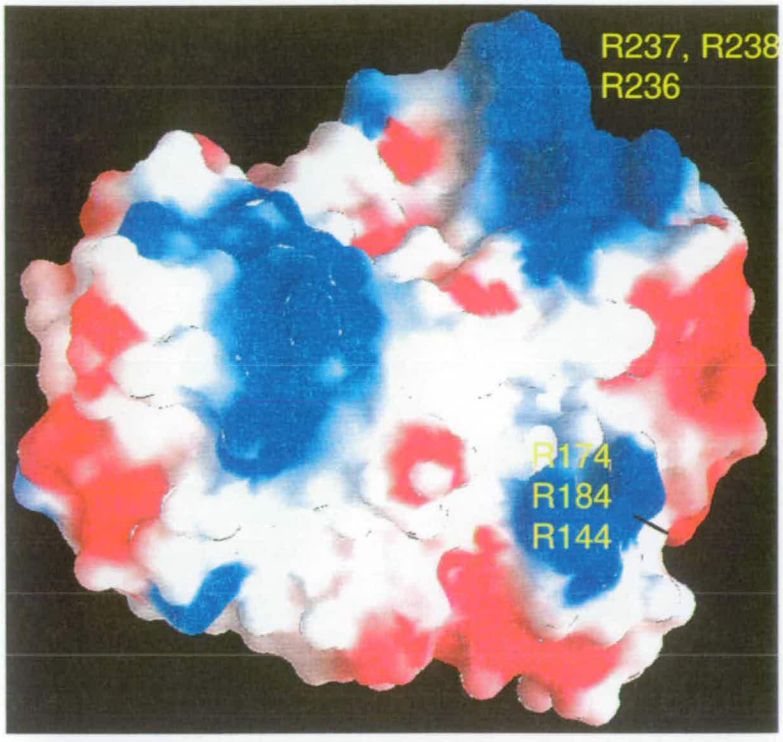


**Fig 1.12 Potential Map of FLD**
Scale –5eV (red) to + 5 eV (blue)

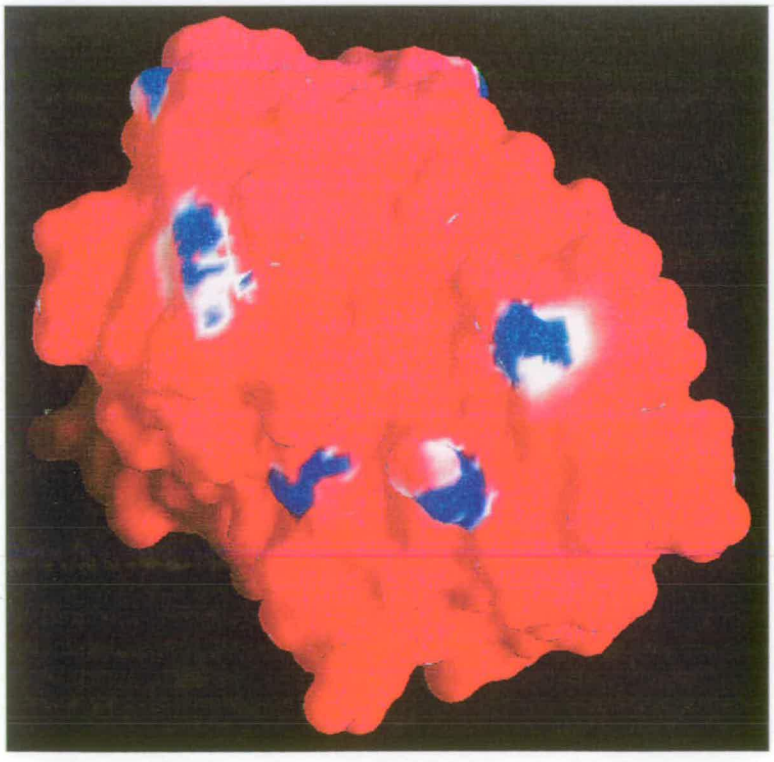

'binding' site of the enzyme, see fig 1.11. Flavodoxin, which exhibits a large number of negative residues on its surface and it is one of the most negatively charged proteins known, see fig 1.12. It appears likely that at least some of the positive residues on FLDR are involved in the binding of flavodoxin (Hoover & Ludwig 1997, Ingleman *et al.* 1997).

Interaction between proteins has long been speculated on. How does the interaction occur? Is it specific? How does the alignment of the proteins occur? All these factors are important for redox enzymes. The different theories are discussed below with particular emphasis upon redox enzymes.

Redox enzymes are often involved in more than one physiological system, interacting with various very different donor and acceptor molecules. Similarly, different redox proteins are able to mediate electron transfer between two particular donors and acceptors. An example of this is pseudoazurin, which can donate electrons to a range of structurally diverse enzymes in the periplasm of *T. pantotripha* (Williams *et al.* 1995). However, only one of them, cytochrome $cd_1$ nitrite reductase, has its 3-D structure solved. Cytochrome $cd_1$ nitrite reductase can, in turn, accept electron from a range of donors, including pseudoazurin, azurin, cytochrome $c_{550}$ and cytochrome $c_{551}$(Williams *et al.* 1995). In fact it is known that FLDR can use either FLD or ferredoxin as its electron acceptor, although its main redox partner is thought to be FLD (Bianchi *et al.* 1993a). It is obvious that the traditional theory of the lock and key mechanism, where a protein has one specific site on its surface only suitable for a particular substrate, does not necessarily apply to electron transfer proteins which appears to exhibit promiscuous behaviour.

One possibility is that electron transfer can occur without complex formation. In this case the donor and acceptor molecules exchange electrons without actually docking. According to the 'Marcus theory' the speed of electron transfer could not be very fast in this case (Marcus1956, Marcus 1964, Marcus 1965). It is more likely that redox proteins dock to form a complex in order to promote electron transfer. The molecular recognition event could be promiscuous in nature, and very specific

interactions such as salt brides and hydrogen bonding would not be involved. The interaction is more likely to involve less specific and transient electrostatic and hydrophobic attractions.

A basic electrostatic theory is the velcro theory (McLendon 1991), where positive charges on one protein and negative charges on the other bring the two proteins together. This allows a certain flexibility in docking enabling the sampling of a number of sites until the electron transfer complex is achieved. The proteins can be imagined to be rolling over each other until the ideal position is achieved.

The velcro theory has been developed into the "pseudospecfic docking theory" (Williams *et al.* 1995). This takes into account both hydrophobic and electrostatic interactions, and has been used to explain the behaviour of pseudoazurin from *Thioshaera pantotropha*. Pseudoazurins are small copper containing redox enzymes, which are involved in the flow of electrons between various donors and acceptors in the bacterial periplasm. The interaction between pseudoazurin, cytochrome $C_{550}$ and cytochrome $cd_1$ nitrite reductase have been investigated (Williams *et al.* 1995). The crystal structure of pseudoazurin was studied to look for residues which may be involved in its binding motif. A hydrophobic patch was found surrounding the copper ion. Hydrophobic interactions are thought to be important, because they are relatively less specific and directional than electrostatic interactions. An important aspect is that a hydrophobic interface has a low dielectric constant, which is favourable for electron transfer. In conjunction with this there are a large number of positively charged residues, which may be involved in docking along with the hydrophobic residues surrounding the copper ion of pseudoazurin. This feature is highly conserved in other pseudoazurins. Cytochrome $cd_1$ nitrite reductase, one of pseudoazurin's redox partners from *T. pantotropha* structure was examined, and it was found that it showed a hydrophobic patch surrounded by negative residues. Modelling studies of the docking of these two proteins show that the interaction of the two hydrophobic patches on each protein, surrounded by the oppositely charged residues brings the copper ion of pseudoazurin to the closests possible distance to the heme iron of cytochrome $cd_1$ nitrite reductase (19-20Å) (Williams *et al.* 1995).

In pseudoazurin there are a large number of negatively charged residues on the opposite side of the protein from the positively charged patch. This bipolarity of the molecule induces a dipole movement. This may help to steer the pseudoazurin and cytochrome $cd_1$ nitrite reductase together from long range distances, bringing them together in an orientation so that their prosthetic groups are orientated to an optimal position for an electron transfer complex to form. This asymmetrical distribution of charge is observed in numerous other redox proteins, including cytochrome *c*. It has been observed that electron transfer between cytochrome *c* and its physiological partners occurs at rates, $10^8$-$10^9$, which are close to diffusion control. The asymmetric distribution of charges helps the molecules to attain the correct orientation for electron transfer (Koppenol & Margoliash 1982). Electron transfer between cytochrome *c* and flavodoxin has been extensively studied (Matthew *et al.* 1983), the electrostatic interactions pre-orient the molecules before they make physical contact, facilitating the formation of an optimal reaction complex. This suggests that the reactants may orientate themselves as they approach each other to form the electron transfer complex.

Neither electrostatic nor hydrophobic interactions are highly specific, since these surface motifs allow partners to take up related but different orientations relative to each other. Both electrostatic and hydrophobic interactions are important in the docking of redox partners, and experimental conditions determines which dominates.

The above discussion has indicated that there are interactions between redox coupled protein molecules before collision occurs. This type of interaction has been discussed by Janin (Janin 1997) and developed into a theory. The Janin model incorporates the basic feature of protein-protein recognition with the rigid body approximation and assumes that no large conformational changes occurs in the molecules. The process starts (if long range electrostatic interactions are ignored), with a random collision at the rate ($k_{coll}$) predicted by the Einstein-Smoluchowski equation (Atkins 1990). An encounter complex is formed, which may evolve into a stable complex if the two molecules are correctly aligned. The probability of a

correct alignment is defined as $p_r$ and the bimolecular rate of association is defined as $p_r k_{coll}$. However, long-range interactions can affect both constants. Coulombic attraction makes collisions more frequent and the collision rate can be multiplied by a factor qt. This factor is larger than one if the proteins carry net charge of opposite sign. The probability factor $p_r$ is multiplied by a factor $q_r$ that represents the steering effect of electric dipoles, which pre-orientate the molecules before they collide. This gives an association rate constant $Ka = q_t q_r p_r k_{coll}$, making collisions more frequent and pre-orienting proteins so that the collision is more successful one. This has been applied, to the barnase-barstar system. The presence of barnase in a cell is lethal, giving to rise the need for an inhibitor of bastar which has a femtomolar binding constant. These proteins have an asymmetric charge distribution, which is important in bringing them together. The model predicted a $K_a$ of $10^5$ $M^{-1}s^{-1}$ under these conditions a $p_r$ is $1.5 \cdot 10^{-5}$, its value is compatible to computer docking simulations. At low ionic strength, long-range electrostatic interactions accelerate the interaction of the barnadse-barstar association by a factor of $q_t q_r$ of up to $10^5$ as favourable charge-charge and charge-dipole interactions work together to make it much faster than free diffusion. From this information it should be possible to gain an understanding of how FLDR and FLD interact, by a variety of experimental techniques.

The aim of this work, is to gain a greater understanding of FLDR and its interaction with NADPH and FLD. The initial step was to optimise the expression and purification of FLDR allowing a full characterisation of the protein. The crystal structure of FLDR does not fully elucidate the interaction of FLDR with either FLD or NADPH. It is of great interest to understand how these substrates interact with FLDR. This will be an important aim of this project.

# Chapter 2 (FLDR).

# Materials and Methods

## Materials

Chemicals were purchased from Pharmacia, Promega, Sigma, Biorad, Gibco BRL, Amicon, New England Biolabs, Invitrogen and Difco.

### Cell lines

| Strain | Genotype | Description/Applications |
|---|---|---|
| TOP10 One Shot™ Cells | F⁻mcrA(mrr-hsdRMS-mcrBC)80lacZM15lacX74 deoR recA1 araD139 (ara-leu)7697 ga/U ga/K rpsL endA1 nupG | Used for transforming DNA ligations |
| BL21(DE3) | -Fomp Thsds$_b$ ($r_B^-$ $m_B^-$) gal dcm (DE3) | General purpose expression host |
| JM101 | sup E, thi, Δ (lac-proAB)[F' tra D36, pro AB, lac $1^9$ΔM15] | Storing plasmid DNA |
| JM109 | F' traD36 lac$1^q$ (lac Z) M15 proA$^+$B$^+$/e14$^-$(McrA$^-$) (lac-proAB) thi gyr A96 (Na1$^1$) endA1 hsdR17 ($r^-_{K12}$-$m_{K12}^+$) relA1 supE44 recA1 | Storing plasmid DNA<br>Expression of flavodoxin |
| HMS174(DE 3) | F-recA1 hsdR($r^-_{K12}$-$m_{K12}^+$)Rif$^R$(DE3) | recA-K-12 expression host |
| B834(DE3) | F-ompT hsdS$_B$($r_B$-$m_B$-)gal dcm met (DE3) | Met auxotroph, parent of BL21 control non-expression host |

**Plasmids**

| Plasmids | |
|---|---|
| pCL21 | pET-16b + fldr |
| pCL22 | pUC18/RBS + fldr R144A |
| pCL23 | pUC18/RBS + fldr R174A |
| pCL24 | pUC18/RBS + fldr R184A |
| pCL25 | pUC18/RBS + fldr R237A |
| pCL26 | pUC18/RBS + fldrR238A |
| pDH1 | pTRC-99A + *fld* |

## Growing cells

Overnight cultures were grown up by inoculating in sterile conditions. A loop full of bacterial culture was added to 10ml of Luria Bertani (LB) medium, [bactotryptone (10g/l), bacto yeast extract(5g/l), NaCl (10g/l), pH adjusted to 7.5 with NaOH, autoclaved at 121°C for 15 min at 15psi.], containing ampicillin (100μg/ml). For larger cultures the same procedure was used scaled up by the necessary factor. The cultures were grown overnight with shaking (37°C).

To prepare agar plates bacto-agar (15g/l)was added to the LB medium, the plates were then poured (40ml per plate). If antibiotics were required they were spread to dryness after the plate had dried. The bacterium was added in sterile conditions by spreading a loopful of bacterium over the plate. The plate was then incubated overnight (37°C).

## SDS-PAGE

SDS-Page gels were used for the analysis of proteins present in cells (Laemmli 1970).

## Transformation

LB broth (10ml) was inoculated with cell line (0.2ml) and 1M MgCl (0.2ml), and then grown for 1 hour. The cells were chilled on ice (5mins), and then centrifuged at 2000rpm (15 min). The supernatant was discarded and the cells resuspended in chilled transformation buffer (TB) (50mM $CaCl_2$, 10mM Tris, pH 8). The cells were left on ice (30 mins), and were then centrifuged at 3000rpm (15min).

The cells were resuspended in 400µl of TB buffer and to 100µl fractions of this, up to 10µl of DNA was added and left on ice (1-2 hours). The cells were then heat shocked at 37°C (5 min), LB medium (1ml) was added and then the cells were grown at 37°C (1 hour). The cells were centrifuged (10mins) and then resuspended in 100µl of LB and spread to dryness on selective plates.

Transformation of DNA into TOP10 One Shot™ Cells (Novagen) was done as per the manufacturer's instructions.

## Polymerase chain reaction (PCR)

The template and primer were added in appropriate proportions to Ready To Go PCR beads (Pharmacia Biotech), this was then made up to 25µl as per the manufacturer's instructions. The PCR reaction was then carried out in Perkin Elmer DNA thermal cycler, with a typical cycle of 95°C 1min, 54°C 1min and 72°C 1min

## Agarose gel

Required amount of agarose was added to TE buffer (40mM Tris, 1mM EDTA) and heated to dissolve the agarose. The solution was allowed to cool to 60°C and ethidium bromide added to a final concentration of 0.5µg/ml. The gel was then

poured into a casting mould and allowed to set at room temperature. The DNA sample was loaded onto the agarose gel using blue/orange loading dye. The DNA was size separated by running the gel at 100V (40 mins). The gel was then visualised under UV light.

### Purification of DNA from agarose gels

DNA was prepared from agarose gels using Prep-A-Gene® DNA Purification Systems (BIO-RAD), as per the manufacturer's instructions.

### Digestion of DNA with restriction endonuclesaes

The required amount of DNA was treated with the appropriate enzyme(s) and buffer. This was incubated at the required temperature for a specified time.

### Ligation of DNA

DNA was cut with appropriate restriction enzymes was incubated with DNA ligase and the ligase buffer at room temperature (two days). A control reaction was also carried out. Both the control and ligation reaction were transformed into an appropriate cell line.

### PCR screen

Colonies were picked from a plate, and then touched on to another plate at a known position. The remaining colonies were suspended into 50µl of water. The cell suspension was then boiled for five minutes, and the solution centrifuged (14 000rpm) for two minutes. A sample (5µl) was taken and used as a template in a PCR reaction to amplify the required gene using the appropriate primers. The resulting reaction was run on an agarose gel and visualised using UV light.

## Preparation of plasmid DNA

Plasmid DNA was prepared using Wizard ® *Plus* SV Minipreps DNA Purification System (Promega), following the manufactures instruction.

## DNA sequencing

The sequencing was carried out by combining the following together for each template to be sequenced: sequencing reagent pre-mix (Amersham), DNA template, primer (5pmol), and $H_2O$ to final volume of 20µl. The PCR reaction was carried out with the following cycle 96°C for 30s, 45°C for 15s and 60°C for 4 mins. The DNA was then precipitated, and submitted for sequencing by Sanger dideoxy chain termination method on ABI Prism 377 DNA sequencer. Nicola Preston provided the sequencing service.

## DNA Precipitation

DNA was precipitated with 3M sodium acetate (pH 5.3): ethanol (0.1:2 v/v), which was mixed well with the DNA solution, and kept at -20°C (1 hour). The solution was then centrifuged (15mins), and the supernatant discarded. The precipitated DNA was then washed with a 70% solution of ethanol and the supernatant discarded. The DNA pellet was then dried under vacuum.

## Purification of flavodoxin NADPH reductase & mutants

Fermenter containing LB medium (9l) was inoculated with HMS174 (DE3) cells (1l), containing the plasmid pCL21, which had been grown overnight. The cells were grown (37°C) until an OD=1 @ 600nm was reached. The over-expression of the *fldr* gene was achieved by the addition of IPTG (100µM), and the cells were then grown for a further 3 hours. The cells were harvested by centrifugation (5 000rpm, 20 mins). The wet weight of the cells was recorded. The cells were washed with Tris buffer A ( Tris 50mM, pH 7.5) The cells were lysed by sonication (20*30 s bursts).

The cell free extract was separated by anion exchange chromatography (Q-Sepharose column) using a gradient of 0-1M NaCl in 50 mM Tris pH 7.5, over 20 column volumes. The FLDR elutes at 150mM NaCl and is yellow in colour. The fractions containing FLDR were combined and applied to an adenosine 2′,5′-diphosphate (ADP) sepharose column. The column was washed with three column volumes of binding buffer (10mM sodium phosphate, 0.15M NaCl, pH 7.5). FLDR was eluted with elution buffer (10mM sodium phosphate, 0.5M NaCl, pH7.5). FLDR was then dialysed against assay buffer (10mM sodium phosphate, pH 7.5). Glycerol was added to a concentration of 10%, and FLDR was stored at -20°C.

## Flavodoxin $NADP^+$ reductase extinction coefficient

To calculate the concentration of ferredoxin $NADP^+$ reductase the extinction coefficient was used, (Jenkins & Waterman 1993).

$\varepsilon_{456nm}=7100M^{-1}cm^{-1}$

## Preparation of $^{15}N$ labelled Flavodoxin $NADP^+$ Reductase

HMS174 cells(1l) containing the *pCL21* plasmid were grown with shaking (37°C) overnight in LB medium. The cells were then washed with M9 media. This was then used to inoculate 10 l of $^{15}N$-M9 minimal media, [$Na_2HPO_4$ (6g/l), $KH_2PO_4$ (3g/l), NaCl (0.5g/l), $^{15}NH_4Cl$ (1g/l), $MgSO_4$, (1M 2ml)]. This was grown for 10 hours in a fermentor at 37°C, until an OD=1 @ 600nm. The cells were then induced with IPTG (100μM) for a further 12 hours. FLDR was then purified as previously described.

## NMR Spectroscopy

The NMR spectroscopy was performed with the assistance of Dr. Emma Beatty. 2-D HSQC (heteronuclear single quantum coherence) was performed on $^{15}N$-FLDR (0.33mM). NADPH (0.4mM) and flavodoxin (0.27mM) were titrated into FLDR separately and HSQC spectra was recorded.

## Purification of flavodoxin

Fermenter containing LB medium (9l) was inoculated with JM109 cells (1l) containing the plasmid pDH1, which had been grown overnight. The cells were grown (37°C) until an OD=1 @ 600nm was reached. The overexpression of the *fld* gene was achieved by the addition of IPTG (100μM) and riboflavin (5mg/l), the cells were grown for a further 6 hours. The cells were harvested by centrifugation (5000 rpm, 20 mins). The wet weight of the cells was recorded. The cells were washed with Tris buffer A (Tris 50mM, pH 7.5) The cells were lysed by sonication (20*30 s bursts). Protamine sulphate (0.1%[w/v]) was added to the cell free extract.

The cell free extract was separated by anion exchange chromatography (Q-sepharose) using a gradient of 0-1M NaCl in 100mM sodium acetate, pH 5, (20 column volumes). The FLD elutes at 450mM NaCl and is blue in colour. The fractions containing the FLD were combined, and dialysed against 50mM Tris pH 7.5 over night. The FLD re-oxidised to an orange colour. FLD was then applied to RESOURCE Q column and eluted with a gradient 0-1M NaCl in Tris 50mM, pH 7.5 (20 column volumes). The fractions containing FLD were collected and combined. Glycerol was added to a concentration of 10%, and FLD was stored at -20°C.

## Flavodoxin extinction coefficient

The concentration of flavodoxin was calculated using the extinction coefficient.

$\varepsilon_{466}$= 8250 $M^{-1}cm^{-1}$ (Fuji & Huennekens 1974)

The purity of flavodoxin was estimated using a ratio.

$A_{274}/A_{466}$=5.8 (Bianchi *et al.* 1993 b)

## Steady-state kinetic assay of flavodoxin $NADP^+$ reductase

Steady-state kinetic parameters for wild-type and mutant forms of FLDR were measured at 30 °C in 10 mM sodium phosphate (pH 7.5) (assay buffer) on a Shimadzu 1201 UV/Vis spectrophotometer. Reduction of cytochrome *c* (horse heart, type 1) was monitored by absorbance increase at 550 nm, using an absorbance

coefficient ($\varepsilon_{red\text{-}ox}$) = 22640 $M^{-1}$ $cm^{-1}$. Reduction of potassium ferricyanide was monitored by absorbance decrease at 420nm, using absorbance coefficient ($\varepsilon_{red\text{-}ox}$) = 1010 $M^{-1}$ $cm^{-1}$.

## Pre-steady-state kinetic

Stopped-flow measurements of transient absorbance changes associated with reduction of FLDR flavin (decrease in absorbance at 456nm), FLD flavin (increase in absorbance at 583nm) and reduction of cytochrome *c* (550 nm) were made using an Applied Photophysics SF.17 MV stopped-flow kinetics spectrophotometer. Reactions were performed at 30 °C in assay buffer (7.5) (unless otherwise stated). Analysis of stopped-flow data were performed using the SF.17 MV software and Origin (Microcal), both of which use non-linear least-squares regression analysis. The reduction of wild-type and mutant forms of FLDR by NADPH and NADH were measured by rapid mixing of NAD(P)H (10 μM - 10 mM) with enzyme (10 - 50 μM) and monitored at 456 nm (total flavin reduction). Rates of FLDR-to-FLD electron transfer were measured after enzyme and buffer solutions had been degassed and bubbled for 15 minutes with oxygen-free nitrogen. The solutions were then transferred to the stopped-flow syringes and sealed within the glove box before transferring to the stopped-flow apparatus. Wild-type and mutant FLDRs (at a fixed concentration between 30 – 50 μM) were placed in one stopped-flow syringe, with FLD (20 μM), and NADPH (2mM) in the other syringe, the rate of electron transfer from FLDR to FLDs FMN was monitored by absorbance change at 583 nm. Reduction of cytochrome *c* was measured at 550 nm after reaction of reduced FLDR (10 - 50 μM enzyme + 2 mM NADPH) with cytochrome *c* (horse heart, type 1; 20-3 μM). All solutions were degassed as described above.

## CD Spectrometry

Protein samples were in assay buffer (10 mM sodium phosphate, pH 7.5) throughout. CD measurements were made in the far UV (190-260 nm), near UV (260-320 nm)

and visible (320-600 nm) regions on a Jasco spectropolarimeter at protein concentrations of *ca.* 15 - 20 μM (far UV) and *ca.* 30 - 80 μM (near UV-visible).

## UV/Vis Spectroscopy

Protein samples were in assay buffer (10 mM sodium phosphate, pH 7.5) throughout. All UV-visible spectra were run on a Shimadzu 2101 scanning spectrophotometer.

## Fluorescence

Protein samples were in assay buffer (10 mM sodium phosphate, pH 7.5) throughout. Fluorescence from protein aromatic residues (primarily tryptophan) was measured on a Shimadzu RF-5301 spectrofluorophotometer with excitation wavelength set at 290 nm and emission measured between 300-400 nm, using ~ 0.5 μM protein. Flavin fluorescence was measured with excitation at 456 nm and emission measured between 500-600 nm, also using ~ 0.5 μM protein. Excitation and emission slit widths on the Shimadzu instrument were set at 5 nm / 5 nm for tryptophan fluorescence, and at 10 nm / 10 nm for flavin fluorescence.

## Mass Spectrometry

Electrospray mass spectrometry was performed on a micromass Platform quadrupole mass spectrometer equipped with an electrospray ion source. The cone voltage was set to 70V and the source temperature to 65$^0$C. A waters 2690 HPLC unit with a Waters 486 Tunable Absorbance Detector was connected to the mass spectrometer. Protein samples (10μg protein in buffer) were separated on a Jupiter 5μg C-4 300A column at a constant TFA concentration of 0.01% using a linear gradient of 10-100% acetonitrile in water over 40 min flow rate of 0.05ml/min. The total ion count of all ions in the range m/z 500 to 2000 and the UV chromatogram at 280nm were recorded for the reversed-phase HPLC separation. The mass spectrometer was scanned at intervals of 0.1s, the scans accumulated, the spectra combined and the average molecular mass determined using the MaxEnt and Transform algorithms of MassLynx software. Dr. Scott Webster provided this service.

## Potentiometric titrations

All redox titrations were conducted within a Belle Technology glove box under a nitrogen atmosphere, with oxygen maintained at less than 5 p.p.m. Degassed, concentrated enzyme samples were passed through an anaerobic Sephadex G25 column (1 x 20cm) (Sigma) immediately on admission to the glove box to remove all traces of oxygen. The column was equilibrated and proteins were eluted with 0.1M phosphate buffer (pH 7.0), which was used throughout the experimental procedures. Protein solutions were titrated electrochemically according to the method of Dutton (Dutton 1978) using sodium dithionite as reductant and potassium ferricyanide as oxidant. Mediators were introduced prior to titration; typically 2-hydroxy-1,4-napthaquinone (5μM), benzyl viologen (1μM) and methyl viologen (1μM) within sample volumes of 5-10ml. After 10-15 minutes equilibration following each reductive/oxidative addition, spectra were recorded on a Shimadzu 1201 UV/Vis spectrophotometer (typically between 350 and 800nm) contained within the anaerobic environment. The electrochemical potential of the sample solutions were monitored using a CD740 meter (WPA) coupled to either Pt/calomel or Pt/Ag.AgCl combination electrodes (Russell pH Ltd.) at 25 ± 2°C. The electrodes were calibrated using the $Fe^{III}/Fe^{II}$ EDTA couple as a standard (+108mV). The calomel and Ag.AgCl electrodes were corrected by +244 ± 2mV and +198 ± 3mV respectively, both relative to the normal hydrogen electrode. For experiments involving FLDR, UV/Vis spectra were affected by the slow formation of a protein precipitate, which resulted in a small increase in baseline absorbance with time. This was corrected for by transforming each spectrum with a $1/\lambda$ subtraction calculated to return the absorbance at 800nm back to zero (at this wavelength chromophore absorbance is minimal). All data manipulations and non-linear least squares curve fitting of electrochemistry data were conducted using Origin (Microcal). This experiment was undertaken with the assistance of Dr. Simon Daff.

## Molecular modelling

Dominikus Lysek carried out molecular modelling studies studying the interaction of FLDR with NADPH. Atomic co-ordinates for protein were taken form the 1.7Å resolution X-ray structure of flavodoxin reductase from *E. coli* (Protein Data Bank number = 1FDR) (Ingleman *et al.* 1997). All modelling studies were carried out using residues 2-248, excluding residues 44-46, which could not be refined in the original structure. The graphics program SYBYL (Tripos) was used to dock the NADPH onto flavodoxin reductase, and to rotate W248 by 90°. The restraints for this preliminary model were that the hydride to isoalloxazine distance should be less than 8Å and residues R144, 174 & 184 should be close to, or should form part of, the intermolecular recognition surface.

A number of possible orientations were selected as starting points for further molecular mechanics refinement to remove any short non-bonded contacts and to optimise any intermolecular hydrogen bonds and salt bridges using the program Biopolymer-flexidock within SYBYL, using the maximum of 3000 generations allowed. All non-hydrogen atom positions of the amino acid residues and prosthetic groups in flavodoxin reductase and NADPH were refined using a Powel least squares minimisation algorithm with the standard geometry definitions. No water or other solvent molecules were included in any of the models.

## Sequence Alignment

Amino acid sequence alignments of *E. coli* FLDR with other proteins were performed initially using the MSA (Multiple Sequence Alignment) program from Washington University, and refined manually.

# Chapter 3 (FLDR)

## Investigation into wild type flavodoxin NADP$^+$ reductase

### Introduction

The aim of this work is to clone the *fldr* gene into an efficient vector to achieve a high level of protein expression, and to develop a simple and effective purification system. This will allow the production of large amounts of homogenous protein for characterisation. The characterisation of FLDR is essential because it is involved in many important systems in *E. coli*, and a thorough knowledge of FLDR is essential to provide an understanding of these pathways. The interaction of FLDR with its redox partner enzyme FLD and cytochrome P-450 will also be discussed in this section. This latter work was carried out by Miss Lisa McIver and is included for the sake of completeness. I thank Miss McIver for permission to use her data.

### Results

#### Cloning of *fldr* gene

The fldr gene was cloned from the plasmid pEE1010 (a gift from Dr. Elizabeth Haggård-Ljungquist, Department of Chemistry, Karolinska Institute, Stockholm, Sweden) (Bianchi *et al.* 1993a) using primers "RED FOR" (5' CAGGAGAATTCCATGGCTGATTGGGTAACAGGC 3') and "RED REV" (5' ATAAGGATCCGCTTACCAGTAATGCTCCGCTGTCAT 3'). "RED FOR" contains a *Nco*I site (red) encompassing the start codon (underlined) of the *fldr* gene). "RED REV" contains a *Bam*HI site (red) encompassing the stop codon (underlined) of *fldr*. A PCR reaction was carried out, and the PCR product was cleaved with *Nco*I and *Bam*HI. The digested product was ligated into plasmid pET16b (Novagen Inc., Madison) under the control of a T7*lac* promoter to produce the plasmid pCL21, see fig 3.1

**Fig 3.1 Picture of the plasmid pCL21 (pET16-b/*fldr*)**

Diagram showing the construct of pCL21 plasmid which is a construct of pET16-b and the *fldr* gene. The *fldr* gene was cloned into pET 16-b using the restriction sites *Nco*I and *Bam* HI. The ampicillin resistance gene (*amp*) is present on the construct. The vector is under the control of the T7 promotor system.

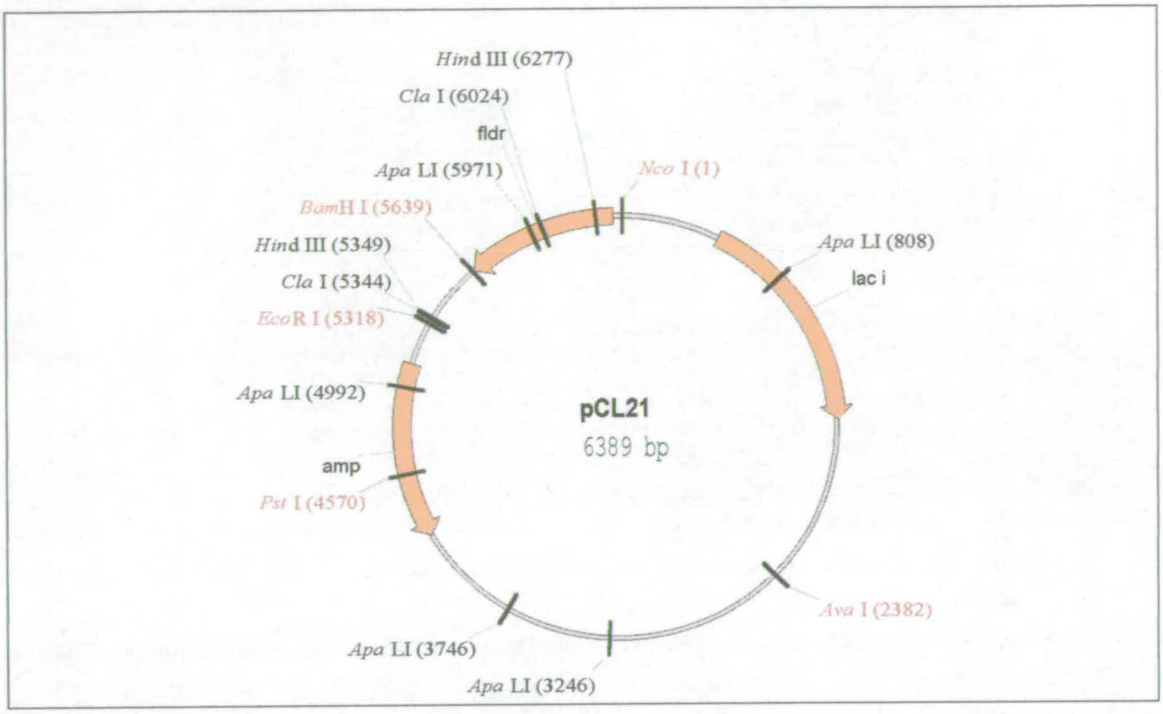


## Expression & purification of wild-type FLDR

Flavodoxin $NADP^+$ reductase (FLDR) is a monomeric (247 amino acids, $M_r$ 27648) enzyme containing FAD. *E. coli* HMS174 (DE3)/pCL21 was used to overexpress FLDR. Expression level of 15mg/liter was achieved. The protein was purified by sequential chromatography steps on Q-Sepharose and 2', 5'-ADP Sepharose (Table 3.1). Transformants of pCL21 in strain BL21 (DE3) resulted in even higher expression of *fldr* (*ca* 35mg/l); but the specific activity of the purified FLDR was considerably lower than that purified from the HMS174 (DE3) strain. Samples were analysed at all steps by SDS-PAGE (Fig 3.2) and UV-visible spectroscopy.

**Table 3.1 Purification table for *E. coli* NADP$^+$ flavodoxin oxidoreductase (FLDR)**

Total protein was estimated by absorbance at 280nm. FLDR was estimated by measurement of absorbance at the peak of the longer wavelength flavin band (456nm).

| Purification step | Total volume (V) (ml) | Total protein ($VxAbs_{280}$) | Total FLDR ($VxAbs_{456}$) | $Abs_{456}/Abs_{280}$ | Purification fold |
|---|---|---|---|---|---|
| Lysate | 55 | 833.9 | 18.26 | 0.0207 | 1 |
| Q-Sepharose | 80 | 119.1 | 9.28 | 0.0779 | 3.77 |
| 2',5'-ADP Sepharose | 35 | 37.5 | 5.74 | 0.1531 | 7.41 |

**Fig 3.2 SDS –page gel of the purification steps of wt FLDR**

1a: SDS PAGE of *E. coli* Flavodoxin NADP$^+$ oxidoreductase (FLDR) purification steps. Lane 1: Molecular weight standards (94000, 67000, 43000, 30000, 20100, 14400 Da), Lane 2:CFE, Lane 3: Q-Sepharose Lane, 4: 2', 5'-ADP Sepharose.

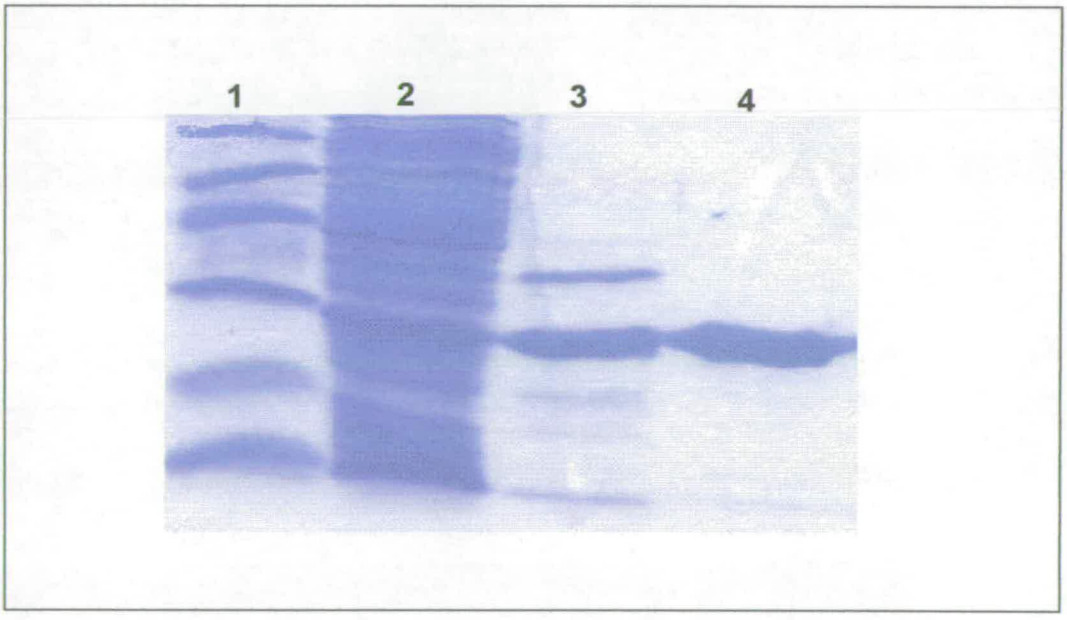

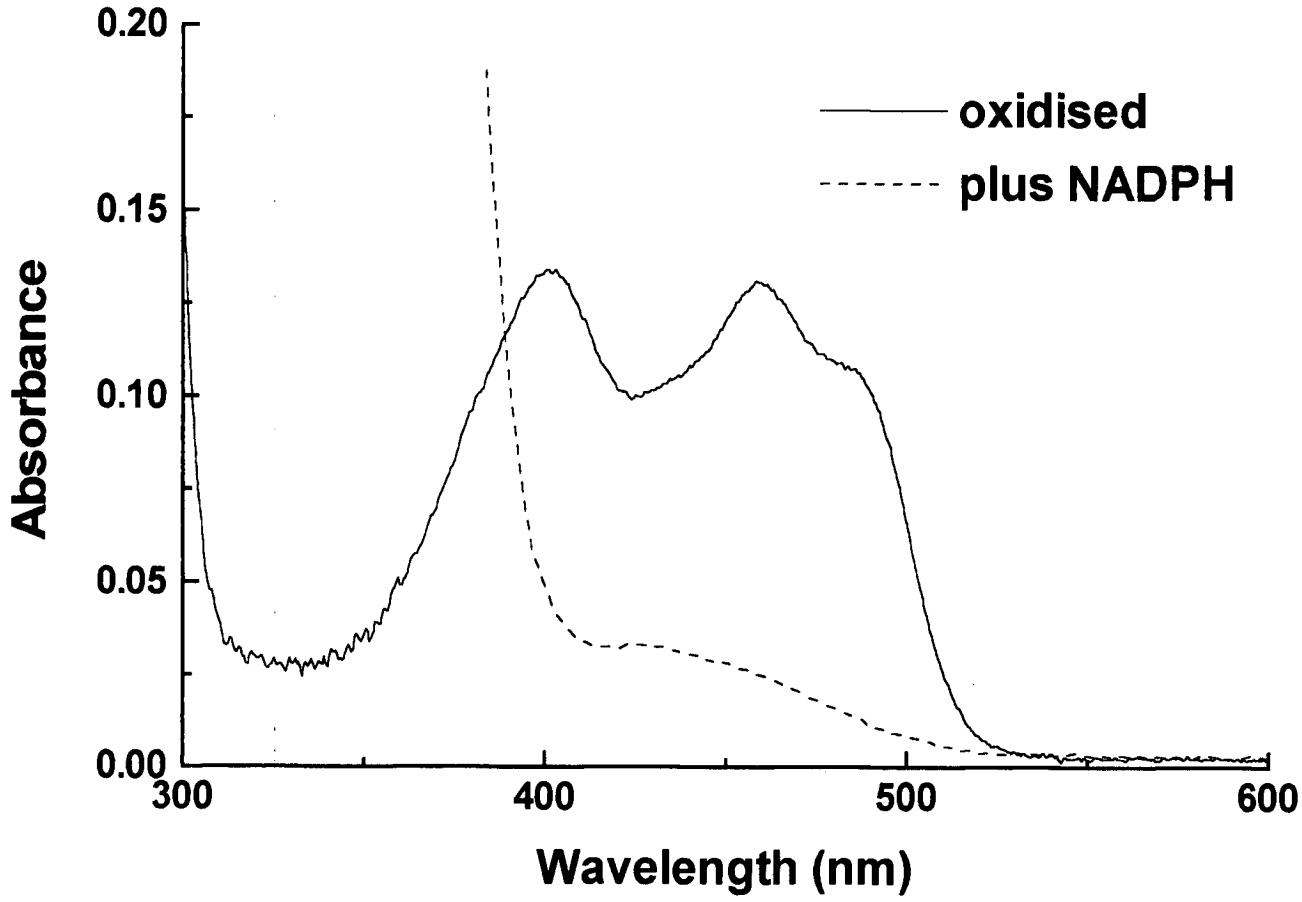


**Fig 3.3 UV/Vis spectra of wt FLDR**

Spectra was carried out as described in the *Materials & Methods* section.

The molecular weight of the expressed FLDR apoprotein was determined as 27648 Da by electrospray mass spectroscopy. This is 28 Da higher than the predicted molecular mass of 27620 Da calculated from the amino acid sequence derived from the database gene sequence (Bianchi *et al.* 1995) (less the N-terminal methionine). However, the recent solution of the atomic structure of the *E. coli* FLDR indicates that an arginine is present at position 126, as opposed to a glutamine predicted from the gene sequence (Ingleman *et al.* 1997). The difference in molecular mass of these two residues is exactly 28 Da, corresponding to the apparent discrepancy. The *fldr* gene was sequenced by Sanger dideoxy chain termination method and this also confirmed that arginine was present at position 126 and not glutamine.

FLDR is bright yellow in its oxidised form and it is converted to a neutral blue semiquinone by the addition of one reducing equivalent. FLDR has an extinction coefficient of 7100 $M^{-1}cm^{-1}$ at 456nm (Jenkins & Waterman 1993). The oxidised FLDR had flavin absorbance maxima at 456nm and 400nm, with a shoulder on the longer wavelength band at 483nm see fig 3.3. Based on the 7.41-fold purification value calculated using flavin absorbance at this wavelength, the overexpressed FLDR comprises 13.5% of the total soluble protein in the *E. coli* extract.

## NMR Spectrscopy

2-D HSQC spectra was carried out on $^{15}N$ labelled FLDR (0.33mM), NADH (20mM) and flavodoxin (20mM) were titrated in separately. A shift in some peaks was observed, when both FLD and NADPH were titrated into FLDR.

## Enzyme activities

Purified FLDR shows NADPH-dependent reductase activity towards a variety of electron acceptors (Table 3.2). In previous studies a buffer of 100 mM sodium phosphate (pH 7.5) was used. However, we established in the current study that interaction with the cytochrome was primarily electrostatic and was enhanced at lower ionic strength, being optimal at 10 mM sodium phosphate (pH 7.5) (assay buffer).

**Table 3.2 Steady-state kinetic parameters for FLDR.**

Rates of reduction of artificial electron acceptors were measured at 550nm for cytochrome *c* (22640 $M^{-1}cm^{-1}$) and 420nm for potassium ferricyanide (1010 $M^{-1}cm^{-1}$). Rates were measured at 30°C in 10mM sodium phosphate buffer (pH 7.5) with saturating (200 μM) NADPH. The $K_m$ for NADPH was determined under conditions of saturating cytochrome *c* (200 μM). The $K_m$ for the FLD was determined under conditions of saturating cytochrome *c* and NADPH, with the FLDR at 16.65 nM.

| Substrate | $k_{cat}$ (mol/min/mol) | $K_m$ (μM) |
|---|---|---|
| Potassium ferricyanide | 673.9 ± 16.3 | 3.95 ± 0.54 |
| Cytochrome c | 340 ± 7 | 17.6 ± 2.15 |
| NADPH | ---- | 3.85 ± 0.5 |
| FLD | ---- | 6.84 ± 0.68 |

Using cytochrome *c* (horse heart) as the acceptor, a $k_{cat}$ of 340± 7 mol/min/mol and a $K_m$ of 17.6 ± 2.15 μM were measured using homogeneous FLDR at 30°C in 10mM sodium phosphate buffer (pH 7.5). With saturating cytochrome *c*, the $K_m$ for NADPH was estimated at 3.85 ± 0.5 μM. Under similar conditions, potassium ferricyanide was reduced with a $K_m$ of 3.95 ± 0.54 M and a $k_{cat}$ of 673.9 ± 16.3 mol/min/mol. Purified FLD acts as a single electron shuttle and is able to stimulate the rate of FLDR-dependent cytochrome *c* reduction approximately 6-fold under the above conditions. With saturating cytochrome *c* (200μM) and FLDR at 16.65 nM, a Michaelis curve was obtained for the stimulation of cytochrome *c* reductase activity by FLD indicating an apparent $V_{max}$ of 272 ± 11.5 mol/min/mol and an apparent $K_m$ of the FLD for the FLDR of 6.84 ± 0.68 μM.

## Stopped-flow characterisation

Investigations of the rates of reduction of FLDR (40 μM) with NADPH (4 μM – 2 mM) were performed with measurement of the rate of decrease in absorbance at 456nm, the oxidised FLDR absorbance maximum. The rate observed was 21± 2 $s^{-1}$,

regardless of the concentration of NADPH. A similar value was obtained when the concentration of FLDR was altered.

Attempts to measure the rate of electron transfer between NADPH-reduced FLDR and FLD (following the formation of FLD semiquinone at 583nm) proved difficult under aerobic conditions due to the slow rate of this process and the relatively rapid reoxidation of the FLDR. To solve this problem, solutions were degassed and made up anaerobically prior to performing the stopped-flow experiments. The rate of formation of FLD semiquinone was seen to be very slow when reduced FLDR (40 μM) was mixed with FLD (20μM). Over the first 60 seconds, a single exponential rate of only $(3.4 \pm 0.2) \times 10^{-2}$ $s^{-1}$ was recorded in the presence of 2mM NADPH.

## Cytochrome P-450 reduction

Miss Lisa McIver also analysed the nature and kinetics of the reduction of cytochrome P-450 by the FLDR/FLD system. The ability of these flavoproteins to support the oxidation of arachidonic acid by the haem domain of flavocytochrome P-450 BM3 was studied by Miles *et al.* ( 1992). The FLDR/FLD system proved able to transfer electrons to the P-450. At concentrations of 0.762 μM P-450, 0.25 μM FLDR and 25 μM FLD, a rate of 5.48 ± 0.95 mol arachidonic acid oxidised/min was measured. Data were collected from three sets of fatty acid oxidation assays in which the P-450 was maintained at one of three different concentrations (0.76 μM, 2.54 μM or 3.81 μM), FLD was kept constant at 25 μM (4-fold in excess of its apparent $K_m$ for FLDR) and FLDR was varied between 0.25 μM and 10 μM. The plots of the reciprocal rates of these data *v.* the reciprocals of the [FLDR]. The lines plotted were parallel (not convergent) indicates that the P-450 reduction mechanism is ping-pong in nature, rather than involving a ternary complex between the P-450, FLDR and FLD.

## Potentiometric titrations

The absorbance *v.* potential data is fitted in figure 3.4 to an equation (equation 1) comprising the sum of one 2-electron redox function designed to model the absorbance of a flavin passing through 3 different oxidation states.

$$\text{Flavin absorbance} = \frac{a10^{(E-E'_1)/59} + b + c10^{(E'_2-E)/59}}{1 + 10^{(E-E'_1)/59} + 10^{(E'_2-E)/59}}$$

**Equation 1**: a, b, c ≡ absorbance coefficients for oxidised, semiquinone and reduced flavin, respectively. E ≡ electrode potential; $E'_1$, $E'_2$ ≡ midpoint potentials for the semiquinone/reduced couple and the oxidised/semiquinone couple, respectively.

**Figure 3.4 a plots the proportion of FLDR oxidised based on the sum of the absorbance values between 440nm and 480nm against the potential of the enzyme solution.**

**Figure 3.4 b the redox titration of the *E. coli* FLDR at *ca* 72μM monitored by UV/Vis spectrophotometry between 350 and 800nm.**

The 1st electron reduction of FLDR does not result in the accumulation of a stable semiquinone intermediate with long wavelength absorbance. Thus potentiometric data for both 1st and 2nd electron reductions are determined from the continuous decrease in absorbance between 440-480nm. Using absorbance between 440-480nm fitted to Equation 1. From these data $E'_1$ (ox/sq) = -308 ± 4 mV and $E'_2$ (sq/red) = -268 ± 4 mV.

Fig 3.4 a

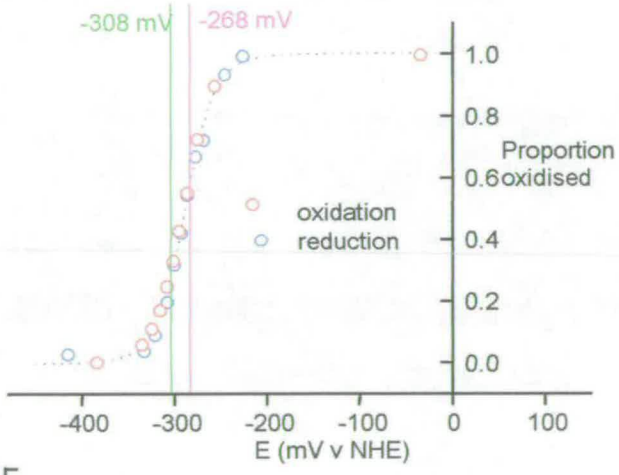


Fig 3.4 b

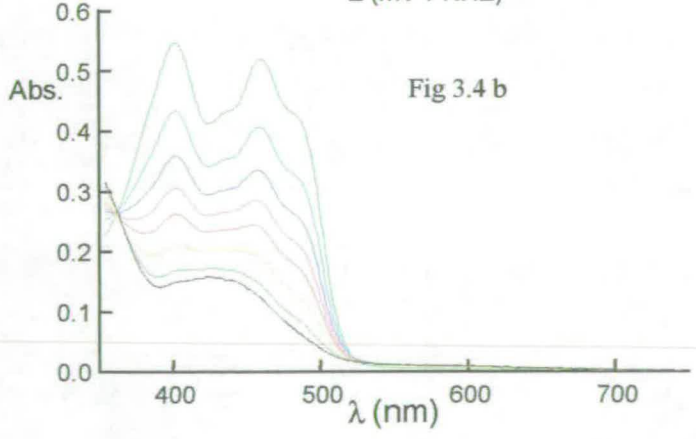

Lisa McIver carried out further redox titration studies, of interest, which will be reported here. The redox titration of FLDR was carried out in the presence of a saturating concentration (5mM) of 2' adenosine monophosphate (2' AMP), in order to investigate the effects of binding of a nucleotide analogue to the NADPH site on the redox properties of the FAD in FLDR. 2' AMP is non-redox active and thus can be used to in reductive titrations to mimic the effects of binding of $NADP^+$ on the FAD redox properties. In preliminary experiments, the affinity of 2' AMP for FLDR was estimated by measurement of its $IC_{50}$ (~ 1mM) for FLDR-mediated cytochrome *c* reduction. The concentration of 5mM used in the titration was based on this result. An increase in the reduction potentials of both the oxidised/semiquinone ($E'_1$ elevated by 15mV to -293 ± 6mV) and semiquinone/reduced ($E'_2$ elevated by 38mV to -230 ± 7mV) couples of FLDR was observed in the presence of 2' AMP (table 3.3). Lisa McIver also determined the redox potential of FLD, FLDR's redox partner. Values for the reduction potentials of FLDR and FLD flavins are collected in table 3.3

**Table 3.3 Redox potentials**

Midpoint reduction potentials (E' in mV) for the flavin cofactors in purified *E. coli* FLDR ($NADP^+$ flavodoxin oxidoreductase) and FLD (flavodoxin), calculated from electrode potential *v.* absorbance data. $E'_{12}$ refers to the midpoint potential for the 2-electron reduction of the flavins in each protein, while $E'_1$ and $E'_2$ refer to the midpoint reduction potentials for the ox/sq and sq/hq couples, respectively, for FLD and FLDR. The values for FLD and FLDR are compared with the values for free FAD and FMN (Massey 1991, Draper & Ingraham 1968).

| | $E'_{12}$ | $E'_1$ | $E'_2$ |
|---|---|---|---|
| FLDR FAD | -288 ± 4 | -308 ± 4 | -268 ± 4 |
| FLDR FAD (+2′ AMP) | -261 ± 6 | -293 ± 6- | 230 ± 7 |
| FLD FMN | -343 ± 6 | -254 ± 5 | -433 ± 6 |
| FREE FAD | -207 | ----- | ----- |
| FREE FMN | -205 | -172 | -238 |

## Discussion

The reduction potentials for the flavins in the flavodoxin $NADP^+$ reductase (FLDR) have not been previously reported. An understanding of the FLD and FLDR system is central to our understanding of the roles these flavoproteins play in electron-transfer to the various systems in *E. coli* for which they are essential. These systems include cobalamin-dependent methionine synthase, biotin synthase anaerobic ribonucleotide reductase and pyruvate formate lyase.

The quantities of pure FLDR and FLD recovered in our expression system are considerably higher those reported previously (Jenkins & Waterman 1993, Bianchi *et*

*al.* 1995). The high levels of expression achievable with the T7 polymerase/promoter system, coupled with efficient purification regimes (including a 2', 5'-ADP Sepharose affinity step for FLDR) facilitate good recovery. Protein purification data indicate that the FLDR can be overexpressed to at least 10% of total cell protein without notable detrimental effects on cell growth. However, it was noted that transformants of the *fldr* gene in the faster growing BL21 (DE3) strain yielded protein with considerably lower specific activity than that from HMS174 (DE3). This is possibly due to failure of the cells to match FAD synthesis and/or incorporation to the production of FLDR apoenzyme with strong induction under fast growth conditions.

It is worthy of note that *E. coli* FLDR is capable of reduction of cytochrome *c* in the absence of flavodoxin or alternative protein mediators. This has not been reported previously. However, the rate is elevated by the presence of *E. coli* FLD. In a recent publication, Jenkins and co-workers (Jenkins *et al.* 1997) reported the kinetics of cytochrome *c* reduction with the *Anabaena variabilis* flavodoxin $NADP^+$ reductase/flavodoxin system. In this system, there is negligible flavodoxin-independent cytochrome *c* reduction by the *Anabaena* FLDR. However, the cytochrome *c* turnover number of $1200min^{-1}$ for the *Anabaena* FLDR/FLD system is much higher than that of its *E. coli* homologue reported here. From stopped-flow studies, the first reduction of cytochrome *c* by reduced FLDR can occur at up to 1740 $min^{-1}$ compared with only 339 $min^{-1}$ during steady state. Clearly, the reduction of cytochrome *c* by FLDR is rate-limited by processes other than its binding and the transfer of an electron to the ferric haem.

The mass of the FLDR shows a discrepancy of 28 Da from that predicted by translation of the determined nucleotide sequence (Bianchi *et al.* 1995). The recently determined atomic structure of FLDR (Ingleman *et al.* 1997) indicated the presence of an arginine as opposed to a glutamine residue at position 126. The difference in mass between these two residues is precisely 28 Da; thus our data indicate that the discrepancy is in the DNA sequence and not the atomic structure, and that residue 126 is an arginine. It is worthy of note, also, that the mass determined for FLDR

indicate that insignificant proportion of the purified protein retains its initiator methionine residue, and that there are no covalent modifications of the flavoprotein in the homologous host.

Very good NMR data was obtained for $^{15}$N-FLDR. Although FLDR is a relatively large protein in NMR terms. When NADPH was added to FLDR some peaks were seen to shift, some of these peaks were inferred to be arginines from their chemical shift and the nitrogen dimension. Shifts in other peaks were seen when FLD was added to $^{15}$N-FLDR, again some of these peaks were inferred to be arginines from the chemical shift and the nitrogen dimension. However, these peaks could not be assigned to specific arginine residues as a full structure determination of FLDR by NMR has not been carried out. Movement was also seen in other peaks when FLD and NADPH were added, however it was not possible to identify the corresponding residues. When the crystal structure was examined three arginines residues, R144, R174 and R184 were proposed to be present in the NADPH binding site (Ingleman *et al.* 1997). As mentioned previously citrate present in the crystallisation buffer had precipitated in the proposed NADPH binding site, and FLDR has not been co-crystallized with NADPH. Three other arginine residues, R236, R237 and R238 are clearly visible on the surface of FLDR, and these form a positive patch which can be inferred to be a potential docking site for flavodoxin, as flavodoxin is one of the most negatively charged proteins known. Ingleman *et al* (Ingleman *et al.* 1997) have suggested that the residues R236, R237 and R238 of FLDR would be able to dock FLD. All these arginine residues clearly warrant further exploration into their role in the interaction with both FLD and NADPH, and the results of our investigations are discussed in the next chapters.

Lisa McIver collected potentiometric data for *E. coli* flavodoxin, and it was demonstrated that FLD stabilises a neutral blue semiquinone form of FMN. The FLD hydroquinone cannot be proposed as a realistic electron transferase to the biotin synthase enzyme or cytochrome P-450; since the midpoint reduction potential for the sq/hq couple is some 100mV more negative than that of the NADPH/NADP$^+$ couple (and 165mV and 125mV more negative than those of the FLDR ox/sq and sq/hq

couples, respectively). The midpoint reduction potential values for the FLD (-254mV [ox/sq] and -433mV [sq/red]) are similar to those obtained from non-recombinant *E. coli* FLD and flavodoxins from other species (Skyes & Rogers 1984). Repeats of the FLDR titration in the presence of a saturating concentration of 2' AMP indicated that the midpoint potentials of both the ox/sq and sq/red couples are elevated by binding this nucleotide analogue and that $E'_{12}$ is increased by 27mV from -288 ± 4 mV to -261 ± 6 mV, respectively. The effect of bound nucleotide analogue is similar to that observed previously for the homologous FAD-containing enzymes adrenodoxin reductase (Lambeth & Kamin 1976) and cytochrome $b_5$ reductase (Iyganagi 1977) and indicates that the binding of $NADP^+$ to FLDR may exert an important controlling influence on the catalytic properties of the enzyme. The elevation of both of the reduction potentials of FLDR places them even closer to that of the ox/sq couple of FLD and decreases further the driving force for electron transfer to FLD. This may at least partially explain the very slow rates of electron transfer measured between FLDR and FLD using stopped-flow spectrophotometry. Though it is possible that when FLD and FLDR interact their ox/red midpoint potentials may shift to make electron transfer more favourable. A study of two electron transfer partners isolated from *Paracoccus denitrificans*, a pyrroloquinoline quinone containing enzyme methylamine dehydrogenase, and the copper containing electron carrier amicyanin (Gray *et al.* 1988), demonstrated a changed ox/red midpoint potential when they were measured while complexed together. The oxidation-reduction midpoint potential ($E_m$) of methylamine dehydrogenase was found to be +100mV, and the $E_m$ for amicyanin was +294mV. Amicyanin serves as an electron shuttle between methylamine dehydrogenase and cytochrome $c_{551}$. However, the $E_m$ value of cytochrome $c_{551}$ is +190mV, suggesting that this reaction is thermodynamically unfavourable. Complex formation of amicyanin with methylamine dehydrogenase shifted the oxidation-reduction midpoint potential of amicyanin by 73mV, from +294 to +221mV, making electron transfer from amicyanin to cytochrome $c_{551}$ thermodynamically possible.

The potentiometric data have important implications for the mechanism of the reduction of cytochromes P-450 (and other enzyme systems). They indicate that

(unless there is a very large increase in the FLD sq/hq couple caused by binding of FLD to P-450) the 2 electrons required for P-450 catalysis must be delivered through 2 consecutive single electron-transfers from FLD sq; as opposed to the first FMN-to-haem electron transfer being mediated by FMN hq and the second by FMN sq. This raises the question as to whether these transfers occur in a ternary complex of FLDR/FLD/P-450 or through a ping-pong mechanism in which the FLD may interact firstly with the FLDR and secondly with the P-450. The fact that the flavins in both proteins are relatively exposed, suggests that electron transfer between them is likely to be through close approach of the isalloxazine rings, as opposed to involving a protein pathway (Bianchi *et al.* 1995, Hoover & Ludwig 1997). The atomic structure of a eukaryotic P-450 reductase also indicates that the edges of the FAD and FMN ring systems in this protein are only 4Å apart and that inter-flavin electron transfer must occur without mediation by any amino acid side chains (Wang *et al.* 1997). Thus, it appeared most likely that reduced FLDR and FLD would dock, an electron would be transferred to form the FLD sq and the FLD would then dissociate from the FLDR and associate with a P-450 to reduce this enzyme, again *via* the exposed FMN. The ping-pong kinetic properties of the FLDR/FLD/P-450 BM3 haem domain system are consistent with this model, suggesting that the FLD acts as a shuttle between FLDR and the P-450, as opposed to the three proteins forming a ternary complex for electron transfer.

The data presented here clearly define the electron-transfer route through this system as NADPH → FLDR (FAD) → FLD (FMN) and then onto other enzyme partners. This is a similar flavin electron-transfer path to that described previously for the *E. coli* sulfite reductase and for the diflavin reductases of cytochromes P-450 (P-450 reductase or CPR) and nitric oxide synthase (Abu-Soud *et al.* 1994). In fact, the FLDR and FLD proteins show structural homology to the FAD and FMN domains of CPR (Porter 1991), and these domains have been expressed independently for both a eukaryotic P-450 reductase and the reductase of flavocytochrome P-450 BM3 - a natural CPR/P-450 fatty acid hydroxylase fusion protein (Smith *et al.* 1994, Govindarj & Poulos 1997). However, it is of particular interest to note here that the FAD and FMN domains of P-450 BM3 show very different redox characteristics to

FLDR and FLD; with the blue semiquinone being formed on the FAD domain of P-450 BM3 (Daff *et al.* 1997). In P-450 BM3, the FAD hydroquinone is thermodynamically unfavourable, compared the FMN of FLD in the *E. coli* system. In all three systems the high and low potential flavins are the FMN and FAD, respectively. However, both the $E'_1$ and $E'_2$ values for FLDR are considerably less negative than those for the related reductases. Also, the ox/sq and sq/red couples for FLD are both more negative than those for the BM3 (Daff *et al.* 1997) and CPR (Iyanagi1974) systems. Indeed, the sq/red couple of FLD has a very negative potential (-433mV) which makes electron-transfer *via* an NADPH-driven system virtually impossible. The results indicate that the overall driving force (*i.e.* the difference in reduction potential) for single electron-transfer from NADPH-reduced FLDR to oxidised FLD is considerably less than those for CPR and BM3. In addition, the binding of nucleotide ($NADP^+$) to FLDR may result in further increase in the flavin reduction potentials (as we have shown with 2′ AMP) and decrease further the driving force for electron transfer to FLD. Our stopped-flow data are consistent with these findings. The rate of reduction of FLDR ($20s^{-1}$) is markedly slower than that seen in the P-450 BM3 system ($> 700s^{-1}$) and the reduction of FLD by reduced FLDR is also very slow ($0.034\ s^{-1}$).

These results are published (McIver *et al* 1998), a copy of the publication forms appendix of this thesis.

# Chapter 4 (FLDR)

# Investigation into the binding site of NADPH in flavodoxin $NADP^+$ reductase

## Introduction

The aim of this study is to gain insight into the interaction between FLDR and NADPH. FLDR has not been co-crystallised with $NADP^+$/NADPH or any anlogues. However, citrate has been found bound in a site proposed to accommodate the adenine ribose of NADPH (based on homology with the spinach FNR) (Ingleman *et al.* 1997, Karplus *et al.* 1991). On the basis of modelling three arginine residues, R144, R174 and R184 have been proposed to bind the 2′ –phosphate of NADPH. The amino acid R174, is a conserved residue described as part of a "fingerprint" region for $NADP^+$-binding members of the FNR (ferredoxin reductase)-like family of flavoenzyme (Correll *et al.* 1993). In this project we wanted to elucidate the roles of these positively charged residues, R144, R174 and R184 in the interaction with NADPH, and in the transfer of hydride ions from the reduced pyridine dinucleotide to generate the FAD hydroquinone. We also want to investigate the relative importance of each of these residues in the interaction with the pyridine nucleotide and the distinct roles that each of these residues plays in the discrimination between NADPH/NADH, and in the catalysis of electron transfer from NAD(P)H to flavin and on to an electron acceptor (cytochrome *c*). To achieve this we decided to mutate each of these residues (R144, R174, R184) from arginine to alanine, and examine the effects of charge neutralisation in the putative NADPH binding site.

## Results

### Mutagensis and cloning of R144A, R174A and R184A

The wild-type *fldr* gene was expressed under the control of an IPTG-inducible T7 promoter in pCL 21, in the cell line HMS173(DE3) as reported in chapter 3. For the generation of mutants R144A, R174A and R184A, the *fldr* gene was sub-cloned into pUC 18/RBS (Yanisch-Perron *et al.* 1985) using *Nco* I and *Bam* HI restriction sites. Site-directed mutagenesis was performed using the "mega-primer" PCR method (Sarkar & Sommers 1990) using vector forward (5′ CGC CAG GGT TTT CCC

AGT CAC G 3′) and reverse (5′ GTT GTG TGG AAT TGT GAG CGG 3′) oligonucleotides, and the following mutagenic primers:

R144A: 5′ CAC GCG GCC GCC TAT GCC GCC GAC 3′
R174A: 5′ GTG GTC AGT GCA GAA ACG GCA GCG 3′
R184A: 5′ CTC ACC GGC GCC ATA CCG GCA TTA 3′

The bases underlined in each primer indicate the position at which the arginine codon is replaced by one encoding an alanine. Mutated *fldr* genes were digested with *Nco*I and *Bam*HI and re-cloned into pUC 18/RBS (Yanisch-Perron *et al.* 1985), to form plasmids pCL22(pUC18/RBS/*fldr*R144A), pCL23 (pUC18/RBS/*fldr*R174A), pCL24 (pUC 18/RBS/*fldr*R184A). The *E. coli* strain TOP10 One Shot™ (Invitrogen) was used for transformation of the mutant ligation mixes. Mutant clones were sequenced by the Sanger dideoxy chain termination method to establish that secondary mutations had not occurred, and expressed in strain C6007, which is deficient in the host *fldr* gene (Bianchi *et al.* 1995) which was a kind gift from Vera Bianchi (Department of Biology, University of Padua, Pauda, Italy).

## Protein expression and purification

Wild-type and mutant FLDRs were successfully overexpressed in *E. coli* and purified to homogeneity in two column chromatography steps (Q-Sepharose and 2′, 5′-ADP Sepharose). The expression of mutant forms from plasmids pCL22-24 under the *lac* promoter system in the background of strain C6007 (*fldr*$^-$) (Bianchi *et al.* 1995) was not as high ≥ 2 mg of pure enzyme/litre of cells (~ 2 % of total cell protein) as that obtained for the wild-type under the T7-promoter from plasmid pCL21, necessitating purification from a larger *E. coli* transformant cell mass (10 - 20 l *vs.* 2 l for wild-type FLDR). However, the use of strain C6007 guaranteed lack of contamination with the wild-type FLDR, which is normally expressed naturally at high levels. The purity of the mutant and the wild-type proteins were anaylsed by SDS-PAGE (Fig. 4.1).

**Fig 4.1 SDS-PAGE gel of purified wt and mutant (R144A, R174A and R184A) of *E.coli* FLDR**

Lane 1: Molecular weight standards (94000, 67000, 43000, 30000, 20100, 14400 Da), Lane 2: Pure wild-type FLDR, Lane 3: Pure R144A FLDR, Lane 4: Pure R174A FLDR, Lane 5: Pure R184A FLDR, Lane 6: Molecular weight standards (as lane 1).

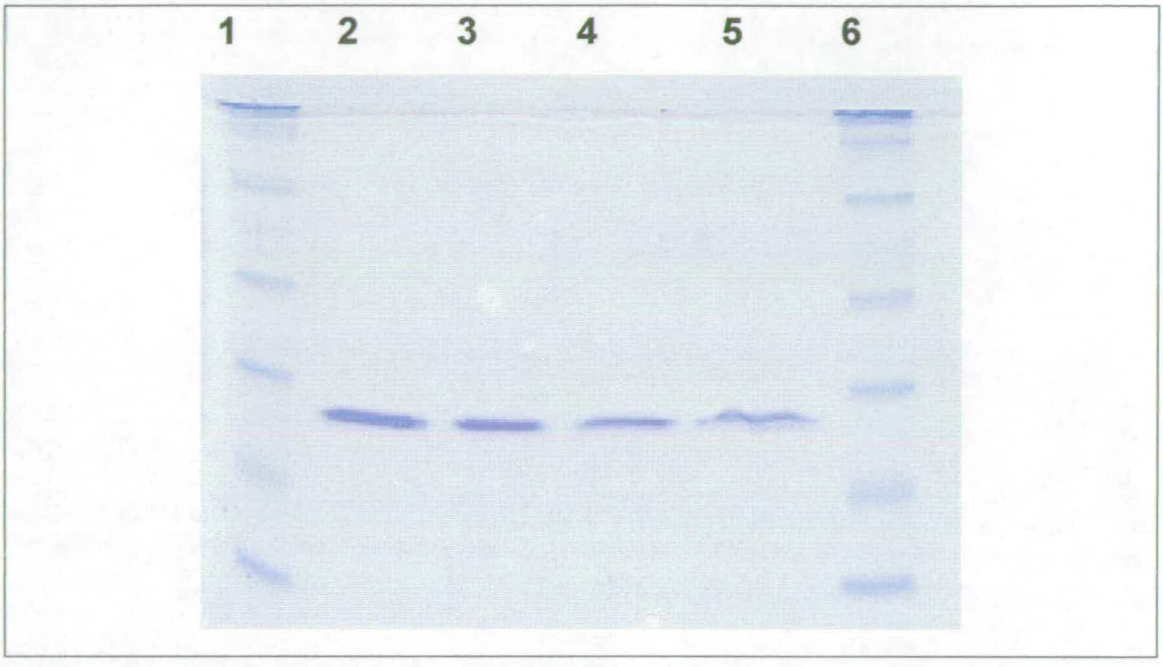


The stability of the FLDR proteins enabled the collection of high resolution mass spectrometric data, confirming the isolation of homogeneous, non-proteolysed protein. Mass spectrometric data was obtained for wt and the mutants of FLDR, confirming the predicted molecular weight analysis. Fig 4.2 shows an example of the mass spectrum data collected, table 4.1 shows the predicted and obtained molecular weights for wt and mutants FLDR.

**Fig 4.2 Typical ESMS spectrum of a purified FLDR enzyme.**

The mass spectrum shown is that of mutant R174A. The inset shows the total ion count of all ions in the m/z range 500 to 2000 (peaks at 785.3, 788.4, 811.7, 836.2, 862.2, 890.1, 919.7, 951.2, 985.2, 1021.7, 1060.9, 1103.3, 1149.3, 1199.3, 1253.7, 1268.7, 1313.3, 1329.2, 1379.0, 1395.5, 1451.4, 1468.5, 1532.1, 1550.2, 1622.0, 1641.5, 1723.3, 1744.1, 1838.3 and 1969.3). The molecular mass of FLDR R174A (27 558.5 Da).

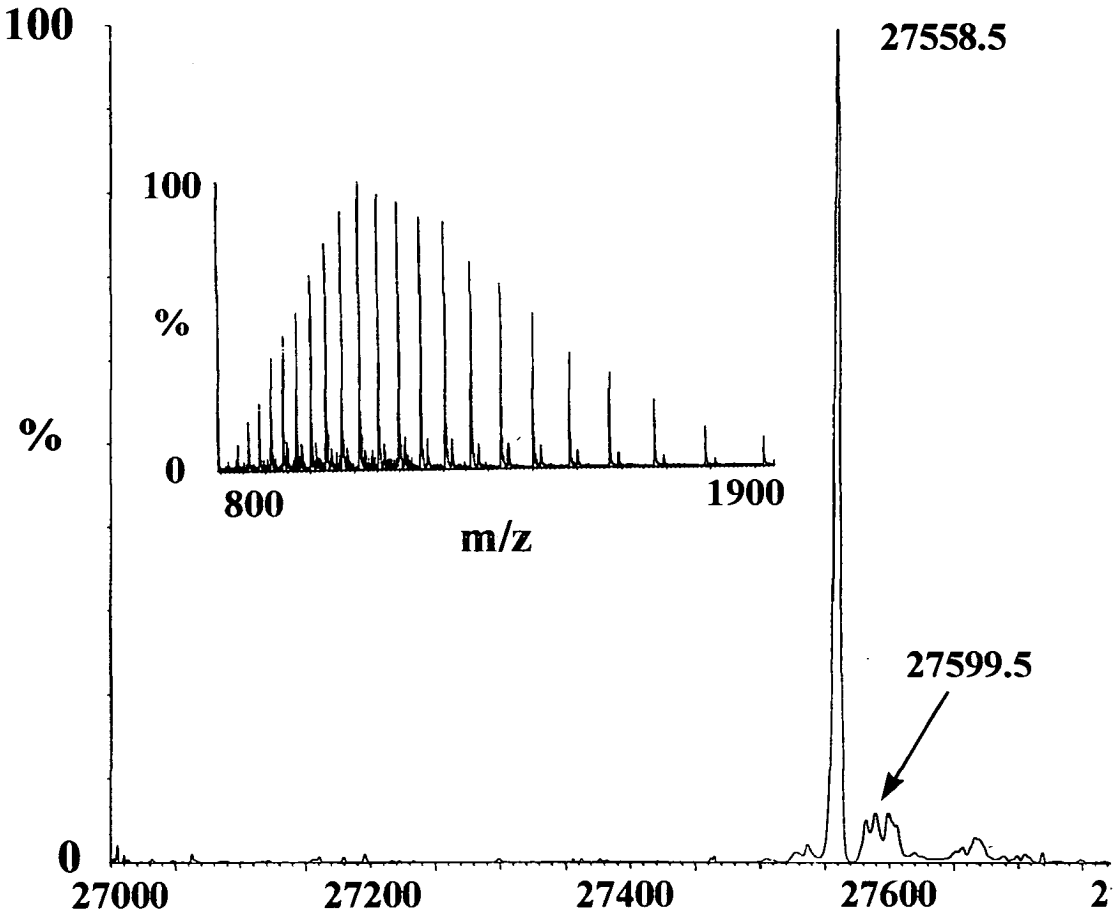

**Table 4.1 Predicted and obtained mass by ES-MS for wt and mutant FLDR**

| | Predicted Mass (Da) | Obtained Mass (Da) |
|---|---|---|
| Wt | 27 647 | 27 641 |
| R144 | 27 562 | 27 552 |
| R174 | 27 562 | 27 558 |
| R184 | 27 562 | 27 554 |

## Spectroscopic characterisation

### UV-visible spectrophotometry

Wild-type and mutant FLDRs have essentially identical visible absorption spectral characteristics, with absorbance maxima at 456nm and 400nm, and a shoulder on the longer wavelength band at 483nm (Fig. 3.3, chapter 3). The far UV absorption maxima are at 280 nm for all forms. The ratio of absorbance at 280 nm/456 nm (protein/flavin) is 6.5 ± 0.2 for both wild-type FLDR and mutants. Occasional pure preparations of mutants had slightly lower flavin content. However, preparations always contained > 85 % holoenzyme and those used for kinetic studies contained > 95 % flavin.

### CD spectroscopy

Wild-type and mutant FLDRs had very similar far UV CD spectra, exhibiting a negative Cotton effect from 202 nm to ~ 250 nm, and positive ellipticity at wavelengths lower than the abcissa at 202 nm. The mimimum is at ~ 215 nm for all FLDRs. The visible CD spectra of the proteins were also very similar, showing positive ellipticity in the region of the first flavin visible absorption band (385 nm) with a peak at 388 nm and a less intense band of negative ellipticity in the region of the second flavin visible band (456 nm), centred at 454 nm (Fig. 4.3). In the near UV region, all FLDRs exhibit a very strong, sharp signal of positive ellipticity, centred at 272 nm. The intensity of the signal indicates that it may derive from stacking interactions between the FAD and one or more aromatic residues in FLDR. The R144A and R184A mutations do not alter significantly the intensity or position of this

near UV band. However, the intensity (but not position) of the band appears slightly lower in mutant R174A (Fig. 4.3), which also exhibits unusual aromatic amino acid fluorescence properties.

**Fluorescence spectroscopy**

The fluorescence properties of wild-type and mutant FLDRs were compared to probe further for effects on tertiary structure (aromatic amino acid fluorescence) and flavin environment (flavin fluorescence). Flavin emission (excitation 456 nm, emission 500 - 600 nm) from all FLDRs was low, due to strong quenching of the chromophore by the surrounding protein matrix. By comparison of the fluorescence of the FLDRs with that of free FAD under the same conditions, and with the knowledge of the quantum yield ($Q_f$) for FAD (0.032) (Harvey 1980), the $Q_f$ values for the FLDR-bound flavins were all measured to be < 0.001, *i.e.* negligible fluorescence. Using high flavoprotein concentrations (~ 0.5 μM) and wide slit widths (10 nm/10 nm excitation/emission on the Shimadzu instrument) the flavin emission maxima was found to be at 528 nm for both wild-type and mutant FLDRs.

Aromatic amino acid (primarily tryptophan) fluorescence (excitation 290 nm, emission 300 - 400 nm) was measured for wild-type and mutant FLDRs (0.05 μM) with excitation/emission slit widths set at 5 nm on the Shimadzu instrument. Emission spectra were of similar intensity and had similar emission maximum (328 nm) for wild-type and for R144A and R184A FLDRs. However, the emission from mutant R174A was of slightly greater intensity and was maximal at a longer wavelength (336 nm) (Fig. 4.4).

## Enzyme activities

The reduction of wild-type and mutant FLDRs by NAD(P)H, and the catalysis of cytochrome *c* reduction by the enzymes were investigated using steady-state and stopped-flow methods. All experiments were performed in 10 mM sodium phosphate buffer (pH 7.5) (assay buffer).

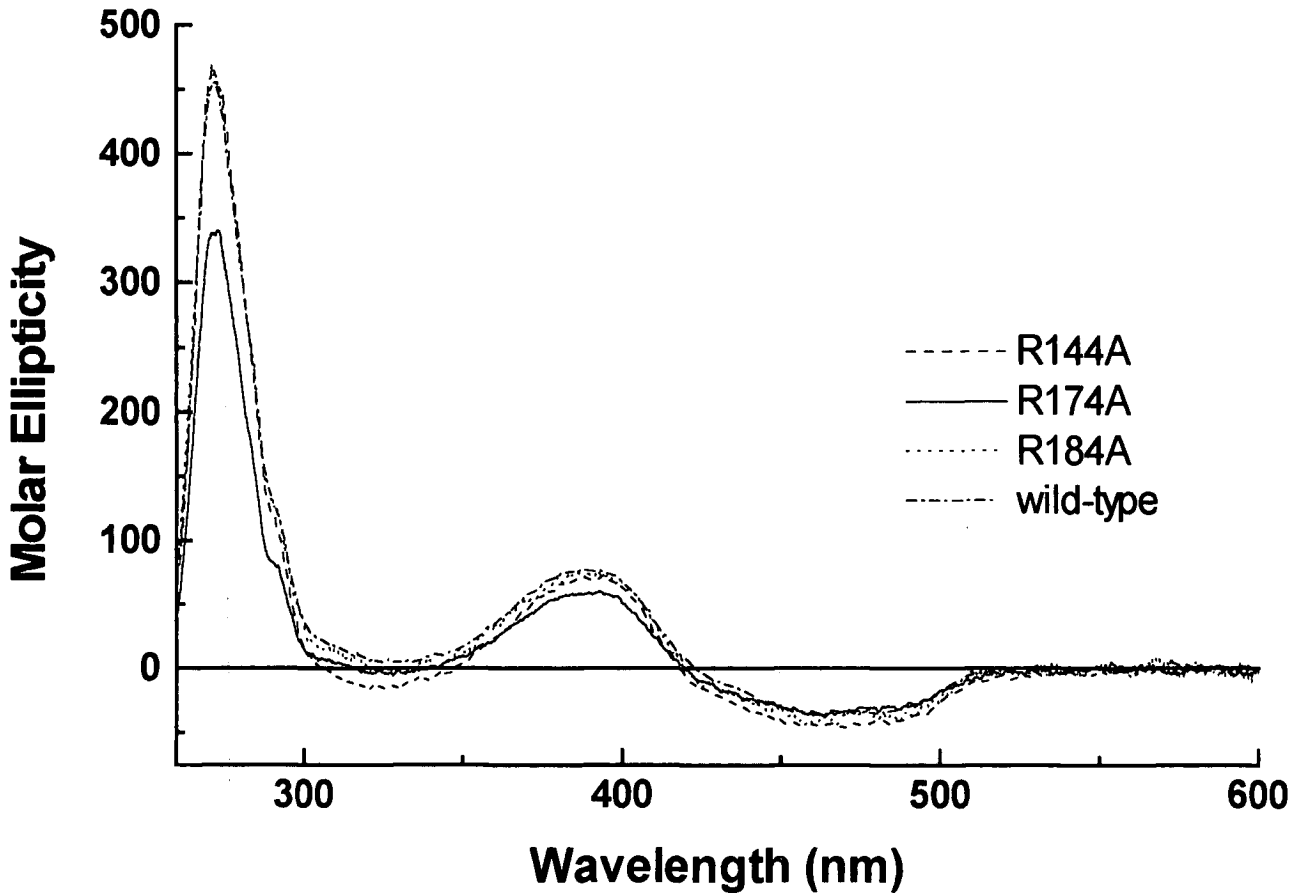


**Fig 4.3 Near UV-visible CD spectra of wt FLDR and mutants**

Wild-type (dotted-dashed line) and mutant forms (R144A - dashed line; R174A - solid line; R184A - dotted line) of *E. coli* flavodoxin reductase.

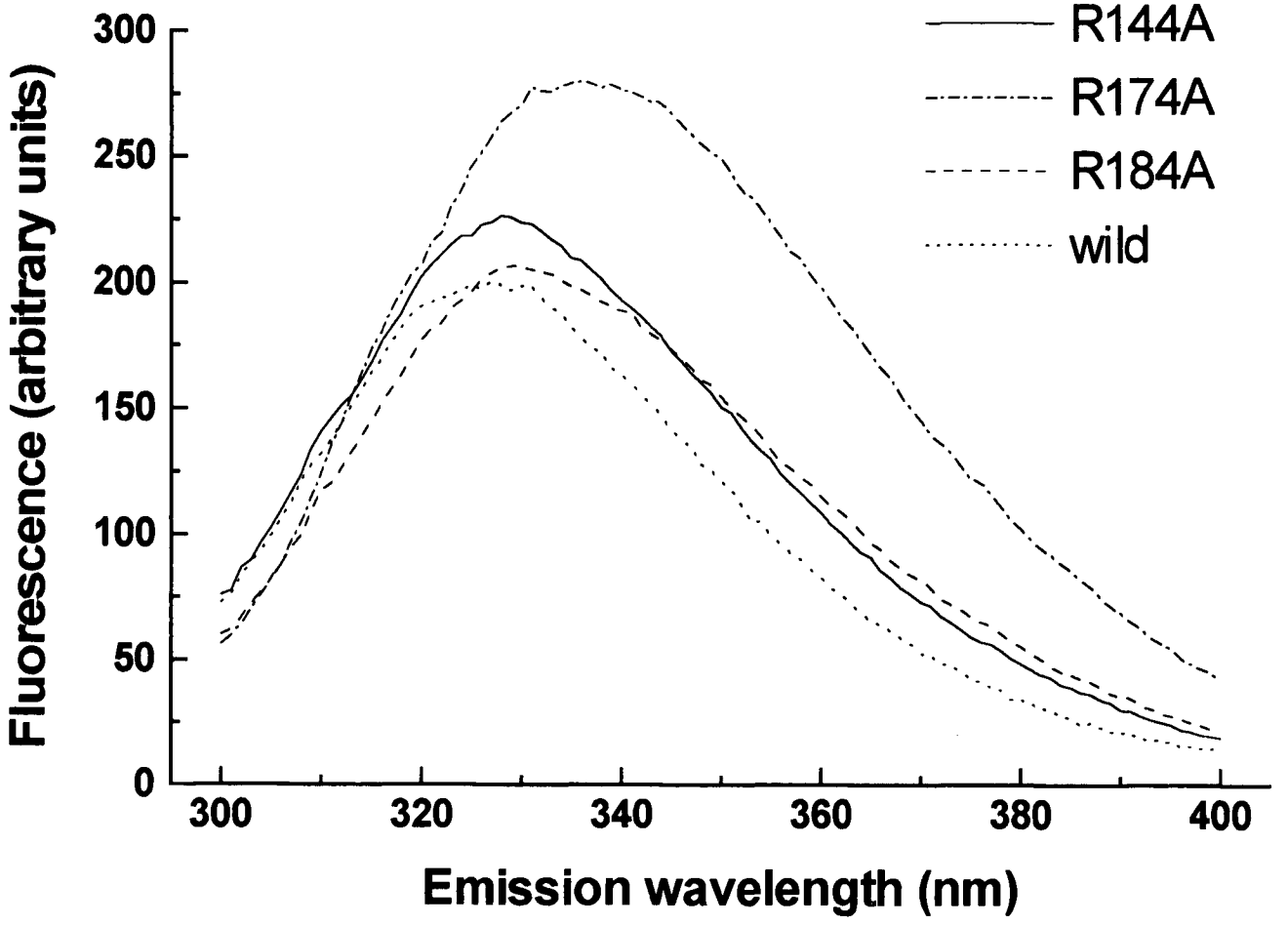


**Fig 4.4 Aromatic fluorescence spectra from wild-type and mutant (R144A, R174A and R184A) *E. coli* FLDR.**

Fluorescence spectra were measured as described in the *Materials & Methods* section.

## Steady-state kinetics

The steady-state kinetic behaviour of wild-type and mutant FLDR enzymes was investigated using cytochrome *c* as an electron acceptor and either NADPH or NADH as the donor. Preliminary experiments indicated that the $K_m$ for NADPH was ~ 4 μM and for NADH was ~ 2 mM. A set of experiments was performed with NADPH/NADH at saturating or near-saturating conditions (200 μM and 10 mM, respectively) and cytochrome *c* varied between 0-200 μM. With NADPH, wild-type FLDR catalysed cytochrome *c* reduction with a $k_{cat}$ of 338.9 ± 7.2 $min^{-1}$ and a $K_m$ of 17.6 ± 1.6 μM for cytochrome *c*. The $k_{cat}$ value was lower for mutants R144A and R174A, and their $K_m$ values were also higher. In particular, R174A had a $K_m$ of 64.8 ± 7.2 μM - almost 4 times that for wild-type FLDR. However, mutant R184A was a slightly superior cytochrome *c* reductase to wild-type FLDR, with a $k_{cat}$ of 384.1 ± 8.4 $min^{-1}$ and a $K_m$ of 16.7 ± 1.3 μM (Table 4.2).

With NADH as the donor, all $k_{cat}$ values were greatly reduced relative to NADPH (Table 4.2). The apparent $K_m$ values for cytochrome *c* were also markedly decreased (3.2 ± 0.19 μM [wild-type], 0.82 ± 0.04 μM [R144A], 5.9 ± 0.46 mM [R174A] and 4.4 ± 0.35 μM [R184A]), although this may indicate only that cytochrome *c* is able to saturate the FLDR at much lower concentrations due to constraints on catalytic activity imposed by the use of NADH as the reductant. However, the $k_{cat}$ values for mutants R174A and R84A with NADH are both higher than that for wild-type, while R144A has a lower $k_{cat}$ value (Table 4.2).

With cytochrome *c* maintained at a saturating concentration (200 μM), the $K_m$ values for NAD(P)H were also determined by steady-state kinetic analysis. As expected, wild-type FLDR had the lowest $K_m$ for NADPH (3.9 ± 0.3 μM). Mutant R184A was the most affected in affinity for NADPH ($K_m$ = 54.4 ± 6.0 μM) (Table 4.2). The $K_m$ for NADH was also much greater for mutant R144A and R174A than for wild-type FLDR (2.0 ± 0.15 μM). However, affinity for NADH was slightly enhanced in mutant R184A ($K_m$ = 1.6 ± 0.2 μM) (Table 4.2).

**Table 4.2 Steady-state kinetic parameters for cytochrome *c* reduction with NAD(P)H by wild-type, R144A, R174A and R184A mutants of *E. coli* FLDR.**

| | $K_m$ NADPH (μM) | $K_m$ NADH (mM) | $k_{cat}$ ($min^{-1}$) NADPH | $k_{cat}$ ($min^{-1}$) NADH | $k_{cat}/K_m$ NADPH ($\mu M^{-1}$ $min^{-1}$) | $k_{cat}/K_m$ NADH ($mM^{-1}$ $min^{-1}$) |
|---|---|---|---|---|---|---|
| wild-type | 3.86 ± 0.28 | 2.04 ± 0.17 | 339 ± 7.2 | 33.0 ± 0.35 | 87.8 ± 7.3 | 16.2 ± 1.6 |
| R144A | 5.3 ± 0.76 | 5.14 ± 0.51 | 237 ± 7.1 | 13.7 ± 0.12 | 44.7 ± 7.9 | 2.67 ± 0.31 |
| R174A | 20.2 ± 0.95 | 9.86 ± 0.79 | 153 ± 5.6 | 42.3 ± 1.4 | 7.6 ± 0.6 | 4.29 ± 0.53 |
| R184A | 54.4 ± 5.9 | 1.66 ± 0.22 | 384 ± 8.4 | 50.4 ± 1.1 | 7.1 ± 1.1 | 30.4 ± 5.4 |

## Stopped-flow kinetics

Stopped-flow absorption spectrophotometry was used to investigate the effects of mutations on the microscopic rate constants for the NAD(P)H-dependent flavin reduction step in the catalytic cycle. This was achieved by rapid mixing of wild-type and mutant FLDRs (at a fixed concentration between 10 – 40 μM) in one stopped-flow syringe with an excess of NADPH (100 μM - 10 mM) or NADH (100 μM - 25 mM) in the other syringe, and monitoring the rate of hydride transfer from NAD(P)H to reduce the FAD to its hydroquinone form by following the absorbance change at 456 nm.

*NADPH*

With wild-type FLDR, negligible variation in the rate of NADPH-dependent reduction ($k_{red}$) of FLDR (34 μM) was seen between 10 μM and 10 mM reductant. FLDR was reduced at 22 $s^{-1}$ and the $K_m$ was clearly < 5 μM. A similar phenomenon ($K_m$ < 5 μM) was observed with mutant R174A, with reduction rate constant over the entire NADPH concentration range. However, $k_{red}$ was considerably lower than in the wild-type (8.8 $s^{-1}$). For mutants R144A and R184A, a clear flavin-reduction rate-dependence on [NADPH] was observed. A plot of reduction rate *vs.* [NADPH] described a rectangular hyperbola, from which a $K_m$ and $k_{red}$ could be determined by

fitting the data to the Michaelis function in Origin. The apparent affinity for NADPH was dramatically weakened in both R144A ($K_m$ = 0.64 mM) and R184A ($K_m$ = 2.3 mM), although the $k_{red}$ values were not lowered to the same extent (12.9 $s^{-1}$, R144A; 15.2 $s^{-1}$, R184A). The $k_{red}/K_m$ ratio for each enzyme indicates the relative efficiency of the NADPH-binding and flavin reduction process. The ratios for wild-type FLDR (> 4500 $mM^{-1}$ $s^{-1}$) and R174A are massively (> 100-fold) higher than those for R144A (20.4 $mM^{-1}$ $s^{-1}$) and R184A (6.7 $mM^{-1}$ $s^{-1}$) (Table 4.3).

*NADH*

The affinity of wild-type and mutant FLDRs for NADH was considerably lower that for NADPH. The rate of flavin reduction showed a clear [NADH]-dependence for all enzymes, allowing calculation of $k_{red}$ and $K_m$ by fitting of data points to the Michaelis function. Wild-type FLDR had the highest apparent affinity for NADH ($K_m$ = 1.7 mM), while R144A had the lowest ($K_m$ = 56.2 mM). R174A and R184A had apparent affinities approximately 3-fold higher than wild-type ($K_m$ = 4.1 mM [R174A] and 4.4 mM [R184A]). Less variation was observed for the $k_{red}$ values - with both R144A (10.1 $s^{-1}$) and R174A (9.0 $s^{-1}$) giving higher rates than wild-type (7.8 $s^{-1}$). R184A had the lowest $k_{red}$ (4.2 $s^{-1}$). The $k_{red}/K_m$ ratio for wild-type FLDR (4.7 $mM^{-1}$ $s^{-1}$) is the highest, followed by R174A (2.2 $mM^{-1}$ $s^{-1}$), R184A (0.97 $mM^{-1}$ $s^{-1}$) and R144A (0.18 $mM^{-1}$ $s^{-1}$) (Table 4.3).

**Table 4.3 Stopped-flow kinetic parameters for NAD(P)H-dependent flavin reduction in wild-type and mutant (R144A, R174A and R184A) forms of *E. coli* FLDR.**

| | $K_d$ NADPH (μM) | $K_d$ NADH (mM) | $k_{red}$ NADPH ($s^{-1}$) | $k_{red}$ NADH ($s^{-1}$) | $k_{red}/K_d$ NADPH ($\mu M^{-1}$ $s^{-1}$) | $k_{red}/K_d$ NADH ($mM^{-1}$ $s^{-1}$) |
|---|---|---|---|---|---|---|
| wild-type | <5μM | 1.67 ± 0.38 | 22.63 ± 0.67 | 7.79 ± 0.61 | > 4.53 ± 0.13 | 4.66 ± 1.09 |
| R144A | 635 ± 10 | 56.15 ± 4.55 | 12.94 ± 0.73 | 10.09 ± 0.61 | 0.0204 ± 0.0015 | 0.18 ± 0.027 |
| R174A | <5μM | 4.14 ± 0.49 | 8.82 ± 0.52 | 9.05 ± 0.47 | 1.76 ± 0.11 | 2.18 ± 0.43 |
| R184A | 2300 ± 60 | 4.35 ± 0.60 | 15.22 ± 0.14 | 4.24 ± 0.39 | 0.00667 ± 0.00019 | 0.97 ± 0.26 |

## Discussion

In their report of the atomic structure of the *E. coli* flavodoxin $NADP^+$ reductase, Ingelman *et al.* (Ingleman *et al.* 1997) identified arginines 144, 174 and 184 as essential components of the NADPH-binding site of the enzyme, although this site was occupied by citrate in the crystal. Examination of the structure highlights this cluster of three positively charged arginine residues located at the cleft between the NADP(H)-binding and FAD-binding sub-domains of the enzyme (Fig. 4.5).

We decided to probe the effects of charge-neutralising (R→A) mutations to these on the catalytic activities, pyridine nucleotide affinity and preference, and spectroscopic properties of the mutant flavodoxin reductase enzymes. We expected to find that one or more of the arginines would play key roles in pyridine dinucleotide recognition and/or distinguishing between NADPH/NADH (which differ only in the presence of a phosphate group, rather than a hydroxyl, at the 2′ position of the ribose). The results of steady-state kinetic studies on R144A, R174A and R184A mutants (Table 4.2) indicate that the removal of the positively charged arginines at each of these positions results in decreased NADPH-dependent cytochrome *c* reductase activity. In addition, stopped-flow studies show that each mutation has clear effects on the binding of

**Figure 4.5**

Ribbon diagram of the 3D structure of *E. coli* Flavodoxin $NADP^+$ reductase (PDB number, 1FDR). The positions of the three mutated arginine residues (R144, R174 and R184) are indicated in black, relative to the FAD moiety (also in black). The positively charged $NH_2$ groups of the arginines are exposed, providing potential interaction sites with the negatively charged phosphate groups of NADPH. A binding cavity for the NADPH cofactor is obvious between the arginines and theFAD

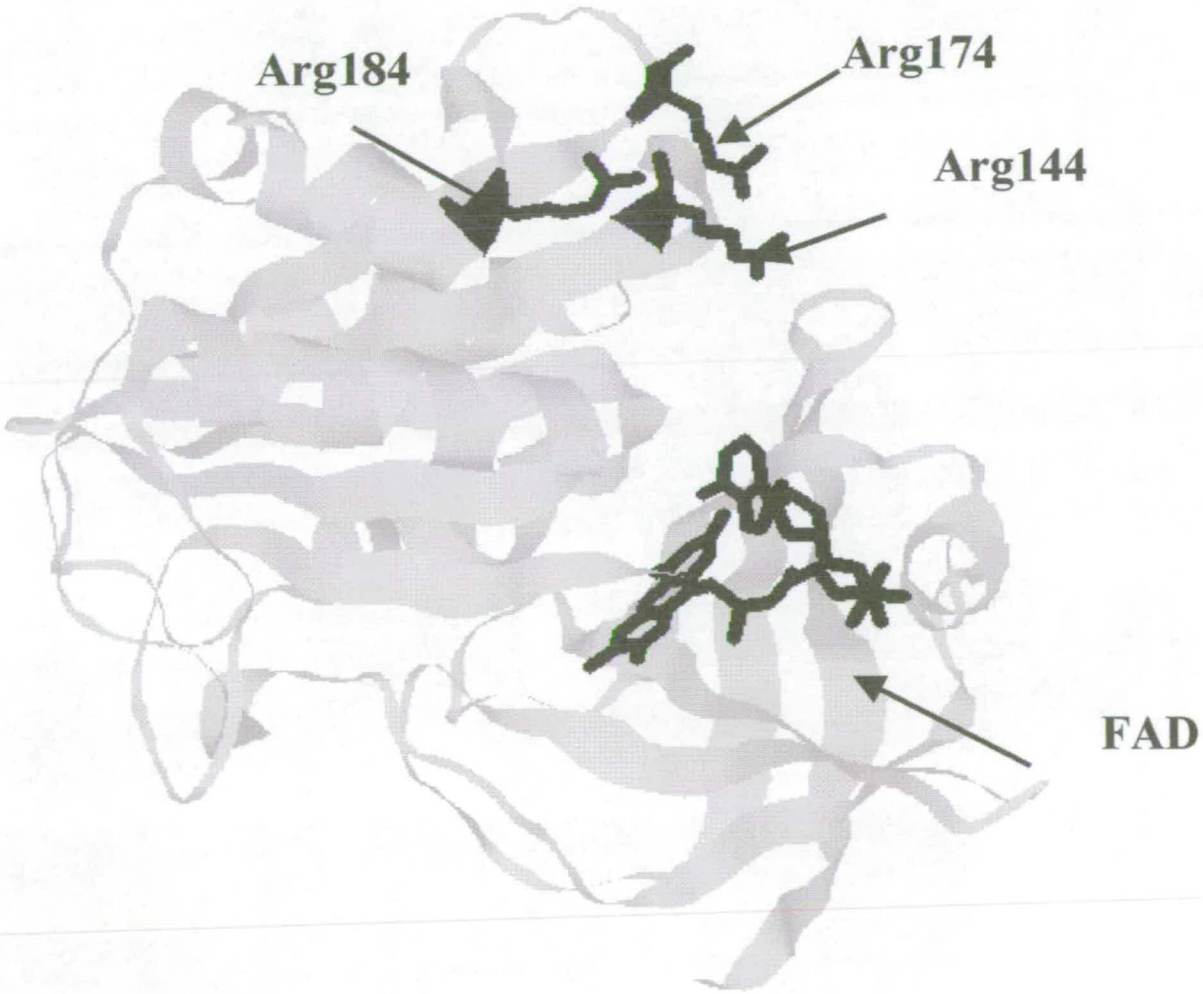

NADPH and/or the process of hydride transfer to the flavin (Table 4.3). Thus, kinetic data indicates that all mutations have major consequences for FLDR catalysis.

In terms of the severity of the overall effects of the mutations, R174 and R184 appear much more important to NADPH-dependent activity than does R144. From steady-state studies, the $k_{cat}/K_m$ ratio for R174A and R184A (a measure of catalytic efficiency with NADPH) is decreased 11-fold and 12-fold, respectively, compared to wild-type. By contrast, the $k_{cat}/K_m$ is decreased less than 2-fold for R144A. Despite their apparent similarity in efficiency and NADPH-dependent cytochrome *c* reductases ($k_{cat}/K_m$ = 7.6 and 7.1 $\mu M^{-1}$ $min^{-1}$, respectively), R174A and R184A are affected rather differently. Both the $k_{cat}$ and the $K_m$ for R184A are ~ 2.5-fold greater than the same parameters for R174A (Table 4.2). Indeed, the $k_{cat}$ for R184A is actually slightly higher than for the wild-type FLDR.

Since the $K_m$ is a complex measure of NADPH affinity, we decided also to analyse the NAD(P)H-dependent reduction of the FAD in FLDR using stopped-flow absorption spectroscopy. By this technique, we were able to examine the effects of mutations on only the binding of NAD(P)H and the hydride transfer to oxidised FAD, the first two steps in FLDR catalysis. By this method, the $K_d$ for NADPH for wild-type FLDR was determined to be very tight (< 5 μM, Table 4.3), *i.e.* the flavin reduction rate was seen to remain constant even when the NADPH concentration was lowered to a level equimolar with that of the FLDR (10 μM). The $K_d$ for NADPH remained very low for mutant R174A (< 5 μM). However, the apparent NADPH affinity was much reduced for mutants R144A ($K_d$ = 635 μM) and R184A ($K_d$ = 2.3 mM).

From stopped-flow studies, the limiting rate of reduction ($k_{red}$) of FAD by NADPH in wild-type FLDR was determined to be 22.63 $s^{-1}$ (Table 4.3). Since each hydride transfer to the flavin involves transfer of two electrons, the theoretical maximal rate of cytochrome *c* reduction by the reduced wild-type FLDR is ~ 45 $s^{-1}$. The actual steady-state rate is only 5.65 $s^{-1}$, some 8-fold lower. Clearly, cytochrome *c* reduction is rate-limited by its binding to FLDR and/or the flavin-to-cytochrome *c* haem electron

transfer. Although the $K_d$ for NADPH remains low in mutant R174A, it is the worst affected in the catalysis of hydride transfer to the FAD. For R174A, the $k_{red}$ falls to 8.82 $s^{-1}$, only 39 % of the wild-type value (Table 4.3). It would appear that although this mutant maintains a low $K_d$ for NADPH, it is badly affected in the catalysis of electron transfer to the flavin. It is notable also for this mutant that CD properties are altered (the near UV band showing a positive Cotton effect at 272 nm is reduced in intensity [Fig. 4.3]). The aromatic amino acid fluorescence emission from R174A is of slightly greater intensity than wild-type or the other mutants, with a maximum at a longer wavelength (336 nm *vs.* 328 nm, Fig. 4.4). Both these parameters indicate a perturbed tertiary structure in mutant R174A, the effects of which must underlie its diminished hydride transfer rate.

From alignments of the amino acid sequences of FLDR with other pyridine dinucleotide-dependent oxidoreductase superfamily of enzymes, it is evident that an arginine corresponding to R174 is strongly conserved in virtually all the $NADP^+$-dependent members of the ferredoxin $NADP^+$ reductase (FNR) family of enzymes (Fig. 4.6).

**Fig 4.6 Amino acid alignment of *E. coli* FLDR ("*E. coli*", Swiss-Prot code P28861, [Bianchi 1993]) with other members of the ferredoxin $NADP^+$ oxidoreductase (FNR) family of enzymes.**

Alignments were performed by comparing other protein sequences with the region of FLDR from L139 to E190 (encompassing all three of the mutated arginines). Flavodoxin reductase arginine residues 144, 174 and 184 are highlighted in red, as are positively charged amino acids (arginines and lysines) conserved in the aligned enzymes. Serine 173 is highlighted in blue. "Spinach" = spinach ferredoxin $NADP^+$ reductase (Swiss-Prot code P00455, (Karplus *et al.* 1991); "*Anabaena*" = ferredoxin reductase from *Anabaena variabilis* (Q4459) (Serre *et al.* 1996); "P450 BM3" = flavocytochrome P450 BM3 from *Bacillus megaterium* (P14779, [Ruettinger *et al.* 1989]); "Hum CPR" = Human NADPH-cytochrome P450 reductase (P16435, [Haniu *et al.* 1989]); "Rat CPR" = Rat NADPH-cytochrome P450 reductase (P00388,

[Porter & Kasper 1985]); "B5 R′ase" = Bovine NADH-cytochrome $b_5$ reductase (P07514, [Ozols *et al.* 1985]); "Hum iNOS" = Human inducible nitric oxide synthase (P35228, [Geller *et al.* 1993]); "Hum nNOS" = Human neuronal nitric oxide synthase (P29475, [Hall *et al.* 1994]); "Hum eNOS" = Human endothelial nitric oxide synthase (P29474, [Janssens *et al.* 1992]); "Corn NIR" = corn nitrate reductase (P17571, [Gowri & Campbell 1989]). Bovine cytochrome $b_5$ reductase and corn nitrate reductase are NADH-dependent reductases, all other enzymes shown are NADPH-dependent.

```
                144                                 174        184
                 ↓                                   ↓          ↓
E. coli     LVHAARYAADLS-YLPLMQELEKRYEGKLRIQTVVSRETAAGSLTGRIPA-LIE
Spinach     LFLGVPTSSSLL-YKEEFEKMKEKAPDNFRLDFAVSREQTNEK-GEKMYI-QTR
Anabaena    LVFGVPTTPNIL-YKEELEEIQQKYPDNFRLTYAISREQKNPQ-GGRMYI-QDR
P450 BM3    LYFGCRSPHEDYLYQEELENA-QSEGIIT-LHTAFSRMPNQPKTYVQHVMEQDG
Hum CPR     LYYGCRRSDEDYLYREELAQF-HRDGALTQLNVAFSREQS-HKVYVQHLLKQDR
Rat CPR     LYYGCRRSDEDYLYREELARF-HKDGALTQLNVAFSREQA-HKVYVQHLLKRDR
B5 R′ASE    LLFANQTEKDILLRPELLEELRNEHSARFKLWYTVDRAPEA-WDYSQGFVNQEM
Hum iNOS    LVFGCRRPDEDHIYQEEMLEMAQK-GVLHAVHTAYSRLPGKPKVYVQDILRQQL
Hum nNOS    LVFGCRQSKIDHIYREETLQAKNK-GVFRELYTAYSREPDKPKKYVQDILQEQL
Hum eNOS    LVFGCRCSQLDHLYRDEVQNAQQR-GVFGRVLTAFSREPDNPKTYVQDILRTEL
Corn NIR    LVYANRTEDDILL-RDELDRWAAEYPDRLKVWYVIDQV-KRPEEGWK-YSVGFV
```

In addition, a serine is also conserved in the majority of related enzymes at a position corresponding to S173 in FLDR. However, the serine is replaced by an acidic residue in many of the NADH-dependent members of the FNR family (Wierenga *et al.* 1986). For instance, in the bovine NADH-cytochrome $b_5$ reductase, an aspartate replaces the serine. This is also the case for *e.g.* the human and porcine $b_5$ reductases, the nitrate reductase from corn and the NADH-putidaredoxin reductase component of the *Pseudomonas putida* cytochrome P450cam camphor hydroxylase system (Correll *et al.* 1993, Karplus *et al.* 1991). By analogy with the NADPH- and NADH-dependent glutathione reductases (Scrutton *et al.* 1990), the aspartate side chains may be involved in hydrogen bonding to the 2′ hydroxyl of the adenosine ribose in NADH, *i.e.* the functional group which is replaced by phosphate in NADPH. However, it should be remembered that glutathione reductases are not members of the FNR family. Karplus *et al* from their crystallographic studies of the 2′ AMP-bound form

of spinach ferredoxin reductase (the "prototype" enzyme for the FNR family) (Karplus *et al.* 1991), identified S234, R235, K244 and Y246 as a cluster of residues whose side chains provide hydrogen bonds to the 2′ phosphate group of bound 2′-phospho-5′-adenosine monophosphate (2′-phospho-AMP), and hence hydrogen bond to the same position on $NADP^+$ and aid in the discrimination against $NAD^+$, which has a $K_m$ 400-fold greater than $NADP^+$ (Shin & Arnon 1965). The first three of these residues correspond to S173, R174 and R184 in *E. coli* FLDR (a positively charged arginine replaces the lysine at position 184 in FLDR), but an aromatic residue corresponding to Y246 is not conserved in FLDR (Fig. 4.6 sequence alingnment). By comparison with data for related FNR enzymes, it appears clear that R174 and R184 of *E. coli* FLDR interact with the $NADP^+$ 2′ phosphate group, but that R144 may not. However, other amino acid side chains are also implicated in stabilising interactions with $NADP^+$. In addition, chemical modification studies of spinach FNR have suggested that K116, K244 (= R184 in FLDR), another lysine, a carboxylate group and a histidine are involved in $NADP^+$-binding (Kaplus *et al.* 1991).

Recent studies have been carried out on the role of Arg100 and Arg264 in *Anabaena* PCC7119 ferredoxin-$NADP^+$ reductase in the reconition and hydride transfer of NADPH. Arg100 was mutated to alanine and Arg264 was mutated to glutamic acid spectroscpoic and kinetic studies were carrid out on the two mutant proteins. It was found that the mutation R100A had a minor affect on the binding of NADPH, and R264E had no effect. Arg100 and Arg264 in *Anabaena* ferredoxin-$NADP^+$ reductase do not correspond to R144, R174 or R184 in *E. coli* FLDR (Martinez-Julvez *et al.* 1998). Studies have recently been carried out into the role of the glutamyl residues 312 in spinach ferredoxin – $NADP^+$ reductase and it was found that this residue is necessary for the binding of the nicotinamide ring of NADPH. In addition it charge modulates the two one-electron redox potential of the flavin to stabilize the semiquinone form. It is stated that this residue is conserved through out the FNR family with the exception of cytochrome $b_5$ reductase, though in our sequence alignment studies we found that the residue was not conserved in *E. coli* FLDR (Aliverti *et al.* 1998).

Scrutton *et al.* (Scrutton *et al.* 1990), carried out a more succeful mutagenesis of residues involved in NADPH binding in glutathione reductase. Scrutton mutated the residues located at positions analogous to S173 and R174 in *E. coli* FLDR, which led to alterations in the pyridine nucleotide specificity of glutathione reductase. However, several successive mutations were required to achieve a complete conversion of specificity from $NADP^+$ to $NAD^+$. Multiple mutations will also doubtless be required to convert *E. coli* FLDR to an NADH-dependent reductase. However, if both R174 and R184 are involved in adenosine ribose 2′ phosphate binding (but R144 is not), then we might expect to observe an increased selectivity for NADH over NADPH in mutants R174A and R184A, but not for R144A. The steady-state and stopped-flow kinetic data presented (Tables 4.2 & 4.3) are largely supportive of this theory. In steady-state cytochrome *c* reduction, the $k_{cat}$ for the NADH-dependent reaction is 1.3- and 1.5-fold higher than wild-type for R174A and R184A, respectively. By contrast, the $k_{cat}$ for R144A is 2.4-fold lower than wild-type FLDR. The $k_{cat}/K_m$ ratio for NADH-dependent catalysis also indicates that R174A and R184A are more efficient NADH-dependent reductases than R144A, with R184A, in particular, being 1.9- and 11.4-fold more efficient than wild-type and R144A, respectively (Table 4.2). The comparative efficiency with NADH *vs.* NADPH ($[k_{cat}/K_m]_{NADH}/[k_{cat}/K_m]_{NADPH}$) for the three mutants also indicates that there is partial conversion to NADH specificity in R174A and R184A, but not 144A. The values for R174A and R184A are 3.1- and 23.2-fold greater than wild-type; while that for R144A is 3.1-fold lower. Stopped-flow studies also indicate that NADH is bound more efficiently by R174A and R184A than by R144A. Although the apparent $K_d$ for NADH is decreased in all three mutants with respect to wild-type (Table 4.3), the $K_d$ is 13.6- and 12.9-fold lower for R174A and R184A, respectively, than for R144A. The $k_{red}$ (limiting flavin reduction rate)/$K_d$ ratio is also much higher for R174A and R184A than for R144A. Comparisons of efficiency with NADH *vs.* NADPH ($[k_{red}/K_d]_{NADH}/[k_{red}/K_d]_{NADPH}$) based on stopped-flow data are confused by the fact that the binding of NADPH is extremely tight ($K_d$ < 5 μM) for wild-type and R174A, but that the apparent $K_d$ is

dramatically increased for both R144A and R184A (Table 4.3). However, if this relative efficiency parameter is compared for only these two mutants, it is found that R184A has a 16.5-fold increase in relative efficiency with NADH over R144A.

The bulk of the kinetic data support the proposal that R174A and R184A are important to binding the adenosine ribose 2′ phosphate of NADPH, although further mutations would clearly be required to convert specificity completely in favour of NADH. The atomic structure of the 2′-phospho-AMP-bound form of spinach FNR indicates that R235 (= R174 in *E. coli* FLDR) and K244 (= R184 in FLDR) each probably provide two hydrogen bonds to the 2′ phosphate, but that K116 is also involved in hydrogen bonding to stabilise the adenosine ribose 5′ phosphate group (Karplus *et al.* 1991). This lysine is also conserved in *E. coli* FLDR (K83), suggesting it may play a similar role here. This raises the question as to the specific role of R144 in NADPH interactions in FLDR. An obvious suggestion would be that it is involved in electrostatic interactions or hydrogen bonding with the nicotinamide ribose 5′ phosphate, which is present in both NADH and NADPH. This would explain that, although mutant R144A is profoundly affected in its binding of NADPH and in its catalytic activity towards an artificial electron acceptor (cytochrome *c*), its relative efficiency with NADH is also diminished (not increased, as in R17A and R184A). An arginine is conserved at a position corresponding to R144 in FLDR in the majority of other $NADP^+$-dependent members of the FNR family, providing further indication for an important role in pyridine nucleotide binding (Fig. 4.6).

To investigate further the binding of NADPH to the *E. coli* flavodoxin reductase, we undertook molecular modelling studies in attempts to dock the pyridine nucleotide in the FLDR structure close to the FAD, in the binding region identified from the atomic structure of Ingelman *et al.* (Ingleman *et al.* 1997). We discovered that the NADPH could not be docked favourably to permit hydride transfer from the nicotinamide ring of NADPH to the FAD, since the C-terminal amino acid side-chain of FLDR (tryptophan 248) blocks the entrance to the flavin in the crystal structure (Fig. 4.7 a). This may at least partly explain the rather slow flavin reduction rates measured in our

stopped-flow studies (Table 4.3). For wild-type FLDR, the limiting rate of flavin reduction ($k_{red}$) was only 22.63 $s^{-1}$. This compares rather poorly with previous studies of the NADPH-reduction of the FAD in its domain of flavocytochrome P450 BM3, another member of the FNR family (Munro *et al.* 1996). For P450 BM3, rates in excess of 700 $s^{-1}$ were obtained for FAD reduction under conditions comparable with those used for FLDR. A conformational change to displace W248 on NADPH binding and permit flavin reduction could explain the relatively low rate of hydride transfer measured in FLDR. Molecular modelling was performed using SYBYL (Tripos Inc.) (by Dominikus Lysek) with the constraints that the NADPH hydride / FAD isoalloxazine distance should be < 8 Å and that W248 should rotate to expose the flavin for interaction with NADPH. This modelling resulted in the best-fit docking structure shown in Fig. 4.7 b, where the nicotinamide ring of NADPH approaches the FAD with a minimum distance of 5.8 Å between the two centres. The modelled structure shown in Fig 4.7 a, also highlights the proximity of the three arginines to the phosphate groups of NADPH. The model indicates that R174 and R184 lie close to the adenosine ribose 2′ phosphate, probably within hydrogen bonding distance. Interaction between R184 and the adenosine ribose 5′ phosphate may also be feasible. However R144 is rather more distant from the adenosine ribose, and makes closest approaches to the nicotinamide ribose 5′ phosphate, as suggested above. The NADPH-bound model structure is consistent with the results from our kinetic studies, placing R174 and R184 much closer to the 2′ phosphate group of NADPH (which is replaced by a hydroxyl in NADH) and R144 closer to another phosphate group.

**Fig 4.7 The atomic structure of *E. coli* flavodoxin reductase and the results of molecular modelling of its interaction with NADPH.**

Structures are depicted in Rasmol. Fig. 4.7 a, shows the polypeptide backbone of FLDR (grey) in the region of the proposed NADPH docking site from the atomic structure of Ingelman *et al.* (Ingleman 1997). The FAD moiety is coloured in yellow, and relevant amino acid side chains (R144, R174, R184 & W248) are also shown, with nitrogen atoms depicted in blue and oxygens in red. Tryptophan 248 obscures access of the nicotinamide ring of NADPH to the flavin in this structure. Fig. 4.7 b,

shows the results of molecular modelling studies, with NADPH binding optimised. Phosphorus atoms in the docked NADPH are depicted in orange. Tryptophan 248 is rotated away from the adenine moiety of FAD to facilitate closer approach of the NADPH nicotinamide ring, which is now located only 5.8 Å from the FAD isoalloxazine ring system. The arginines are now positioned close enough for potential electrostatic or hydrogen-bonding interactions with the adenosine ribose 2′ phosphate (R174 and R184), adenosine ribose 5′ phosphate (possibly R184) and nicotinamide ribose 5′ phosphate (R144), explaining the deleterious effects of mutating these residues on NADPH-binding and catalytic efficiency.

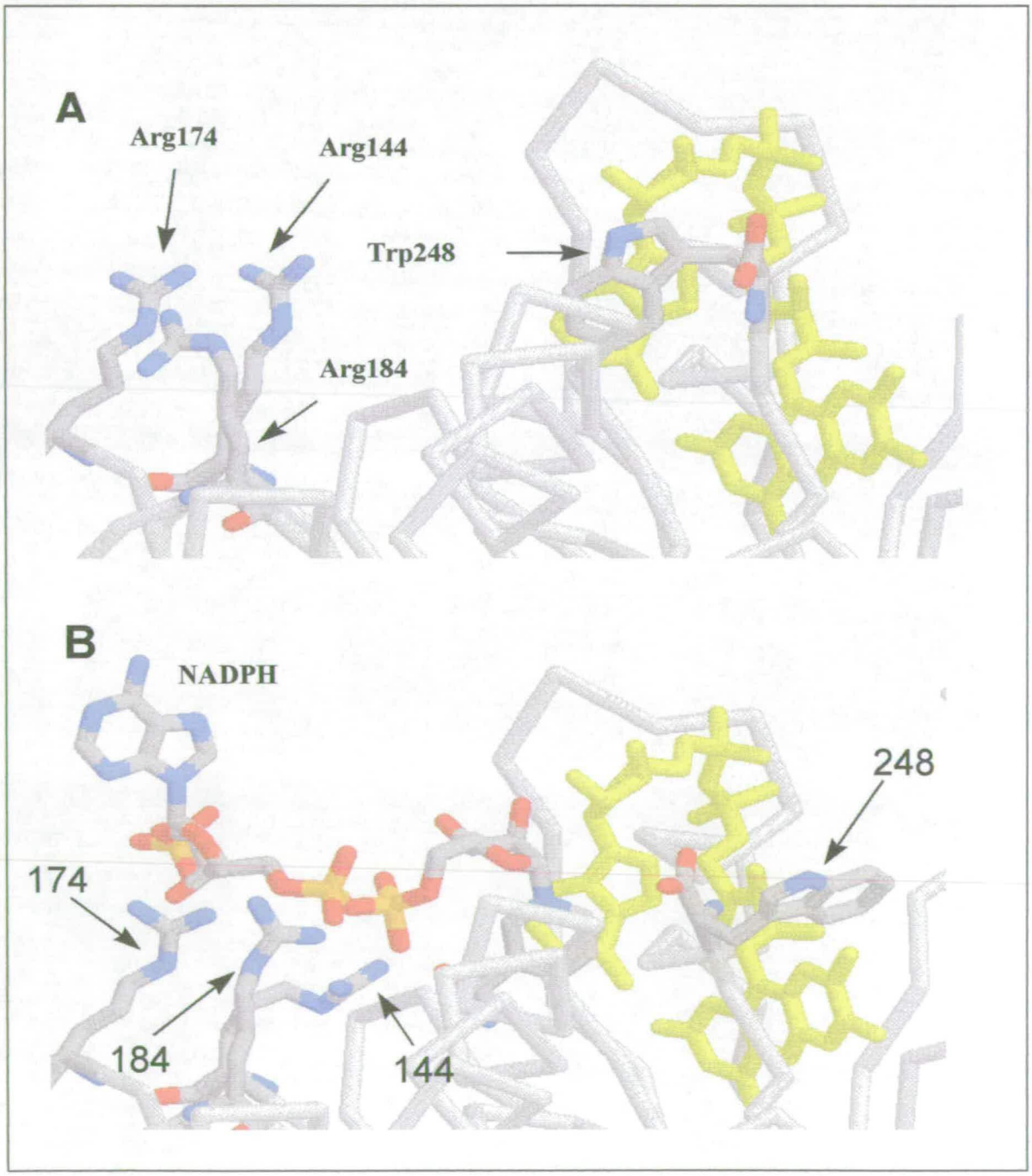

In conclusion, the atomic structure of *E. coli* flavodoxin reductase implicated the positively charged arginine residues at positions 144, 174 and 184 in the interaction with NADPH. Our studies have proven that charge-neutralising mutations (to alanine) at each of these positions have profound consequences for the efficiency of the mutants to act as NADPH-dependent reductases. The mutations increase the $K_m$ for NADPH in all mutants, and the apparent $K_d$ for NADPH in R144A and R184A (possibly R174A also). The efficiency ($k_{cat}/K_m$) of cytochrome *c* reduction is diminished in all mutants, with R174A and R184A worst affected. While R174A maintains a low $K_d$ for NADPH, the mutation also induces alterations in the near UV circular dichroism and flavin fluorescence spectra, consistent with tertiary structure changes in the vicinity of the NADPH-binding site. Indeed, the fact that the near UV CD (resulting mainly from aromatic amino acids) is altered suggests that there may be some movement of the tryptophan (W248) that obscures the FAD in the R174A mutant. These structural changes may explain the low rate of flavin reduction for R174A (only 39 % of wild-type), despite the fact that the $K_d$ for NADPH remains < 5 μM. Molecular modelling studies of NADPH-binding are consistent with the roles of the arginines inferred from structural comparisons with other members of the FNR family, and from our kinetic studies. R174 and R184 appear to interact with the adenosine ribose 2′ phosphate, while R144 is more likely to stabilise NADPH binding by interaction with the nicotinamide ribose 5′ phosphate. R174A and R184A are more efficient enzymes than wild-type or R144A with NADH as substrate, consistent with the proposed phosphate-binding roles for these residues. In particular, from steady-state studies, mutant R184A shows marked conversion in pyridine nucleotide preference, with the $[k_{cat}/K_m]_{NADH}/k_{cat}/K_m]_{NADPH}$ for this mutant being > 23-fold that of wild-type. From stopped-flow studies, the ratio of $K_{d\ (NADH)}/[K_{d\ (NADPH)}$ is also > 175-fold lower for R184A than for wild-type. An interesting possibility which has arisen out of these studies is the possibility of mutating Trp248. If this residue was mutated it may give greater access to the flavin which may increase the electron transfer rate.

# Chapter 5 (FLDR)

# Investigation into the binding site of flavodoxin in flavodoxin $NADP^+$ reductase

## Introduction

The aim of this study was to gain insight into the interaction between *E. coli* flavodoxin $NADP^+$ reductase (FLDR) and *E. coli* flavodoxin (FLD). The interaction between FLD and FLDR is not understood, and none of the redox partners in the FNR families have been co-crystallized. There have however been some hypotheses as to how *E. coli* FLDR and FLD interact. Ingleman *et al* (Ingleman *et al.* 1997) modeled FLDR and FLD together, and suggested that FLD fitted into a depression in the FLDR molecule, with the methyl groups of the FMN of FLD and the FAD of FLDR coming into van der Waals contact to each other. In their model strands βA and βB of FLDR come into contact with negatively charged residues Glu95, Glu127 and Asp 134 in the FLD. In the FLDR crystal structure three arginines residues R236, R237 and R238 form a very large positive patch on FLDR. On this surface R236 is on the strand βA and R237 and R238 are on the strand βB. To elucidate the roles that these residues have to play in the interaction with FLD, we decided to mutate these residues from arginine to alanine in a charge neutralisation mutation, and examine the effects of this on electron transfer.

## Results

### Mutagensis and cloning of R237A and R238A

The wild-type *fldr* gene was expressed under the control of an IPTG-inducible T7 promoter in pCL 21, in the cell line HMS173(DE3) as reported in chapter 3. For the generation of mutants R237A and R238A, the *fldr* gene was sub-cloned into pUC 18/RBS (Yanisch-Perron *et al.* 1985) using *Nco* I and *Bam* HI restriction sites. Site-directed mutagensis was performed using the "mega-primer" PCR method (Sarkar & Sommers 1990) using vector forward (5′ CGC CAG GGT TTT CCC AGT CAC G 3′) and reverse (5′ GTT GTG TGG AAT TGT GAG CGG 3′) oligonucleotides, and the following mutagenic primers:

R237A: 5′ ATG GCC CGG TCG TGC ACG TAA ATG 3′

R238A: 5′ ATG GCC CGG TGC GCG ACG TAA 3′

The bases underlined in each primer indicate the position at which the arginine codon is replaced by one encoding an alanine. Mutated *fldr* genes were digested with *Nco*I and *Bam*HI and re-cloned into pUC 18/RBS (Yanisch-Perron *et al.* 1985), to form plasmids pCL25 (pUC 18/RBS/*fldr*R237A), pCL26 (pUC 18/RBS/*fldr*R238A). The *E. coli* strain TOP10 One Shot™ (Invitrogen) was used for transformation of the mutant ligation mixes. Mutant clones were sequenced by the Sanger dideoxy chain termination method to establish that secondary mutations had not occurred, and were expressed in strain C6007, which is deficient in the host *fldr* gene (Bianchi *et al.* 1995). The C6007 strain was a kind gift from Vera Bianchi (Department of Biology, University of Padua, Pauda, Italy).

## Protein expression and purification

Wild-type and mutant FLDRs were successfully over-expressed in *E. coli* and purified to homogeneity in two column chromatography steps (Q-Sepharose and 2′, 5′-ADP Sepharose). The expression of mutant forms from plasmids pCL25-26 under the *lac* promoter system in the background of strain C6007 (*fldr*$^-$) (Bianchi *et al.* 1995) was not as high (~ 2 % of total cell protein) as that obtained for the wild-type under the T7-promoter from plasmid pCL21 (~ 14 % total cell protein, as reported in *chapter 3*), necessitating purification from a larger *E. coli* transformant cell mass (10 - 20 l *vs.* 2 l for wild-type FLDR). However, the use of strain C6007 guaranteed lack of contamination with the wild-type FLDR.

Wild-type FLDR from HMS174 (DE3)/pCL21 usually yielded ≥ 30 mg of pure FLDR/litre of cells. Mutants R237A and R238A from C6007/pCL25-26 yielded ≥ 2 mg of pure enzyme/litre of cells. Both wild-type and mutant forms of FLDR proved very insensitive to proteolysis in the homologous host organism, as evidenced by SDS-PAGE, see fig 5.1.

**Fig 5.1 SDS-PAGE gel of purified wt and mutant (R237A and R238A) of *E.coli* FLDR**

Lane 1: Molecular weight standards (94000, 67000, 43000, 30000, 20100, 14400 Da), Lane 2: Pure wild-type FLDR, Lane 3: Pure R237A FLDR, Lane 4: Pure R238A FLDR,

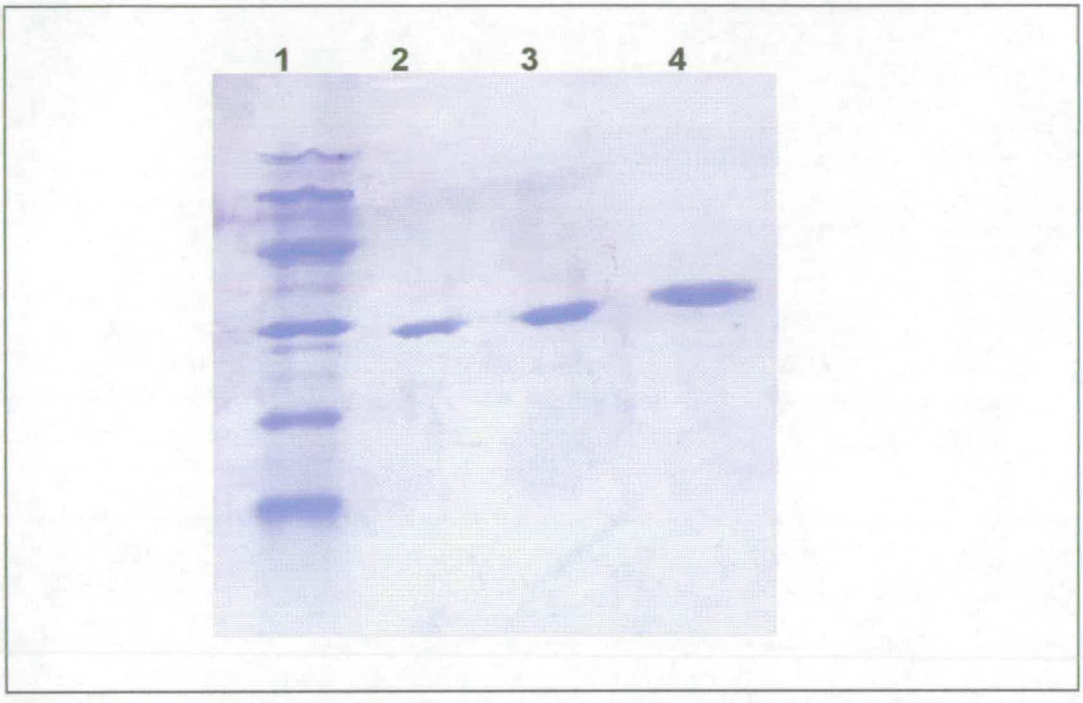


High resolution mass spectrometric data was obtained for wt and the mutants of FLDR, confirming the predicted molecular weight analysis. Table 5.1 shows the predicted and obtained molecular weights for wt and mutants FLDR.

**Table 5.1 Predicted and obtained mass by ES-MS for wt and mutant FLDR**

| | Predicted Mass (Da) | Obtained Mass (Da) |
|---|---|---|
| Wt | 27 647 | 27 641 |
| R237A | 27 562 | 27 560 |
| R238A | 27 562 | 27 560 |

## Spectroscopic characterisation

### UV-visible spectrophotometry

Wild-type and mutant FLDRs have essentially identical visible absorption spectral characteristics, with absorbance maxima at 456nm and 400nm, and a shoulder on the longer wavelength band at 483nm (Fig. 3.3).

### CD spectroscopy

CD spectra were run for *E. coli* FLD, wild-type FLDR, R237A FLDR and R238A FLDR. The spectra was run in both the far UV (190-260nm) and the near UV/Vis (260-600nm), for both the individual proteins and FLDR and FLD mix. In both the far UV region and near UV/Vis region the spectra of the mutant FLDR was essentially the same as wild type FLDR, as reported in *chapter 4*. In the far UV the spectra of the mixture of FLD with the wild-type and mutant FLDRs are essentially identical to those spectra derived by addition of the individual components spectra at the same concentration. In the near UV/Vis region differences were observed between the algebraic and the physical mixtures. Of these proteins differences were small, but the presence of isobestic points at approximately 350nm and 525nm in the overlaid physical and algebraic mixtures indicated that the alterations were genuine, see fig 5.2.

**Fig 5.2 Near UV/Vis CD spectra of R237A and R238A FLDR, and physical and algebraic mixtures of FLD & mutant proteins**

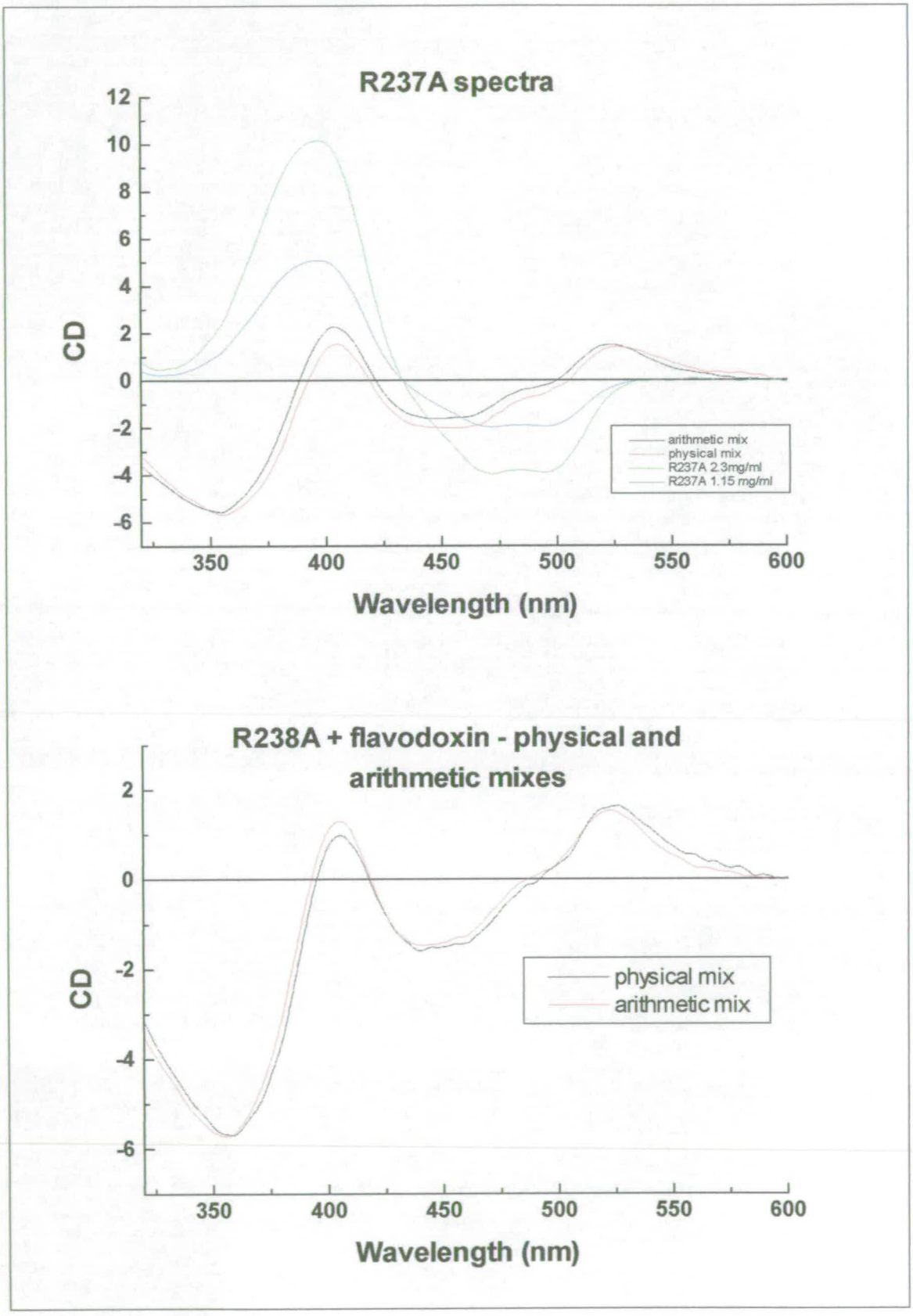

## Fluorescence spectroscopy

The fluorescence properties of wild-type and mutant FLDRs were compared to probe further for effects on tertiary structure (aromatic amino acid fluorescence) and flavin environment (flavin fluorescence). The spectra were found to be essentially identical to the spectra for wild-type FLDR, as described in *chapter 4*.

## Enzyme activities

The reduction of wild-type and mutant FLDRs by NAD(P)H, and the catalysis of cytochrome *c* and potassium ferricyanide reduction by the enzymes were investigated using steady-state and stopped-flow methods. The reduction of FLD by FLDR and mutants was also examined by steady state and stopped-flow methods. All experiments were performed in 10 mM sodium phosphate buffer (pH 7.5) (assay buffer).

## Steady-state kinetics

The steady-state kinetic behavior of wild-type and mutant FLDR enzymes was investigated using cytochrome *c* as an electron acceptor and NADPH as the donor. Preliminary experiments indicated that the wt and mutant enzymes all had a $k_{cat}$ of ~ 340 $min^{-1}$, for cytochrome *c* reduction. The $K_m$ of NADPH for the wild type FLDR was 3.86 ± 0.283μM. Wild-type FLDR had a $K_m$ of 17.6 ± 1.6 μM for cytochrome *c*. The $K_m$ for cytochrome *c* for the mutants R237A and R238A were much greater; that for R237A was 176.3 ± 27 μM and R238A had a $K_m$ of 186.6 ± 36 μM. Steady-state studies were also carried out using potassium ferricyanide as the acceptor, again using NADPH as the donor. Wild-type FLDR catalysed potassium ferricyanide reduction with a $k_{cat}$ of 478.4 ± 28.9 $min^{-1}$. The $k_{cat}$ of R237A potassium ferricyanide was raised at 673 ± 16 $min^{-1}$, whereas the $k_{cat}$ for R238A was slightly lowered at 402 ± 6.2 $min^{-1}$. The potassium ferricyanide $K_m$ for the R237A and R238A were both lowered three fold with respect to wild-type. The $K_m$ for R237A was 3.95 ± 0.54 μM and for R238A was 3.04 ± 0.37 μM, in comparison to 9.68 ± 0.36 μM for the wild type enzyme, see table 5.2.

**Table 5.2 Steady-state kinetic parameters for cytochrome *c* reduction with NAD(P)H by wild-type, R144A, R174A and R184A mutants of *E. coli* FLDR.**

| | $k_{cat}$ ($min^{-1}$) Cytochrome *c* | $K_m$(μM) NADPH | $K_m$(μM) Cytochrome *c* | $K_m$(μM) Potassium ferricyanide | $k_{cat}/K_m$ Cytochrome *c* ($\mu M^{-1}$ $min^{-1}$) | $k_{cat}/K_m$ Potassium ferricyanide ($\mu M^{-1}$ $min^{-1}$) |
|---|---|---|---|---|---|---|
| Wild-type | 339 ± 7.2 | 3.86 ± 0.28 | 17.6 ± 1.6 | 9.68 ± 0.36 | 87.8 | 49 |
| R237A | 319 ± 8.2 | - | 176.3 ± 27 | 3.95 ± 0.54 | 1.81 | 170 |
| R238A | 354 ± 40 | - | 186.6 ± 36 | 3.04 ± 0.37 | 1.91 | 134 |

Purified FLD acts as a single electron shuttle and is able to stimulate the rate of FLDR-dependent cytochrome *c* reduction approximately 6-fold. Clearly FLD must have superior interaction with cytochrome *c* compared to FLDR. As FLDR and FLD are a physiological complex, therefore you may be able infer their affinity for one another on the basis of cytochrome *c* stimulation. With saturating cytochrome *c* (200μM) and FLDR at 16.65 nM, a Michaelis curve was obtained for the stimulation of cytochrome *c* reductase activity when FLD was varied 0.25-10 μM and the reduction rate was plotted *v.* [FLD] and gave an apparent $K_m$ of the FLD for the FLDR of 6.84 ± 0.68μM. When purified FLD was added to the mutant proteins R237A and R238A, it did not stimulate the rate.

## Stopped-flow kinetics

Stopped-flow absorption spectrophotometry was used to investigate the rate of hydride transfer from NADPH to FLDR, to assess if the mutations had had any effect on this stage of the catalysis. The rate of electron transfer for the mutants and the wild-type enzyme was found to be ~ $22s^{-1}$, see table 5.3

Stopped-flow absorption spectrophotometry was also used to investigate the effects of mutations on the microscopic rate constants for the electron transfer from FLDR to FLD. This was achieved by rapid mixing of wild-type and mutant FLDRs (at a fixed

concentration between 30 – 50 μM) in one stopped-flow syringe with FLD (20 μM), and NADPH (2mM) in the other syringe, and monitoring the rate of electron transfer from FLDR to the FMN of FLD. The increase in absorbance at 583nm formation of the semiquinone on FLD was measured. The reaction time was 1000s, as the rate of electrons transfer from FLDR to FLD was apparently very slow. The rate for the wild type enzyme was 0.03407 ± 0.00021 $s^{-1}$. The rate for both mutants were lowered, R237A had a rate of 0.01755 ± 0.00035 $s^{-1}$ and R238A a rate of 0.01871 ± 0.00012$s^{-1}$, see table 5.3.

The affect of ionic strength on the electron transfer from FLDR to FLD for the wild-type and mutants enzymes was also investigated using stopped-flow spectrophototrometry. This was achieved by having FLDR of a fixed concentration (30-50μM) in the assay buffer (10mM sodium phosphate, pH 7.5) in one syringe, with FLD (20μM) pre-reduced by NADPH (2mM) in the other, in the assay buffer at double the required ionic strength. Wild-type enzyme showed the fastest rate at the lowest ionic strength (10mM) whereas the mutants maximal rate was achieved at 100mM and 200mM for R237A and R238A respectively, see fig 5.3.

**Table 5.3 Stopped-flow kinetic parameters for wild-type and mutant FLDR**

| | $K_d$ NADPH (μM) | $k_{red}$ NADPH ($s^{-1}$) | $k_{red}$ FLD ($s^{-1}$) |
|---|---|---|---|
| wild-type | <5 | 22.63 ± 0.67 | 0.03407 ± 0.0024 |
| R237A | <5 | 21.79 ± 0.68 | 0.01755 ± 0.0031 |
| R238A | <5 | 25.43 ± 0.78 | 0.01871 ± 0.0014 |

**Fig 5.3 Ionic Strength studies of wild-type FLDR and R237A and R238A by stopped-flow spectrophotometric studies**

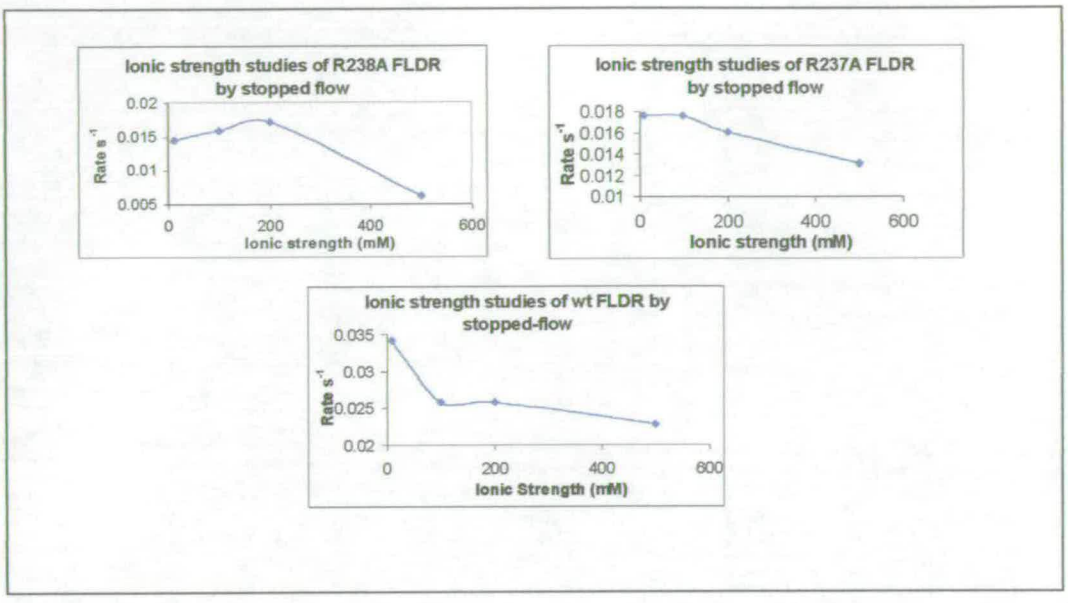


## Discussion

In the crystal structure of FLDR three arginine residues, R236, R237 and R238, near to the C-terminus have been proposed as anchor points for interaction with glutamate residues of the redox partner FLD. The residues R237 and R238 have been mutated to alanine and, the affects of these mutations have been examined by kinetic and spectroscopic studies.

It was expected that the neutralisation of these arginine residues would have an affect on the binding and transfer of electrons to the terminal electron acceptor. The transfer of electrons from NADPH to FLDR was not affected. The results of the pre-steady-state studies showed that the electron transfer from NADPH to FLDR in the mutant enzymes in comparison to the wild-type enzyme is unchanged at ~ $22s^{-1}$. This was also observed in steady state where the $k_{cat}$ for both R237A ($319 \pm 8.2$ $min^{-1}$) and R238A ($354 \pm 40$ $min^{-1}$) was again equivalent to the wild-type enzyme ($339 \pm 7.2$ $min^{-1}$).

These mutations did however affect the terminal electron transfer to both FLD and artificial electron acceptors. This stage of the catalytic cycle was studied by both pre-steady-state and steady-state techniques. For both mutants steady state studies the $k_{cat}$ for cytochrome *c* reduction was roughly equivalent to the wild-type enzyme, although the $K_m$ for both R237A (176 ± 27 μM) and R238A (187 ± 36 μM) had increased ten fold in comparison to wild-type (17.6 ± 1.6 μM). Cytochrome *c* has an asymmetric distribution of charge, which it uses to pre-orientate itself to the optimal position for electron transfer in conjunction with its electron donor. The mutations in FLDR may have disturbed this balance of charge between itself and cytochrome *c*, and this may prevent the two proteins from pre-orientating themselves to the optimal position for the electron transfer complex. This alteration of charge may also disrupt the electrostatic forces, which stabilize the electron transfer complex. However, the $k_{cat}$ for the reduction of cytochrome *c* was not affected. This suggests that the rate limiting step in the catalytic cycle is the transfer of electrons from the FLDRs flavin to the haem group of cytochrome *c*. When potassium ferricyanide is used as the terminal electron acceptor, both the mutants R237A and R238A are three fold more efficient than the wild-type enzyme, see table 5.2. Ferricyanide is a comparatively small artificial electron acceptor and if the protein structure is examined, it can be seen that the R236, R237 and R238 form a positive arm protruding from the main bulk of the protein, see fig 5.4. Potassium ferricyanide may be interacting with these residues and not moving in close enough to the site of the flavin for efficient electron transfer to occur. When one of these positive charges is removed as in the mutants, R237A and R238A, the potassium ferricyanide may approach closer enabling more efficient electron transfer to occur.

The electron transfer from FLDR to its physiological acceptor, FLD, was examined by both steady-state and pre-steady-state kinetics. In steady-state studies, using cytochrome *c* as the terminal electron acceptor with wild-type FLDR, addition of FLD was found to stimulate the reaction six fold and had a *K*m of 6.84 ± 0.68 μM. FLD therefore must transfer electrons at a greater rate to cytochrome *c* than FLDR. Therefore the steady-state reaction with cytochrome *c* as the terminal electron and

**Fig 5.4 Potential Map of FLDR**
Scale -5eV(red) to+5eV (blue)

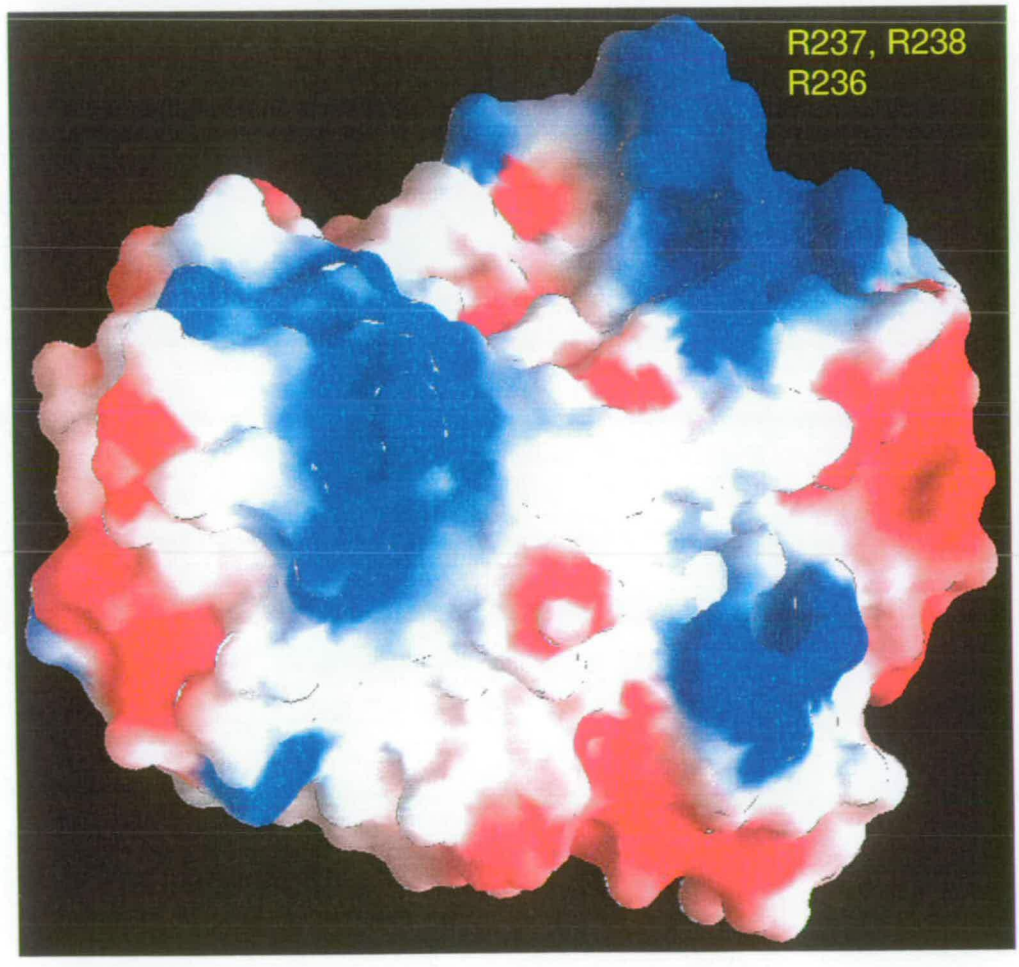

FLDR and FLD present should give an insight into the interaction between FLDR and FLD. In steady-state studies with both of the mutants R237A and R238A, when FLD was added to the assay it was found that the rate was unaffected. This appears logical since these mutations should impair the ability of FLDR and FLD to dock in the optimal electron transfer complex. Either FLDR and FLD cannot pre-orientate themselves or they cannot form the electron transfer complex correctly due to the disruption of electrostatic forces.

The pre-steady-state kinetics showed that the rate of electron transfer between FLDR and FLD for both the mutants R237A and R238A (0.01755 ± 0.0031 $s^{-1}$, 0.01871 ± 0.0014 $s^{-1}$ respectively) is reduced by 50% in comparison to the wild-type ( 0.03407 ± 0.0024 $s^{-1}$). Therefore both mutations R237A and R238A have disrupted the electron transfer from FLDR to FLD. Unfortunately it was not possible to measure the apparent $K_d$ of FLDR and FLD by pre-steady-state, because the rate of electron transfer from FLDR to FLD is very slow. Ionic interactions obviously play an important role in the binding of FLDR and FLD. Ionic strength studies were carried out by stopped-flow spectrophotometry, to try and gain an insight as to how these mutations have affected the electrostatic interactions. The optimal ionic strength for electron transfer in the wild-type enzyme was found to be 10mM NaCl. At higher ionic strengths these ionic interaction are swamped out, therefore FLDR and FLD have trouble forming the optimal electron transfer complex and the rate is reduced. R237A does not appear to be that important in orientating FLDR and FLD, since optimal ionic strength is similar to wild-type at 10mM NaCl but the rate does remain constant until 100mM NaCl then rapidly decreases. In the mutant R238A the optimal ionic strength was found to be 200mM NaCl, so obviously this residue plays an important role in forming the electron transfer complex. When R238 is removed unfavorable electrostatic interactions may dominate. It is plausible that these can be overcome at higher ionic strength. Hence, R238A function best at 200mM NaCl.

All the mutant FLDRs exhibited the same properties as the wild-type enzyme in fluorescence, UV-Vis and CD studies demonstrating that there has been no major

structural change. CD studies were carried out to study the interaction of FLD with the wild-type and mutant FLDR. In the far UV the spectra of the mixture FLD with the wild-type and mutant enzymes were found to be essentially to be identical to those spectra derived by adding the spectra for the individual components at the same concentration. This indicates that the secondary structure of FLDR and FLD are not perturbed by any complex formation. However, in the near UV region there were isobestic points present when the algebraic and arithmetic spectra were overlaid. The changes presumably reflect small re-orientations of one or both of the flavins when complex formation occurs, this would lead to the change in the chiral properties of the flavin observed. Similar small changes were observed with wild-type FLDR and FLD, as when the mutant proteins were mixed with FLD. We were unable to determine from CD if there were any changes in the interaction between the mutant enzymes complex with FLD and the wild-type complex with FLD. CD does not appear to be a particularly sensitive probe for these flavoproteins interaction, but other kinetic data indicates that there are genuine differences in the docking with FLD. When alignment studies were carried out on other members of the pyridine dinucleotide-dependent oxidoreductase super-family of enzymes; it was evident that neither R237 nor R238 are conserved.

Various studies have been carried out into the interaction of various electron transfer partners, including members of the FNR family and their partners. A study has been carried out on the complex between *Azotobacter vinelandii* ferredoxin I and NADPH-ferredoxin reductase (Jung *et al.* 1999). The electrostatic potential of the two proteins were calculated, and it was found that ferredoxin had an asymmetric distribution of charge. The region surrounding the area where the [4Fe-4S] cluster approaches the surface appears to be hydrophobic and surrounded by a ring of negatively charged residues. The surface of NADPH-ferredoxin reductase has an area of positive potential surrounding the area where the flavin approaches the surface of the protein. This asymmetric distribution of charge may help the proteins to pre-orientate themselves for the formation of the electron transfer complex. This

negatively charged ferredoxin and the positively charge ferredoxin reductase surface motif is a common trend in ferredoxin reductase and ferredoxin partners.

In studies using differential chemical modification of spinach ferredoxin reductase De Pascalis *et al* (De Pascalis *et al.* 1993) proposed that a series of basic residues on ferredoxin reductase are involved in the binding of ferredoxin reductase to ferredoxin. As all these residues are conserved in *Anabaena* ferredoxin $NADP^+$ reductase these were used as the basis for mutagensis studies to elucidate ferredoxin $NADP^+$ reductase interaction with ferredoxin (Schmitz *et al.* 1998). These basic residues were either charge neutralized or charged reversed, and their effects on electron transfer to ferredoxin were examined. It was observed that all of these residues are required for efficient electron transfer between ferredoxin $NADP^+$ reductase and ferredoxin. However, only one of these residues is conserved in *E. coli* FLDR, (*Anabaena* R214 ≡ *E.coli* R50). The *Anabaena* residue R214 is implicated in binding of the FAD (Schmitz 1998), as is R50 in *E. coli* FLDR (Ingleman *et al.* 1997).

Mutagenesis studies have also been carried out on *Anabaena* ferredoxin to study its relationship with *Anabaena* ferredoxin $NADP^+$ reductase (Hurley *et al.* 1997). Mutations were carried out on acidic residues which were proposed to interact with basic residues present on ferredoxin $NADP^+$ reductase. Hurley *et al* concluded that it is very specific protein-protein interactions at the ferredoxin/ ferredoxin $NADP^+$ reductase interface that controls the formation of the optimal electron transfer complex. They have demonstrated that hydrophobic interactions play a key role in forming the optimal electron transfer complex and that electrostatic interactions favor less productive orientations between the two proteins (Hurley *et al.* 1996). This was also found to be the case for the interactions between flavodoxin and cytochrome $c_3$ from *Desulfovibrio vulgaris* (Feng & Swenson 1997). Various acidic residues present on flavodoxin were charge neutralised and the interaction with cytochrome $c_3$ was studied. The conclusion was reached that flavodoxin and cytochrome $c_3$ interact by a 'minimal electron transfer mechanism' in which the initial complex formed is stabilized by electrostatic interactions, but is relatively inefficient in electron transfer

terms. The complex then rearranges in a rate limiting step to form a more efficient electron transfer complex.

FLDR and FLD are probably not interacting in this rather inefficient method of electron transfer, as the optimal ionic strength for the interaction of FLDR and FLD is 10mM NaCl, which suggests that electrostatic interactions are important in forming the electron transfer complex. It would be expected that the rate would increase at elevated ionic strength if 'minimal electron transfer mechanism' was the mechanism, as the electrostatic interactions would become weaker. FLDR and FLD are most likely to interact in a more classical electron transfer mechanism. The first step involving the orientation of the two proteins through the interaction of their general electrostatic fields, but it is unclear from our data how important this "steering" process is in the formation of the complex. The two proteins would then dock through electrostatic and hydrophobic interaction, to form the electron transfer complex. Transfer of electrons then occurs and the complex dissociates. Other studies mainly based on hypothetical models have been carried out on protein-protein electron transfer complexes between cytochrome *c* and flavodoxin, (*e.g.*, Stewart *et al.* 1988, Palma *et al.* 1994, Weber & Tollin 1985). The overriding conclusion from these is that the proteins which contain complementary charged patches surrounding the area where the prosthetic group approaches the surface, pre-orientate themselves to form the electron transfer complex.

Unfortunately no atomic structure has been determined for the FLDR/FLD complex, although a structure has been solved for the cytochrome *c*-cytochrome *c* peroxidase complex (Pelletier & Kraut 1992). However, it is unclear whether this complex represents the active form of the electron transfer complex. The crystal structure between the haem-and FMN binding domain of bacterial cytochrome P450BM-3 has also recently been determined (Severioukova *et al.* 1999). However, this is not a good model for the interaction of FLDR and FLD as the BM3-FMN domain differs dramatically from FLD. In this protein the FMN is mainly surrounded by neutral and hydrophobic residues whereas FLD has highly conserved negatively charged residues

surrounding the FMN. This manifest in the very different redox properties of the two FMN containing proteins.

In conclusion, the atomic structure of *E. coli* FLDR (Ingleman *et al.* 1997) suggested that the residues R236, R237 and R238 are involved in the interaction of FLDR and FLD. In our studies, R237 and R238 were mutated and both these residues proved to be involved in the interaction of FLDR with FLD. From our data it is not clear whether these residues are important in pre-orienting the proteins, forming electrostatic interactions with FLD, or a combination of the two. The collection of kinetic data was difficult due to the poor rate of electron transfer between FLDR and FLD, which is at least 100, 000 times lower than similar systems (Hurley *et al.* 1996). One reason for the slow rate of electron transfer, is that the reduction potential of FLDR is very close to that of the ox/sq couple of FLD, which leads to a very low driving force for electron transfer to FLD. The rate may increase when FLDR and FLD are in complex with their terminal electron acceptor. Studies with cytochrome *c* as the terminal electron acceptor, suggest that the rate limiting step of the reaction is the transfer of electrons from FLDR to cytochrome *c* and not the electron transfer complex formation. However, it is not known whether this is also the rate limiting step for electron transfer from FLDR to FLD. Which raises the question as to whether FLDR and FLD are actually physiological redox partners. Nonetheless, the systems that FLDR and FLD support in *E. coli* are not systems that require a fast turnover. It is unfortunate that a $K_d$ for FLDR and FLD has not been determined, but it was not possible to derive it by kinetic studies due to the slow rate of electron transfer.

Various techniques were considered for determining the FLD/FLDR $K_d$, including fluorescence studies. However, the fluorescence of FLDR is very poor and it would not be possible to determine the $K_d$ in this manner. Binding the FLDR to a support column and passing through FLD and then calculating how much of the FLD had bound was also considered. The problem with this method is that we cannot be certain exactly how FLDR is attached to the column. Biacore experiments were

considered, but again it is not possible to ensure that the chip has a homogenous protein covering of FLDR. Obviously further studies are required to gain a fuller understanding of the interaction of FLDR and FLD. The arginine residue R236 should be mutated to gain a fuller understanding of the interaction of the three arginine residues R236, R237 and R238. It would be interesting to make multiple mutations of these arginines to look at the combined effects of these residues.

## References

Abu-Soud, H. M., Feldman, P. L., Clark, P. & Stuehr, D. J. (1994). Electron transfer in nitric oxide synthases: Characterisation of L-arginine analogues that block heme iron reduction. *Journal of Biological Chemistry* **269**, 32318-32326.

Aliverti, A., Deng, Z., Ravasi, D., Piubelli, L., Karplus, P. A. & Zanetti, G. (1998). Probing the function of the invariant glutamyl residue312 in spinach ferredoxin NADP+ reductase. *Journal of Biological Chemistry* **273**(51), 34008-34015.

Andrews, S. C., Shipley, D., Keen, J. N., Findly, J. B. C., Harrison, P. M. & Geust, J. R. (1992). The haemoglobin -like protein (HMP) of *Escherichia coli* has ferrisiderophore reductase activity and its C-terminal domain shares homology with ferredoxin NADP+ reductase. *FEBS* **302**(3), 247-252.

Atkins, P. W. (1990). *Physical Chemistry 4th edition*, Oxford University Press, Oxford.

Beratran, D. N. & Onuchic, J. N. (1989). Electron tunnelling pathways in proteins influences on the transfer rate. *Photosynthetic Research* **22**, 173-186.

Beratran, D. N., Betts, J. N. & Onuchic, J. N. (1991). Protein electron transfer rates set by the bridging secondary and tertiary structure. *Science* **252**, 1285.

Bianchi, V., Reichard, P., Eliasson, R., Pontis, E., Krook, M., Jornvall, H. & Haggard-Ljungquist, E. (1993) a. *E. coli* ferredoxin NADP+ reductase: activation of *E. coli* anaerobic ribonucleotide reduction, cloning of the gene (fpr), and overexpression of the protein. *J. Bacteriol.* **175**(6), 1590-1595.

Bianchi, V., Eliasson, R., Fontecave, M., Mulliez, E., Hoover, D. M., Matthews, R. & Reichard, P. (1993) b. Flavodoxin is required for the activation of the anaerobic ribonucleotide reductase. *Biochemical Biophysical Research Communications* **197**, 792-

797.

Bianchi, V., Haggard-Ljingquist, E., Pontis, E. & Reichard, P. (1995). Interruption of the ferredoxin (flavodoxin) NADP+ oxidoreductase gene of *Escherichia coli* does not affect anaerobic growth but increases sensitivity to paraquat. *Journal of Bacteriology* **177**(5), 4528-4531.

Blaschkowski, H. P., Neuer, G., Ludwig-Festl, M. & Knappe, J. (1982). Routes of flavodoxin and ferredoxin reduction in *Escherichia coli*. *European Journal of Biochemistry* **123**, 563-569.

Bruns, C. M. & Karplus, P. A. (1995). Refined crystal structure of spinach ferredoxin reductase at 1.7 A resolution: oxidized, reduced and 2`-phospho-5`AMP bound states. *Journal of Molecular Biology*(247), 125-145.

Chapman, S. K. & Mount, A. R. (1995). Electron transfer in proteins. *Natural products reports*, 93-100.

Correll, C. C., Batie, C. J., Ballou, D. P. & Ludwig, M. L. (1992). Phthalate Dioxygenase Reductase: A modular structure for electron transfer from pyridine nucleotide to [2Fe-2S]. *Science* **258**, 1604-1610.

Correll, C. C., Ludwig, M. L., Bruns, C. M. & Karplus, P. A. (1993). Structural prototypes for an extended family of flavoprotein reductases: Comparison of phthalate dioxygenase reductase with ferredoxin reductase and ferredoxin. *Protein Science* **2**, 2112-2133.

Daff, S. N., Chapman, S. K., Turner, K. L., Holt, R. A., Govindaraj, S., Poulos, T. L. & Munro, A. W. (1997). Redox control of the catalytic cycle of cytochrome P-450 BM3. *Biochemistry* **36**, 13816-13823.

Demple, B. (1996). Redox signalling and gene control in the Escherichia coli soxRS oxidative stress regulon-a review. *Gene* **179**, 53-57.

Devault, D. (1980). *Review Biophysics* **13**, 387-564.

Draper, R. D. & Ingraham, L. L. (1968). A potentiometric study of flavin semiquinone equilibrium. *Archives of biochemistry Biophysics* **125**, 802-808.

Dutton, P. L. (1978). Redox potentiometry: Determination of midpoint potentials of oxidation-reduction components of biological electron transfer systems. *Methods in Enzymology* **54**, 411-435.

Entsch, B., Ballou, D. P. & Massey, V. (1979). *Journal of Biological Chemistry*.

Feng, Y. & Swenson, R. P. (1997). Evaluation of the role of specific acidic amino acid residues in electron transfer between flavodoxin and cytochrome $c_3$ from *Desulfovibrio vulgaris*. *Biochemistry* **36**, 13617-13628.

Flint, D. H. & Allen, R. M. (1997). Purification and characterisation of biotin synthases. *Methods in Enzymology* **279**, 349-356.

Fuji, K. & Huennekens, F. M. (1974). Activation of methionine synthetase by a reduced triphosphopyridine nucleotide-dependant flavoprotein system. *The Journal of Biological Chemistry* **249**(21), 6745-6753.

Geller, D. A., Lowenstein, C. J., shapiro, R. A., Nussler, A. K., Silvio, M. D., wang, S. C., Nakayama, D. K., simmons, R. L., Snyder, S. H. & Billiar, T. R. (1993). Molecular cloning and expression of inducible nitric oxide synthase from human hepatocyytes. *Proceedings of National Academey of Sciences (USA)* **90**, 3491-3495.

Ghisla, S. & Massey, V. (1989). Mechanisms of flavoprotein-catalysed reactions. *European Journal of Biochemistry* **181**, 1-17.

Govindaraj, S. & Poulos, T. L. (1997). The domain architecture of cytochrome P450 BM3. *Journal of Biological Chemistry* **272**, 7915-7921.

Gowri, G. & Campbell, W. H. (1989). cDNA clones from corn leaf NADH nitrate reductase and chloroplast $NAD(P)^+$ glyceraldehyde-3-phosphate dehydrogenase. *Plant Physiolgy* **90**, 792-798.

Gray, K. A., Davidson, V. L. & Knaff, D. B. (1988). Complex formation between methylamine dehydrogenase and amicyanin from *Paracoccus denitrificans*. *The journal of Biological Chemistry* **263**(28), 13987-13990.

Hall, A. V., Antoniu, H., Wang, Y., Cheung, A. H., Arbus, A. M., Olson, S. L., Lu, W. C., Kau, C. L. & Marsden, P. A. (1994). Structural organisation of the human neuronal nitric oxide synthase gene (NOS1). *Journal of Bioloical Chemistry* **269**, 33082-33090.

Haniu, M., McManus, M. E., Birkett, D. J., Lee, T. D. & Shively, J. E. (1989). Structural and functional analysis of NADPH-cytochrome P-450 reductase from human liver: complete sequence of human enzyme and NADPH binding sites. *Biochemistry* **28**, 8639-8645.

Harvey, R. A. (1980). Flavin 1, N6-Ethaneoadenine dinucleotide. *Methods in Enzymology* **66**, 290--294.

Hoover, D. M. & Ludwig, M. L. (1997). A Flavodoxin that is required for enzyme activation: The structure of the oxidized flavodoxin from *Escherichia coli* at 1.8A resolution. *Protein Science* **6**, 2525-2537.

Hurley, J. K., Fillat, M. F., Gomez-Moreno, C. & Tollin, G. (1996). Electrostatic and hydrophobic interactions during complex formation and electron transfer in the ferredoxin/ferredoxin NADP+ reductase system from Anabaena. *Journal of American Chemistry Society* **118**, 5526-5531.

Hurley, J. K., Weber-Main, A. M., Stankovich, M. T., Benning, M. M., Thoden, J. B., Vanhooke, J. L., Holden, H. M., Chae, Y. K., Xia, B., Ching, H., Markley, J. L., Martinez-Julvez, M., Gomez-Moreno, C., Schmeits, J. L. & Tollin, G. (1997). Structure-function relationship in anabaena ferredoxin: correlations between X-ray crystal structures, reduction potentials and rate constants of electron transfer to ferredoxin NADP+ reductase for site-specific ferredoxin mutants. *Biochemistry* **36**, 11100-11117.

Ifuku, O., Koga, N., Haze, S.-i., Kishimoto, J. & Wachi, Y. (1994). Flavodoxin is required for the conversion of dethiobiotin to biotin in *Escherichia coli*. *European Journal of Biochemistry* **224**, 173-178.

Ingleman, M., Bianchi, V. & Eklund, H. (1997). The three dimensional structure of flavodoxin reductase from *E. coli* at 1.7A resolution. *J. Mol. Biol.* **268**, 147-157.

Iyanagi, T., Makino, N. & Manson, H. s. (1974). Redox properties of the reduced nicotinamide adenine dinucleotide phosphate-cytochrome P450 and reduced nicotinamide adenine dinucleotide-cytochrome $b_5$ reductase. *Biochemistry* **13**, 1701-1710.

Iyanagi, T. (1977). Redox properties of microsomal reduced nicotinamide adenine dinucleotide-cytochrome $b_5$ reductase and cytochrome $b_5$. *Biochemistry* **16**, 2725-2730.

Janin, J. (1997). The kinetics of protein-protein recognition. *PROTEINS: Structure,*

*function, and genetics* **28**, 153-161.

Janssens, S. P., Shimoushi, A., Quertermous, T., Bloch, D. B. & Bloch, K. D. (1992). Cloning and expression of a cDNA encoding human endothelium-derived relaxing factor/nitric oxide synthase. *Journal of Biological Chemistry* **267**, 14519-14522.

Jarrett, J. T., Goulding, C. W., Fluhr, K., Huang, S. & Matthews, R. G. (1997). Purification and assay of cobalamin-dependant methionine synthase from *Escherichia coli*. *Methods in Enzymology* **281**, 196-231.

Jarrett, J. T., Huang, S. & Matthews, R. G. (1998). Methionine synthase exists in two distinct conformations that differ in reactivity towards methyltetrahydrofolate, adenosylmethionine , and flavodoxin. *Biochemistry* **37**, 5372-5382.

Jenkins, C. M. & Waterman, M. R. (1993). Flavodoxin and NADPH-flavodoxin reductase from *E. coli* support bovine cytochrome P450 c17 hydroxylase activities. *Journal of Biological Chemistry* **269**, 27401-27408.

Jenkins, C. M., Genzor, C. G., Fillat, M. F., Waterman, M. R. & Moreno, C. G. (1997). Negatively charged *Anabaena* flavodoxin residues [ Asp (144) and Glu (145)] are important for reconstitution of cytochrome P450c17 alpha-hydroxylase. *Journal of Biological Chemistry* **272**, 22509-22513.

Jenkins, C. M. & Waterman, M. R. (1998). NADPH-Flavodoxin Reductase and Flavodoxin from *E. coli*: Characteristics as a soluble microsomal P450 reductase. *Biochemistry* **37**(17), 6106-6113.

Jung, Y.-S., Roberts, V. A., Stout, C. D. & Burgess, B. K. (1999). Complex formation between *Azobacter vineladii* ferredoxin I and its physiological electron donor NADPH ferredoxin reductase. *The Journal of Biological Chemistry* **274**(6), 2698-2987.

Karplus, P. A., Daniels, M. J. & Herriott, J. R. (1991). Atomic structure of ferredoxin NADP+ reductase: prototype for a structurally novel flavoenzyme family. *Science*, 60-66.

Kauzmann, W. (1957). *Quantum Chemistry*, Academic Press, New York.

Knappe, J. & Sawers, G. (1990). A radical chemical route to acetyl-CoA: the anaerobically induced pyruvate formate-lyase system of *Escherichia coli*. *FEMS Microbiology Reviews* **75**, 383-398.

Koppenol, W. H. & Margoliash, E. (1982). The asymmetric distribution of charges on the surface of horse cytochrome *c*. *The Journal of Biological Chemistry* **257**(8), 4426-4437.

Krapp, A. R., Tognetti, V. B., Carrillo, N. & Acevedo, A. (1997). The role of ferredoxin NADP+ reductase in the concerted cell defence against oxidative damage. *European Journal of Biochemistry* **249**, 556-563.

Laemmli. (1970). Clevage of structural proteins during the assembly of the head of the bacteriophage T4. *Nature* **227**, 680

Lambeth, J. D. & Kamin, H. (1976). Adrenodoxin reductase: Properties of the complexes of reduced enzyme with NADP+ and NADPH. *Journal of Biological Chemistry* **251**, 4299-4306.

Larsson. (1998). Electron transfer in proteins. *Biophysics and biochemi acta* **1365**, 294-300.

Liochev, S. I., Hausladen, A., Beyer, W. F. & Fridovich, I. (1994). NADPH:ferredoxin

oxidoreductase acts as a paraquat diaphorase and is a member of the soxRS regulon. *Proc. Natl. Acad. Sci. USA* **91**, 1328-1331.

Lu, G., Lindqvist, Y., Schneider, G., Dwivedi, U. & Campbell, W. (1995). Structural studies on corn nitrate reductase: refined structure of the cytochrome *b* reductase fragment at 2.5 A, its ADP complex and an active site mutant and modelling of the cytochrome *b* domain. *Journal of Molecular Biology* **248**, 931-948.

Marcus, R. A. (1956). On the theory of oxidation-reduction reactions involving electron transfer. *Journal of Chemical Physics* **24**, 966-978.

Marcus, R. A. (1964). Chemical and electrochemical electron transfer theory. *Annual Review of Physical Chemistry* **15**, 155-196.

Marcus, R. A. (1965). On the theory of electron transfer reaction united treatment for homogeneous and electron reactions. *Journal of Chemical Physics* **43**, 679-701.

Martinez-Julvez, M., Hermoso, J., Hurley, J. K., Mayoral, T., Sanz-Aparicio, J., Tollin, G., Gomez-Moreno, C. & Medina, M. (1998). Role of Arg100 and Arg264 from Anabaena PCC 7119 ferredoxin-NADP+ reductase for optimal NADP+ binding and electron transfer. *Biochemistry* **37**, 17680-17691.

Massey, V., Muller, F., Feldberg, R., Schuman, M., Sullivan, P., Howell, G. L., Mayhew, S. G., Matthews, R. G. & Foust, G. P. (1969). The reactivity of flavoproteins with sulfite. *Journal of Biological Chemistry* **244**, 3999-4006.

Massey, V. & Hemmerich, P. (1980). Active site probe of flavoproteins. *Biochemical Society Transactions* **8**, 246-256.

Massey, V. (1991). A Simple method for the determination of redox potentials. *Flavins*

*and Flavoproteins 1990.*

Mattew, J. B., Weber, P. C., Salemme, F. R. & Richards, F. M. (1983). Electrostatic orientation during electron transfer between flavodoxin and cytochrome *c*. *Nature* **301**(13), 169-171.

McLendon. (1988). Long distance electron transfer in protein and model systems. *Accounts of chemical research* **21**, 160-167.

McLendon. (1991). *Metal ions in biological systems* (Siegel, H. & Sigel, A. J., Eds.), Decker, New York.

McLendon & Hake, R. (1992). Interprotein electron transfer. *Chemical review* **92**, 481-490.

Mewies, M., Basran, J., Padmen, L. C., Hille, R. & Scrutton, N. S. (1997). Involvement of a flavin iminoquinone methide in formation of 6-hydroxyflavin mononucleotide in trimethyl amine dehydrogenase: A rationale for the existence of 8 a-methyl and C6 linked covalent flavoprotein. *Biochemistry* **36**, 7162-7168.

Miles, J. S., Munro, A. W., Rospendowski, B. N., Smith, W. E., Mcknight, J. & Thomson, A. J. (1992). Domains of catalytically self-sufficient cytochrome P-450 BM3: Genetic construction, overexpression, purification and spectroscopic characterisation. *Biochemistry* **288**, 503-509.

Moser, C. C., Keske, J. M., Warncke, K., Farid, R. S. & Dutton, P. L. (1992). Nature of biological electron transfer. *Nature* **355**, 796-802.

Moser, Page, C. C., Farid, R. & Dutton, P. C. (1995). Biological electron transfer. *Journal of bioenergetics and* **27**, 263-274.

Munro, A. W., Daff, S., Coggins, J. R., Lindsay, J. G. & Chapman, S. K. (1996). Probing electron transfer in flavocytochrome P-450 BM3 and its component domains. *European Journal of Biochemistry*.

Ollagnier, S., Mulliez, E., Gaillard, J., Eliasson, R., Fontecave, M. & Reichard, P. (1996). The anaerobic *Escherichia coli* Ribonucleotide Reductase. *The Journal of Biological Chemistry* **271**(16), 9410-9416.

Olson, S. T. & Massey, V. (1979). Purification and properties of the flavoenzyme D-lactate dehydrogenase from *Megasphaera elsdenii*. *Biochemistry* **18**, 4714-4724.

Ozols, J., Korza, G., Heinemann, F. S., Hediger, M. A. & Stittmatter, P. (1985). Complete amino acid sequence of steer liver microsomal NADPH-cytochrome $b_5$ reductase. *Journal of Biological Chemistry* **260**, 11953-11961.

Palma, P. N., Moura, I., Legall, J., Vanbeeumen, J., Wampler, J. E. & Moura, J. J. G. (1994). Evidence for a ternary complex formed between flavodoxin and cytochrome c(3)-H-1-NMR and molecular modelling studies. *Biochemistry* **33**, 6394-6407.

Pascalis, A. R. D., Jelesarov, I., Ackermann, F., Knoppenol, W. H., Hirasawa, M., Knaff, D. B. & Bossshard, H. R. (1993). Binding of Ferredoxin to ferredoxin-NADP oxidoreductase the role of carboxyl groups, electrostatic surface potential and molecular dipole movement. *Protein Science* **2**, 1126-1135.

Pelletier, H. & Kraut, J. (1992). Crystal-structure of a complex between electron transfer partners cytochrome *c* peroxidase and cytochrome *c*. *Science* **258**, 1748-1755.

Porter, T. D. & Kasper, C. B. (1985). Coding nucleotide sequence of rat NADPH-cytochrome P-450 oxidoreductase cDNA and identification of flavin binding domains. *Proceedings of National Academy of Science (USA)* **82**, 973-977.

Porter, T. D. & Kasper, C. B. (1986). NADPH cytochrome P450 oxidoreductase-flavin mononucleotide and flavin dinucleotide domains evolved from different flavoproteins. *Biochemistry* **25**, 1682-1687.

Porter, T. D. (1991). An unusual, yet strongly conserved flavoprotein reductase in bacteria and mammals. *Trends Biochemistry Science* **16**, 154-158.

Prasad, G. S., Kresge, N., Muhlberg, A. B., Shaw, A., Jung, Y. S., Burgess, B. K. & Stout, C. D. (1998). The crystal structure of NADPH:ferredoxin reductase from *Azotobacter vinelandii*. *Protein Science* **7**, 2541-2549.

Reichard, P. (1993). The Anaerobic Ribonucleotide reductase from *Escherichia coli*. *The Journal of Biological Chemistry* **268**(12), 8383-8386.

Ruettinger, R. T., Weng, L. P. & Fulco, A. J. (1989). Coding 5` regulatory and deduced amino acid sequences of P-450 BM-3, a single peptide cytochrome P-450:NADPH P-450 reductase from *Bacillus megaterium*. *Journal of Biological Chemistry* **264**, 10987-10995.

Sarkar, G. & Sommers, S. S. (1990). The mega primer method of site directed mutagensis. *BioTechniques* **8**, 404-407.

Schmitz, S., Martinez-Julvez, M., Gomez-Moreno, C. & Bohme, H. (1998). Interaction of positively charged amino acid residues of recombinant cyanobacterial ferredoxin NADP+ reductase with ferredoxin probed by site directed mutagensis. *Biochimica et Biophysica Acta* **1363**, 85-93.

Scrutton, S., Berry, A. & Perham, R. N. (1990). The design of the coenzyme specificity of a dehydrogenase by protein engineering. *Nature* **343**, 38-43.

Serre, L., Vellieux, F. M. D., Medina, M., Gomez-Moreno, C., Fontecilla-Camps, J. C. & Frey, M. (1996). X-ray Structure of ferredoxin:NADP+ reductase from Cyanobacterium *Anabaena* PCC 7119 at 1.8A Resolution and Crystallographic Studies of NADP+ Binding at 2.25 A Resolution. *Journal of Molecular Biology* **263**, 20-39.

Sevrioukova, I. F., Huiying, L., Zang, H., Peterson, J. A. & Poulos, T. L. (1999). Structure of a cytochrome P450-redox partner electron-transfer complex. *Biochemistry* **96**, 1863-1868.

Shin, M. & Arnon, D. I. (1965). *Journal of Biological Chemistry*.

Skyes, G. A. & Rogers, L. J. (1984). Redox potentials of algal and cyanobacterial flavodoxins. *Biochemistry* **217**, 845-850.

Smith, G. C. M., Tew, D. G. & Wolf, C. R. (1994). Dissection of NADPH cytochrome P450 oxidoreductase into distinct functional domains. *Proc. Natl. Acad. Sci. USA* **91**, 8710-8714.

Stewart, D. E., LeGall, J., Moura, I., Moura, J. J. G., Peck, H. D., Xavier, A. V., Weiner, P. K. & Wampler, J. E. (1988). A hypothetical model of the flavodoxin tetraheme cytochrome $c_3$ complex of sulfate reducing bacteria. *Biochemistry* **27**, 2444-2450.

Vermilion, J. L. & Coon, M. J. (1978). Identification of the high and low potential flavins of liver microsomal NADPH cytochrome P450 reductase. *Journal of Biological Chemistry* **253**, 8812-8819.

Wang, M., Roberts, D. L., Paschke, R., Shea, T. M., Master, B. S. S. & Kim, J. J. (1997). Three dimensional structure of NADPH-cytochrome P-450 reductase: Prototype for FMN and FAD containing enzymes. *Proc. Natl. Acad. Sci. USA* **94**, 8411-8416.

Weber, P. C. & Tollin, G. (1985). Electrostatic interactions during electron transfer reactions between c-type cytochromes and flavodoxin. *Journal of Biological Chemistry* **260**, 5568-5573.

Wierenga, R. K., Terstra, P. & Hol, W. G. L. (1986). Prediction of the occurrence of the ADP-binding βαβ-fold in proteins using an amino acid sequence fingerprint. *Journal of Molecular Biology* **187**, 101-107.

Williams, P. A., Fulop, V., Leung, Y.-C., Chan, C., Moir, J. W. B., Howlett, G., Ferguson, S. J., Radford, S. E. & Hajdu, J. (1995). Pseudospecfic docking surfaces on electron transfer proteins as illustrated by pseudoazurin, cytochrome C550 and cytochrome cd1 nitrite reductase. *Nature structural biology* **2**(11), 975-982.

Yanisch-Perron, C., Vieira, J. & Messing, J. (1985). Improved M13 phage cloning vectors and host strains: Nucleotide sequences of M13mp18 and pUC19 vectors. *Gene* **33**, 103-119.

# Chapter 6 (*S. citricolor*)

## Introduction

Aristeromycin (Fig 6.1) is a carbocyclic analogue of adenosine, and was first synthesised in a racemic form in 1966 (Shealy & Clayton 1966). Shortly thereafter it was isolated from *Streptomyces citricolor* (Kusaka *et al.* 1967). Neplanocin A, which has been shown to be a precusor of aristeromycin (Parry *et al.* 1989), and some closely related compounds have subsequently been identified as metabolites of *Ampullariella regularis* (Hayashi *et al.* 1981, Yaginuma *et al.* 1981).

**Fig 6.1 Structure of Aristeromycin and neplanocin A.**

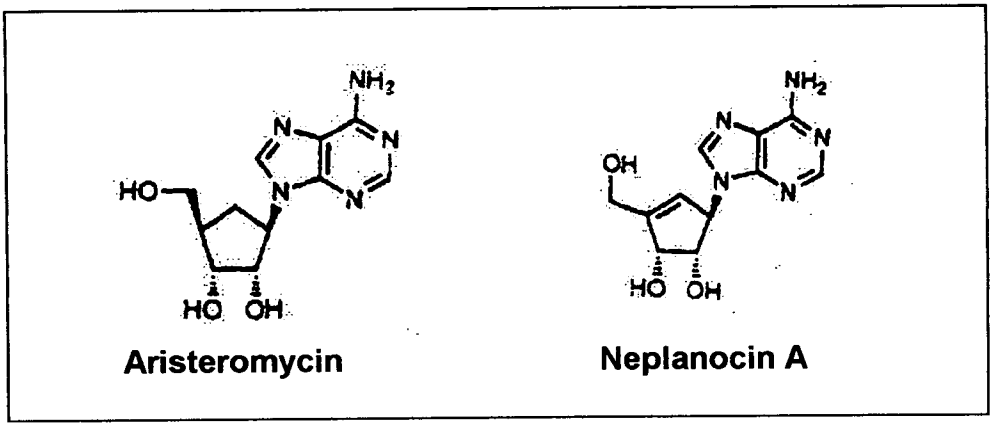


### Biological Activity

Both, neplanocin A and aristeromycin show inhibitory activity against bacteria and fungi, which is presumably due to their close structural relationship to natural nucleosides. Both have been shown to have antiviral activity against (-) RNA viruses (*i.e.*, parainfluenza, measles, and vesicular stomatitis, and double stranded RNA viruses *i.e.*, reo)(De Clercq 1987). They also posses antitumour activity (Yaginuma *et al.* 1981) but unfortunately their cytotoxicity precludes clinical use.

### Inhibition of S-adenosyl-L-homocysteine hydrolase

The mechanism of neplanocin A and aristeromycin antiviral activity is the inhibition of the enzyme *S*-adenosyl-L-homocysteine (AdoHcy) hydrolase. This enzyme catalyses the reversible hydrolysis of *S*-adenosyl-L-homocysteine to adenosine and L-

homocysteine without added cofactors. AdoHcy hydrolase is a key enzyme in transmethylation reactions using *S*-adenosyl-L-methionine (AdoMet) as the methyl donor, including those that are involved in the maturation of viral mRNA. The by-product of these methylations, AdoHcy, serves as a feedback inhibitor for many methyltransferases. AdoHcy hydrolase is the only enzyme known to catalyse AdoHcy catabolism, and is thought to play an important role in allowing the methylation process to proceed at its normal physiological rate, see fig 6.2 (Wolfe *et al.* 1991).

**Fig 6.2 The action of *S*-adenosyl-L-homocysteine hydrolase (De-Clercq 1987)**

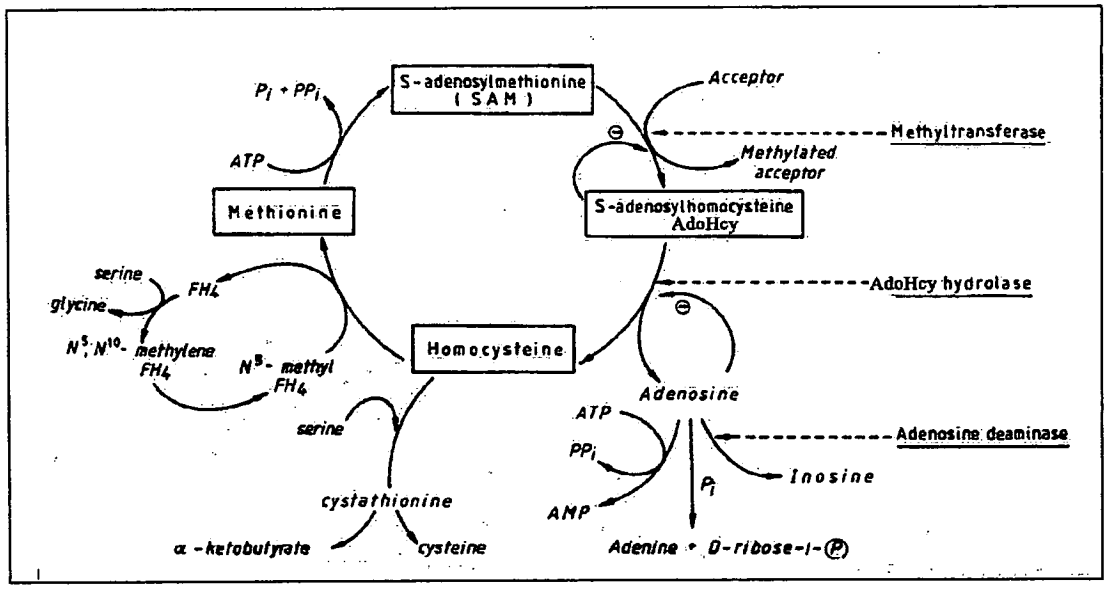


While the equilibrium reaction favours the synthesis of *S*-adenosyl-L-homocysteine, under physiological conditions the reaction proceeds in the hydrolytic direction because the products, adenosine and L-homocysteine, are removed by a number of other enzymes, see fig 6.2 (De-Clercq 1987). Adenosine actually inhibits AdoHcy hydrolase, which means it has to be removed for AdoHcy hydrolase to proceed with its catalytic cycle. It is removed by several pathways, including adenosine deaminase and from fig 6.2 it is clear that the concerted action of three enzymes (methyltransferase, AdoHcy hydrolase and adenosine deaminase) is required.

There is now strong evidence that AdoHcy hydrolase is associated with transmethlyation reactions in the virus replicative cycle. Many plant and animal

viruses require a methylated cap structure at the 5' terminus of their mRNA for viral replication. Virus encoded methlytransferases that are involved in the formation of this structure are inhibited by AdoHcy. Therefore, inhibition of AdoHcy hydrolase would be expected to result in an increased concentration of AdoHcy in the cells, in turn inhibiting the viral methlytransferases (Wolfe *et al.* 1992). The resulting under methylation of the viral mRNA cap structure induced by the inhibition of AdoHyc hydrolase has been correlated to the inhibition of viral replication (Ransohoff *et al.* 1987). The question arises as to how AdoHcy hydrolase inhibitors can impart any specificity towards viral replication. It appears that these may confer their antiviral specificity *via* inhibition of virus specific methlytransferases (De-Clercq 1987).

A detailed knowledge of how neplanocin A and aristeromycin act as inhibitors requires a prior understanding of the enzymatic mechanism of AdoHcy hydrolase. An important feature of the mechanism of the enzyme is the oxidation/reduction at C-3' of the substrate, by the tightly bound $NAD^+$ of the enzyme. Oxidation activates the C-4' proton facilitating the elimination of the C-5' substituent. In the next step, the Michael type addition of water or L-homocysteine is facilitated by the transiently induced ketone functionality (Palmer & Abeles 1979) as shown in fig 6.3.

**Fig 6.3 Mechanism of action of S-adenosylhomomcysteine hydrolase**

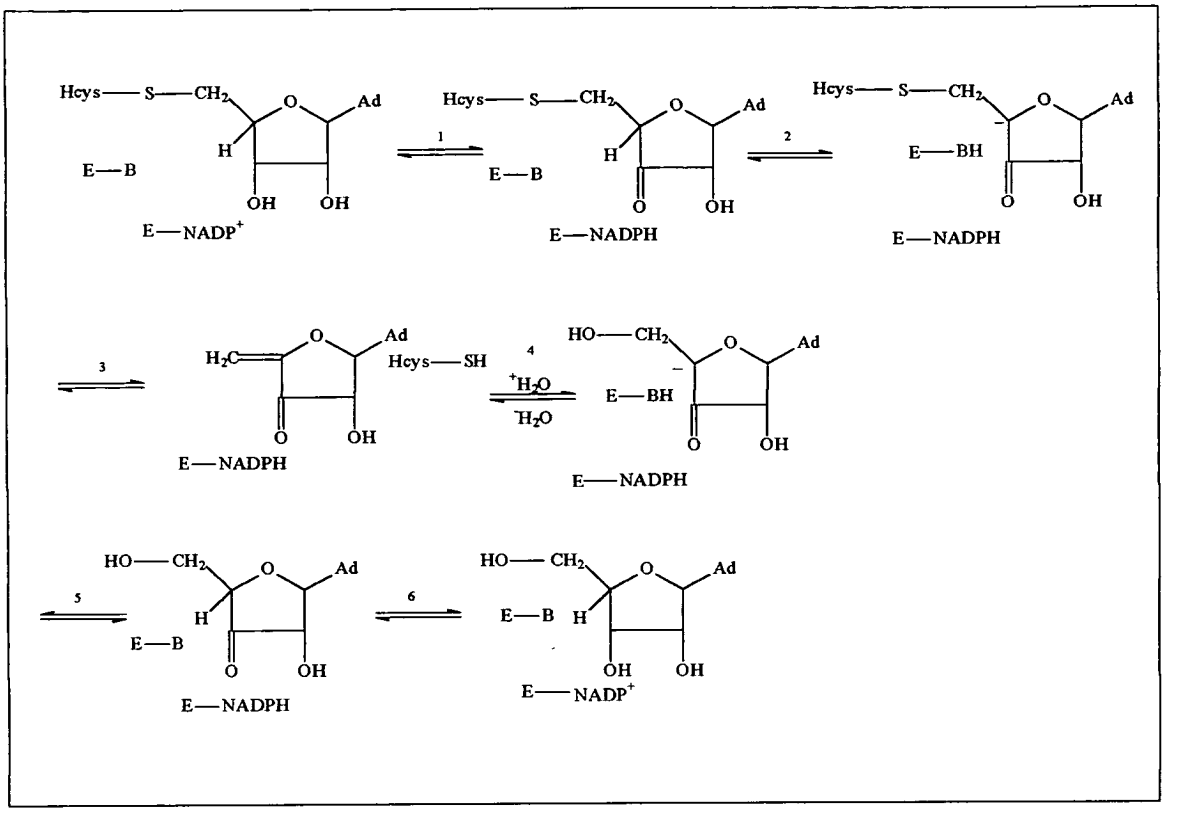


During the inhibition of AdoHyc hydrolase by aristeromycin and neplanocin A they are oxidised at the 3' position by the $NADP^+$ co-factor of the AdoHyc hydrolase resulting in the 3`-keto derivative, which remains tightly bound to the NADPH form of the enzyme leading to inactivity (Paisley *et al.* 1989). This mechanism has been supported by the observation that the binding of neplanocin A to AdoHyc hydrolase involves a stoichiometry of one molecule of enzyme to one molecule of inhibitor (Parry & Bornemann1985).

## Aristeromycin metabolism & antitumour activity

It was found that cells with and without adenosine kinase activity are equally sensitive to aristeromycin. However, the mechanism of cell death is different depending on whether adenosine kinase activity is present or not. Aristeromycin kills cells with no adenosine kinase activity, due to the action of the unphosphorylated nucleoside carbocyclic analogue, presumably by inhibiting *S*-adenosyl-L-homocysteine hydrolase.

It is the metabolites of aristeromycin which confer antitumour activity. Aristeromycin is metabolised to its triphosphate in cells by adenosine kinase *in vivo* (Bennett *et al.* 1986).

Aristeromycin has a potent toxicity to cultured tumour cells (Hill *et al.* 1971) which is increased by the presence of guanine. Aristeromycin inhibits guanine and hypoxanthine utilisation by the cells (Bennett *et al.* 1985). A possible explanation for this is that aristeromycin, in addition to being metabolised to the phosphate derivatives, (Bennett *et al.* 1968) may be also metabolised to the phosphates of the carbocyclic analogue of guanosine (C-Guo). The identification of both 5'-triphosphate of aristeromycin (C-ATP) and the 5'-triphosphate of the carbocyclic analogue of guanosine (C-GTP) as metabolites of aristeromycin indicates that aristeromycin is metabolised along the same pathways as adenosine, see fig 6.4.

**Fig 6.4 The metabolism of aristeromycin.**

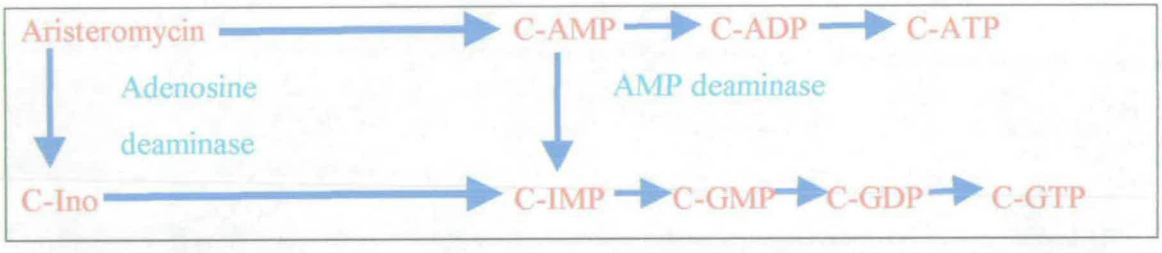


The observation that C-GTP is a metabolite of aristeromycin, when considered with the fact that the carbocyclic analogue of inosine monophosphate (C-IMP) and the carbocyclic analogue of monophospate of guanosine (C-GMP) are present on the metabolic pathway of aristeromycin, gives a possible explanation as to why aristeromycin inhibits the utilisation guanine and hypoxanthine. Both the 5'-phosphates of the carbocyclic analogues of inosine and guanosine strongly inhibit hypoxanthine (guanine) phosphoribosyltransferase (H(G)PRT) (Murray 1966). To date C-GMP is the best known inhibitor for H(G)PRT. In mammalian cells H(G)PRT is present as a salvage pathway of purine synthesis; hence inhibition of H(G)PRT should not lead to excessive cytotoxicity. However many parasites are dependent on pre-formed purines for the synthesis of purine nucleosides, and thus are selectively

inhibited. Hence, inhibitors of H(G)PRT and other salvage enzyme are of potential importance in the therapy of diseases caused by such parasites.

In conclusion, aristeromycin inhibits enzymes in a number of pathways aristeromycin appears an attractive as a drug candidate. Unfortunately, since it is toxic to mammalian cells it cannot be used therapeutically. However, aristeromycin analogues which retain its activity and have less harmful effects, could be potential drug candidates. Due to the therapeutic potential of analogues of aristeromycin, there has been interest in the biosynthetic pathway in *S. citricolor*. If the genes from the biosynthetic pathway were isolated this would possibly enable its manipulation, potentially giving rise to novel analogues as drug candidates.

## Biosynthesis of aristeromycin

The biosynthesis of aristeromycin was first studied by Parry (Parry & Borenemann 1985, Parry *et al.* 1987, Parry *et al.* 1989). On the basis of feeding experiments Parry proposed that D-glucose was the starting point in the pathway. In more recent studies (Jenkins & Turner1995), the intermediates on the pathway have been identified by co-biosynthesis experiments. A series of mutants of *Streptomyces citricolor* which were blocked at different stages of the biosynthetic pathway were isolated by Glaxo in the early 1990's. It was found that combinations of certain mutants could restore the production of aristeromycin. A specific mutant (secretor) emerged that secreted a compound, the tetrol fig 6.5. The tetrol could support the production of aristeromycin in another mutant (converter) which was blocked earlier in the pathway see fig 6.6.

**Fig 6.5 Structure of Tetrol**

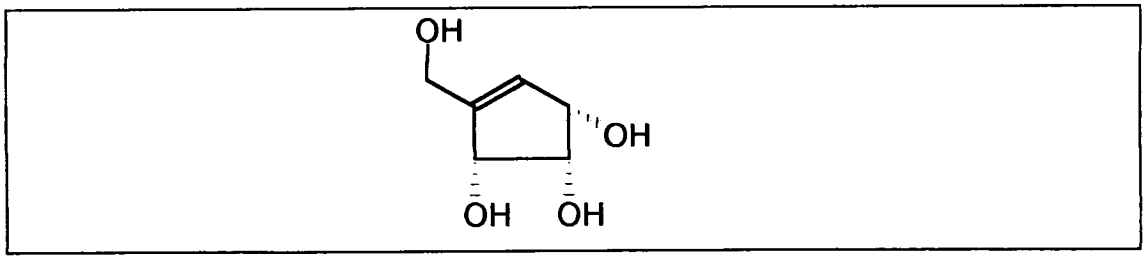

**Fig 6.6 Co-synthesis of aristeromycin using the secretor mutant and the converter mutant (Jenkins & Turner 1995)**

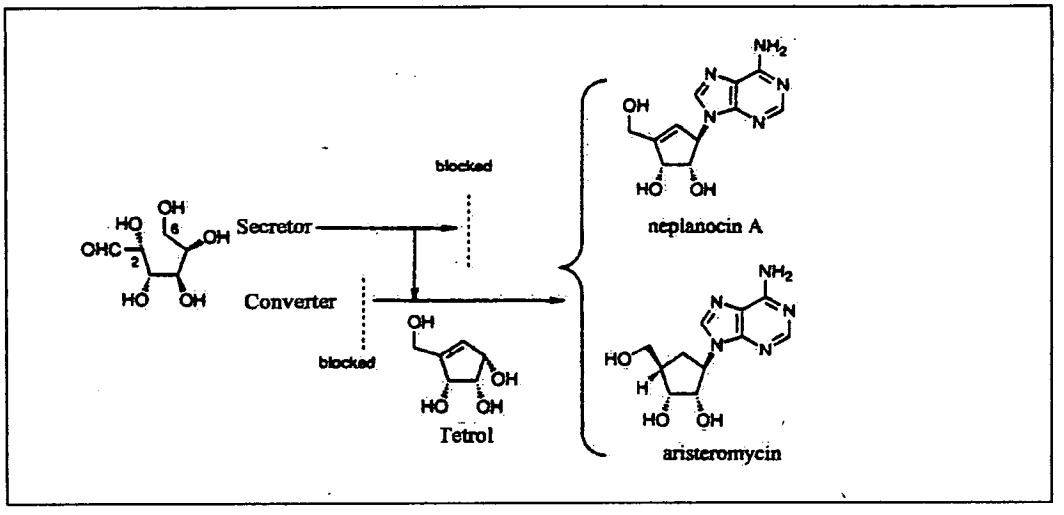


Not much is known about other intermediates on the pathway, though it is speculated that the tetrol may be activated at the C-1 *via* its pyrophosphate, which would allow the introduction of the adenine base. There are two possibilities for the origin of the adenine base of aristeromycin. The adenine ring could be synthesised by the stepwise construction of the purine ring, on a carbocyclic analogue of 5-phosphoribosyl pyrophosphate containing a pre-existing amino group at C-1. Alternatively, the adenine ring could be added directly to a carbocyclic intermediate activated at C-1 by pyrophosphate group. Evidence suggests that the direct incorporation of adenine is the major route to aristeromycin, though this does not eliminate the possibility of a competing *denovo* pathway (Jenkins & Turner 1995).

The co-production of aristeromycin and neplanocin A in cultures of wild type *Streptomyces citricolor* suggested from the outset that they may be closely related on the biosynthetic pathway. In Jenkins work certain mutants of *S. citricolor* could not produce neplanocin A or aristeromycin but were able to convert neplanocin A to aristeromycin (Jenkins & Turner 1995). A mutant of *Streptomyces citricolor*, which produced neplanocin A but no aristeromycin, was fed [6-$^2H_2$]-D-glucose; and 6'-$^2$H-neplanocin A was isolated. 6'-$^2$H-neplanocin A was then fed to a second mutant, which was blocked in the production of both aristeromycin and neplanocin A, but was

able to convert neplanocin A to aristeromycin. 6'-$^2$H -aristeromycin was isolated suggesting that neplanocin A is the direct precursor of aristeromycin (Jenkins & Turner 1995). Parry has produced enzymological evidence which supports this conclusion (Parry & Jiang 1994). A cell free system was prepared from culture of *Streptomyces citricolor*, which was producing aristeromycin. This cell free system was shown to catalyse the NADPH dependant reduction of neplanocin A to aristeromycin. Labelling studies were carried out in the presence of the partially purified enzyme, see fig 6.7. These studies demonstrated that the reaction proceeds with *anti* geometry and involves the transfer of the *pro*-R hydrogen atom of NADPH to the 6'-β-position of aristeromycin, see fig 6.7. The stereochemistry of the double bond is anti. The reaction proceeds with the addition of the hydride to the double bond in an anti Markovnikov fashion. It has been suggested that the mechanism of the conversion may involve initial oxidation of C-5' hydroxymethyl group to an unsaturated aldehyde, followed by the conjugate reduction, and the reduction of the unsaturated aldehyde with NADPH, and finally reduction the aldehyde moiety to the primary alcohol.

**Fig 6.7 Results of labelling studies**

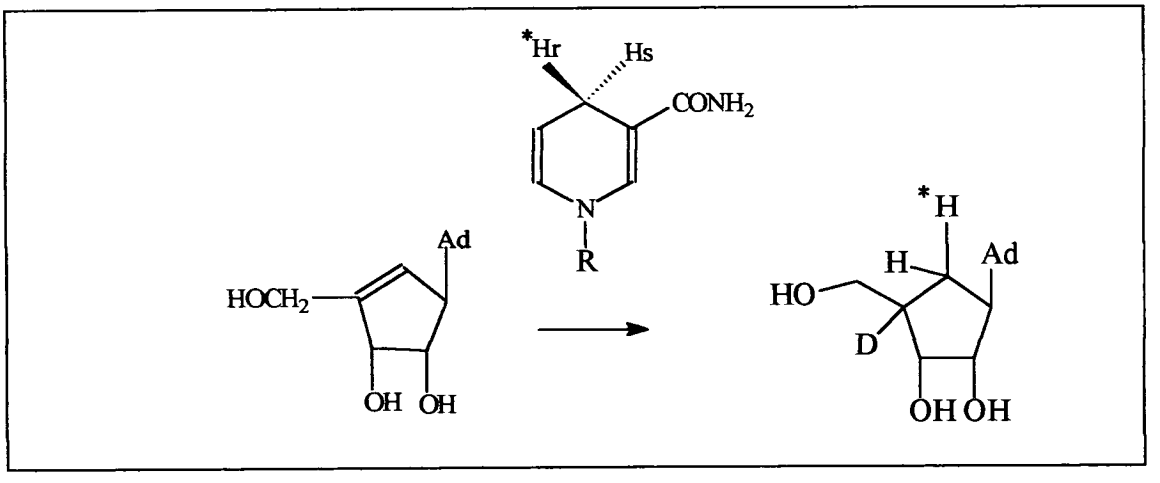


From these studies Jenkins suggested a route; D-glucose → enone → tetrol → neplanocin A → aristeromycin, (Jenkins & Turner 1995) see fig 6.8. D-glucose, tetrol, and neplanocin A have all been shown to be intermediates on the pathway, but the enone is only a proposed intermediate.

**Fig 6.8 The proposed biosynthetic pathway of aristeromycin production (Jenkins & Turner 1995)**

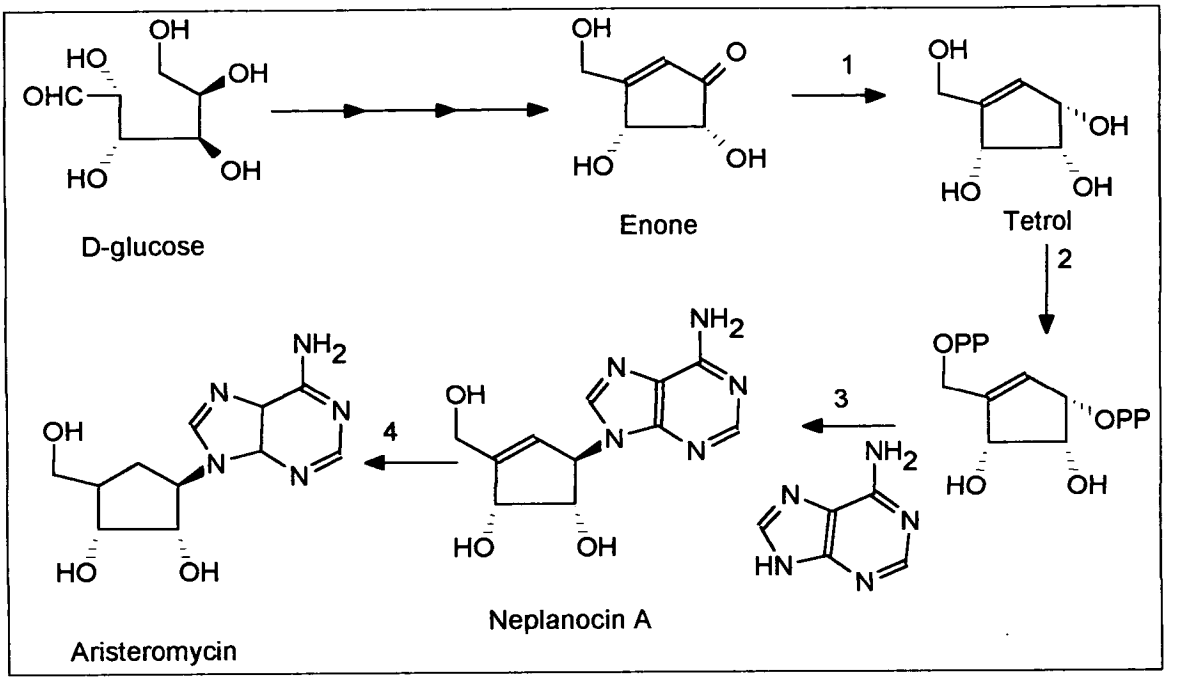


It has been suggested that the aristeromycin pathway may be similar to the O-nucleoside pathway, since coupling of the tetrol and adenine to give neplanocin A could proceed *via* carbocyclic analogues of ribose-5-phosphate and 5-phosphoribosyl-α-1-pyrophosphate (PRPP). Enzymological studies have been carried out on the third defined step, step 2 in fig 6.8, using 5-phosphoribosyl-α-1-pyrophosphate (PRPP) synthases (Nilsson & Hove-Jensen 1987). PRPP synthases catalyse the reaction of ribose-5-phosphate with ATP in the presence of magnesium ions to form 5-phosphoribosyl-α-1-pyrophosphate and AMP. It was therefore suggested that a homolog of PRPP synthases may be used in the biosynthetic pathway. The cyclopentyl analogue of ribose-5-phosphate was synthesised and its behaviour with various PRPP synthases was investigated. However the carbocyclic analogue of ribose-5-phosphate proved not to be a substrate for PRPP synthase, in fact it acted as an inhibitor. Moreover the cyclopentyl analogue showed quite diverse inhibition behaviour against a variety of PRPP synthases (Parry *et al.* 1996).

## Natural product biosynthesis

A major goal of natural product studies is to isolate the enzymes involved in the pathway, and clone their respective genes. Therefore, an initial problem is how to assay for and isolate the enzymes on the pathway. Natural product biosynthesis is frequently a multi-step process, often involving 15-20 gene products. The biosynthetic genes in many biosynthetic pathways are clustered together on the genomic DNA, in what is known as a biosynthetic operon (Roessner & Scott 1996). When the natural product is an antibiotic; the producing organism must have a mechanism of resistance to its own antibiotic. The gene encoding the resistance mechanism is situated on or near the biosynthetic operon, of all the biosynthetic pathways isolated so far. The mechanisms of resistance can take various forms such as the modification of the target site, confinement of the antibiotic to discrete subcellular compartments or the production of them as inert derivatives to be activated during or following export. It maybe a membrane transport enzyme, which would pump the natural product outside the cell. The resistance may also be that the antibiotic undergoes some form of chemical modification such as phosphorylation or acelylation, once it is produced (Cundliff 1984). Often an organism can have multiple resistance genes, incorporating a variety of mechanisms of resistance to an antibiotic. The problem in natural product biosynthesis is to understand all the enzymes present on the biosynthetic pathway. There are numerous methods for gaining an insight into the enzymes situated on the biosynthetic pathway. These include labelling studies to examine the progression of intermediates along the pathway. Isolation and characterisation of individual enzymes on the pathway, which can then give an insight into the catalytic mechanism.

There are also many reasons for cloning an entire biosynthetic pathway. Natural product biosynthesis pathways can be engineered to enhance production or product diversity. Unnatural products may be obtained by supplying unnatural substrates. Limitations *in vivo* (*i.e*, cell toxicity, lack of substrate uptake), may be overcome *in vitro*. Competing pathways can be overcome *in vitro* by using purified enzyme or a large excess of the required enzymes. Inactivating the enzyme that normally uses the

intermediate as a substrate, either by mutating it *in vivo*, or omitting it *in vitro* can induce the accumulation of intermediates. New products may be produced by introduction of genes from heterologous organisms *in vivo*, or by addition of the corresponding enzyme *in vitro*. This may also reduce problems of expression, toxicity and unfavourable culture conditions. Product inhibition may be overcome by replacing regulatory enzymes with isozymes, either naturally occurring or genetically altered, so that they do not exhibit feedback inhibition. Combinatorial biosynthesis is an important result of genetically engineered biosynthetic pathway, where enzymes which have been isolated and characterised these are combinatorially reconstructed to produce libraries of novel compounds which are appropriate for use in screening new drugs, see fig 6.9 (Roessner & Scott 1996). An initial early success in this field by Whiteside and Wong (Wong & Whiteside 1980) who developed the concept of reconstituting a pathway or mixing enzymes from interlinking pathways. They used commercially available enzymes to synthesise ribose-5-phosphate and ribulose-1,5-diphosphate from glucose.

**Fig 6.9 Genetic engineering of natural product biosynthesis (Roessner & Scott 1996)**

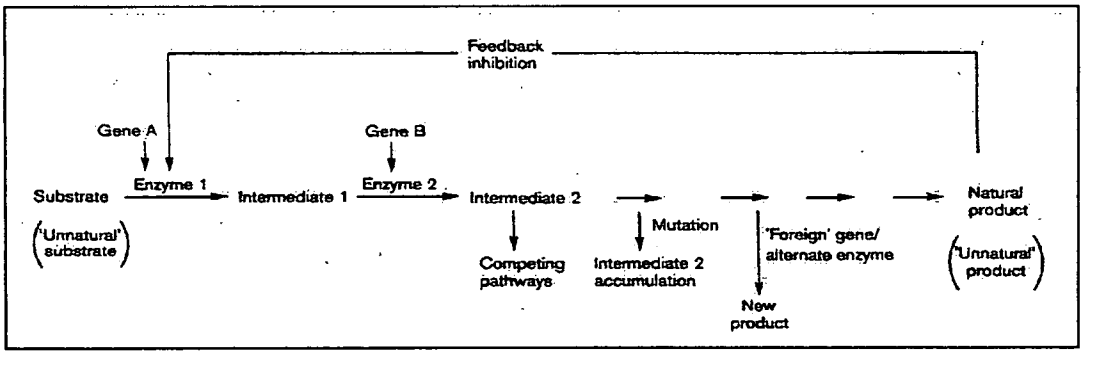


The most successful examples of cloning entire natural product biosynthetic pathways have come from *Streptomyces* and related filamentous bacteria. Many *Streptomyces* produce polyketide natural products. Streptomyces produce over 50% of the clinically known antibiotics. They include antibiotics, anticancer agents, immunosuppressants, antiparasitic agents, antifungals and cardiovascular agents. The

enzymes which catalyse the construction of these molecules are known as polyketide synthases (PKSs). PKSs are multi-enzyme assemblies which catalyse the repeated decarboxylative condensations between coenzyme A thioester. In this way PKSs are similar to fatty acid synthases (FASs) which undergo a similar reaction. The FASs then undergo a full reductive cycle, which consists of a keto reduction, dehydration and enoyl reduction on the β-keto group of the chain. However, unlike FASs PKSs often omit this cycle or shorten it. After the carbon chain of the polyketide has grown to the required length, it is released from the synthase by thiolysis or acyltransfer. The variation among different polyketides is achieved by variations in chain length, chain building units and the differences in the reductive cycles (Khosla & Zawada 1996).

Many polyketide biosynthetic pathways have been cloned and characterised. The cloning of these pathways has enabled combinatorial biosynthesis to be carried out giving rise to novel polyketides that can be either modified further or screened to identify promising drug leads. An important factor is that polyketide enzymes are similar in many ways and contain many conserved motifs, which have similar DNA sequences. These conserved DNA sequences can be used to probe other polyketide producing organisms to enable the isolation of the gene cluster that encodes for their biosynthetic pathway. Therefore, as more polyketides biosynthetic pathways are cloned this leads in turn to it being easier to clone further pathways. An example of combinatorial synthesis being applied to a system is the biosynthetic pathway which catalyses the formation of 6-deoxyerythronolide B (6-dEB). This is catalysed by DEBS synthases 1, 2 and 3, each compromising of two modules. Each module contains a full complement of sites required for one condensation, an acyl transferase, along with a subset reductive active site. Various genetic manipulations and feeding of novel compounds have been performed leading to a variety of products, see fig 6.10 (Khosla & Zawada 1996)

**Fig 6.10 Genetic Manipulations of 9-deoxyerythronolide B synthase (DEBS) genes (Khosla & Zawada 1996)**

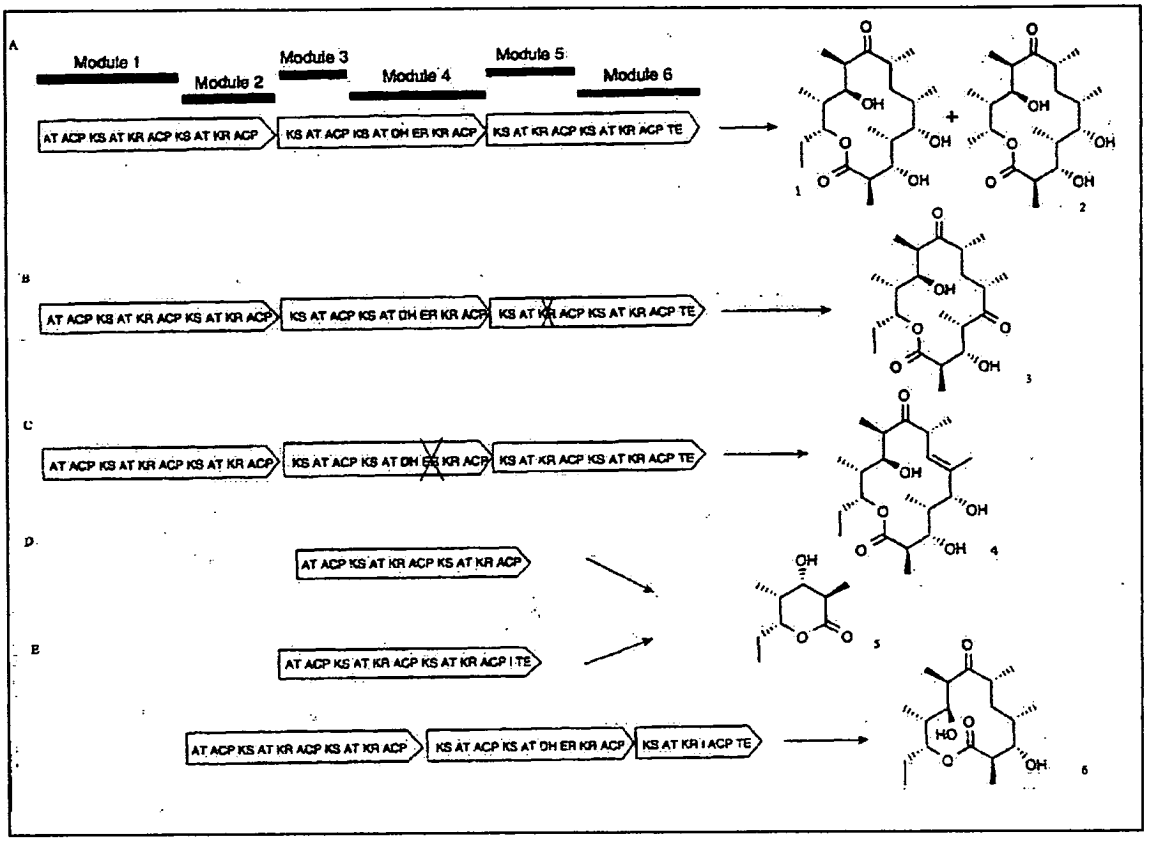


Various other classes of compounds biosynthetic pathways have been cloned, though the most common class is polyketides. One of the most recent biosynthetic pathways to have been cloned is the antitumor antibiotic mitomycin C from *Streptomyces lavendulae*. Probing with *rif*K gene, encoding the rifamycin AHBA synthase from *Amycolatopis mediterranei* (Kim *et al.* 1998) identified the mitomycin C gene cluster. The *rif*K gene was used because mitomycin C is in part derived from 3-amino-5-hydroxybenzoic acid (AHBA), a precursor that is also required for the biosynthesis of the ansamycin antibiotics, including rifamycin. The biosynthetic operon consists of a cluster of forty-seven genes spanning fifty-five kilobases of DNA. The putative mitomycin C pathway regulator has been manipulated, which has led to an increase in the drug production (Mao *et al.* 1999)

## Aims of this project

The aim of this work was to isolate an enzyme whose gene would be situated on the aristeromycin biosynthetic operon in *S. citricolor*. Once the enzyme has been purified, determination of the N-terminal sequence would lead to the design of a degenerate DNA oligonucleotide, and used to probe *S. citricolor* chromosomal DNA. However, unlike many biosynthetic pathways which have recently been cloned, the aristeromycin pathway has the disadvantage that there is not a common probe, for example an acyl carrier protein as in the polyketide biosynthetic pathways, whose N-terminal sequence can be used as a probe for *S. citricolor* DNA. Possible targets in the aristeromycin biosynthetic pathway include the neplanocin A to aristeromycin converting enzyme. Parry (Parry & Jiang 1994) has carried out initial enzymatic studies on this stage of the pathway. Another possible target is an aristeromycin resistance protein, as this could possibly be situated on the biosynthetic operon. To enable the possible isolation of the biosynthetic operon of aristeromycin, chromosomal DNA would need to be packaged into cosmids. A cosmid is a circular piece of DNA, which can hold very large fragments of DNA up to 40Kbp. If a cosmid is isolated which contains the target gene, the cosmid may contain part or the whole of aristeromycin biosynthetic operon. The cosmid would be sequenced and one could "walk down" the operon looking for open reading frames, for the enzymes involved in the biosynthetic pathway. Recognition of known sequence motifs for example nucleotide binding sites *e.t.c* may enable the tentative assignment of function, see fig 6.11.

**Fig 6.11 Procedure for isolating the biosynthetic operon**

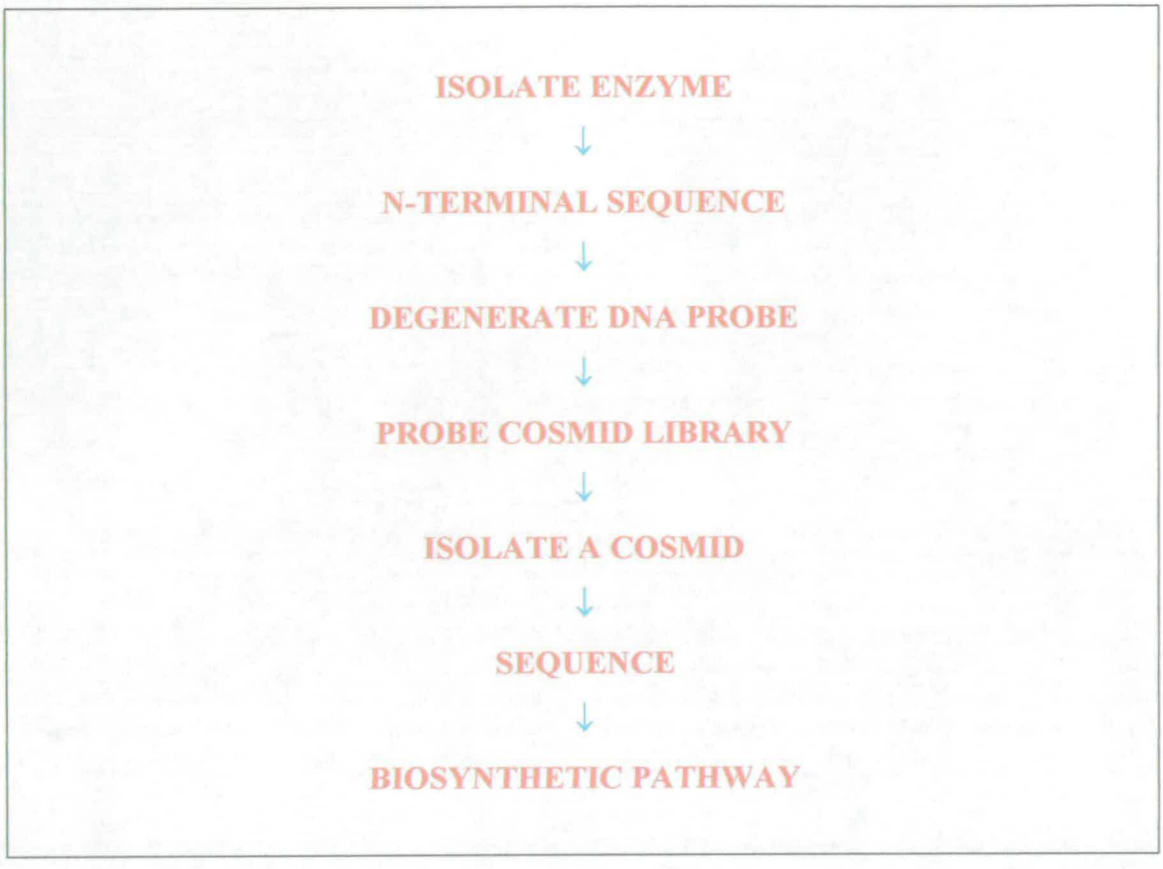

# Chapter 7 (*S. citricolor*)

# Materials & Methods

Any methods which were used in *S. citricolor* project but are not stated here, have been previously stated previously in *chapter 2.*

## Materials

The wild type and mutants of *Streptomyces citricolor* were complimentary from Glaxo.

All other reagents were supplied as stated in *chapter 2*:

## Cell Lines

| Cell Line | Characteristics |
|---|---|
| *Streptomyces citricolor* (cc2667) | Wild type |
| *Streptomyces lividans* | Wild type |

## Oligonucleotides

| Name | Sequence |
|---|---|
| AIP 1 | TCC TTC CAG CTG CCG CCG CTG CTG |
| AIP 2 | TCS TTC CAG CTS CCS CCS CTS CTS |
| AIP 3 | TCS TTC CAG CTS CCS CCS CTS CTS TAC BVS GAS TAC GAC |

B = T + C + G

V = A + C + G

S = C + G

## Growth of *Streptomyces citricolor*

Spore suspension (vol = 1% culture volume) was added to the required media in sterile conditions. 250ml baffled flasks containing 50ml of the required media were used and grown at 30°C with shaking at 225rpm (3-4 days).

GNY Media

| | |
|---|---|
| 20mls Glycerol | |
| 8g Nutrient Broth | per litre |
| 3g Yeast | |
| 5g $K_2HPO_4$ | |

GAM 6.6

| | |
|---|---|
| 60g Glucose | |
| 60g Arkasoy 50 | per litre |
| 21g MOPS | (tap water) |
| 25mg Uracil | adjust pH to7.5 |

autoclave at 121°C for 20mins, stir immediately after autoclaving.

To assess if the culture was uncontaminated, a sample of *Streptomyces citricolor* (10µl) was examined by a light microscope (×40 magnification).

Agar plates, were prepared pouring approx. 40ml of required agar per plate. 100µl of the culture of bacterium was spread over the plate in sterile conditions, and the plate incubated at 30°C (3-4 days)

T/O Agar

| | |
|---|---|
| 20g Tomato puree | per liter |
| 20g Fine milled oatmeal | make in tap water |
| 5g Yeast Extract | adjust pH 7.0 |
| 15g Agar | |
| 25mg Uracil | |

### *Streptomyces citricolor* spore suspension

T/O agar plates of *S. citricolor* were incubated at 30°C until sporulation had occurred (3-4 days). The plate was then covered with sterile water (9mls). Spores were scraped from the plate to form a suspension. This was then sterile filtered, and

centrifuged (3 000 rpm, 15 min). The resulting pellet was resuspended in sterile water (1ml). Spore suspensions were stored at -20°C for future use.

## HPLC analysis

HPLC analysis was used to detect the presence of neplanocin A and aristeromycin. A solution of aristeromycin (1mg/ml) and neplanocin A (1mg/ml) was used to standardize the procedure, when the analysis was carried out.

| | |
|---|---|
| Stationary phase | ODS2 C18 reverse phase (sphericlone) |
| Mobile phase | 97% 50mM ammonium formate buffer pH 3 |
| | 3% acetonitrile |
| Flow Rate | 1ml/min |
| Detection | UV@ 260nm |
| Retention time | 6.6 mins neplanocin A |
| | 9.0 mins aristeromycin |

## Purification of 27kDa aristeromycin induced protein (AIP)

*S. citricolor* was grown in GNY media (1l) in the presence of aristeromycin (100μg/ml). The cells were resuspended in buffer A (50mM Tris, pH 7.5) and were lysed by nebulization. The cell free extract was filtered and applied to a Q-Sepharose column and eluted with a gradient of 0-1M NaCl, using buffer B (buffer A + 1M NaCl). The resulting fractions were analysed by SDS-PAGE. The fractions containing the 27kDa AIP were collected. These fractions were then applied to a RESOURCE-Q column. The fractions were again analysed by SDS-PAGE, and the 27kDa fraction collected.

## Western blotting

A 15% SDS gel was prepared and the sample was run in all lanes. The gel was soaked in electrolyte buffer (100ml 10* CAPS [100mM CAPS, pH 11], 100ml methanol, 800ml $H_2O$) for 5 mins. The membrane was soaked in methanol (20secs).

The protein was transferred to a membrane using the western blot apparatus, at 50V for two hours. The membrane was rinsed in $H_2O$, and stained with SDS PAGE stain (0.1% coomassie blue R-250, 10%[v/v] methanol, 10%[v/v] acetic acid). The membrane was then air dried and the required protein band was cut out (Maniatis 1989).

## N-Terminal sequencing

Dr. Andrew Cronshaw of the Welmet Protein Characterisation Facility, University of Edinburgh carried out this service (Hayes *et al.* 1989). The sequencing was accomplished using the Edman degradation method.

## Southern blotting (Southern 1975)

*Protocol for capillary blotting from agarose gels*

The DNA sample was separated on a 0.8% agarose gel. The DNA was visualized with UV light and photographed. The position of DNA was marked using ink. The gel was then processed for blotting which involves a number of steps:

1. *Denaturation*: the gel was submerged in denaturation buffer (1.5M NaCl, 0.5M NaOH) for with gentle agitation (30 minutes).
2. *Neutralisation*: the gel was placed in neutralisation buffer (1.5M NaCl, 0.5M Tris base, pH 7.5), for with gentle agitation (30 minutes).

Between each step the gel was rinsed with distilled water.
A nylon membrane (Hybond-N, Amersham) was cut to the size of the agarose gel. A tray was half filled with 20*SSC (300mM Tri sodium citrate, 150mM NaCl, pH7.5). A platform was made and covered with a wick of 3MM paper saturated in 20*SSC. The treated gel was placed on the wick, avoiding air bubbles. The gel was surrounded by cling film. The membrane was placed directly onto the gel on top of

this were placed, three sheets of 3MM paper cut to the size of the gel and saturated in 20*SSC. A stack of absorbent towels was then placed on top of the 3MM paper to a height of 15cm. Finally a weight was place on top of the paper stack. The transfer was allowed to proceed overnight. The DNA was then fixed to the membrane by incubating at 80°C (2 hours).

*Colony lifts*

The cells were plated out in the usual way and incubated overnight. The agar plates were cooled (4°C) for at least an hour before the lift. The nylon membrane was pre-wetted on a blank agar plate. The membrane was then placed on the colonised agar (60 seconds), and the position of the membrane was marked using a pin. The membrane then underwent numerous steps to liberate the DNA. This was achieved by placing the membrane disc colony side uppermost on a series of solution saturated 3MM paper filters:

1. Lysis: 10% (w/v) SDS (3 minutes).
2. Denaturation: denaturation buffer (3 minutes).
3. Neutralization: neutralisation buffer (3 minutes), repeated twice.

The membrane was then washed in 2*SSC. The DNA was fixed by incubating the membrane (80°C) for two hours.

*Hybridisation Protocol*

The membrane was pre-wetted with 20*SSC and then rolled between two nylon meshes and placed in hybridsation tubes. Hybridisation buffer (5*SSC, 5*Denhardt's solution (Manatasis 1989), 0.5% (w/v) SDS,) was added which contained denatured salmon sperm DNA. The membrane was then prehybridized (30 minutes) at an appropriate temperature.

The DNA probe was labeled with 32-[γ]–P, by the following reaction:

| | Volume (µl) |
|---|---|
| 32-[γ]-P-ATP | 5 |
| Kinase | 0.8 |
| 10* kinase buffer | 2 |
| Probe (10pmol) | 1 |
| Water | 11.2 |
| Total | 20 |

The reaction is incubated at 37°C (45 minutes).

The reaction was then applied to a gel filtration column (NICK©, Amersham), to separate the un-reacted ATP from the labeled probe. The labeled probe was collected (400µl) and added to the pre-hybridisation buffer. Hybridization was carried out overnight at an appropriate temperature.

The membrane was then washed with SSC solutions, with increasing stringency. The bolt was wrapped in SaranWrap and exposed X-ray film. The film was exposed for an appropriate length of time, at -80°C. The film was then developed.

## Polymerase chain reaction (PCR)

The template and primer were added in appropriate proportions to Ready To Go PCR beads (Pharmacia Biotech). These were then made up to 25µl as per the manufacturer's instructions, with DMSO (5%-10%v/v) included. The PCR reaction was then carried out in Perkin Elmer DNA thermal cycler, with a typical cycle of 95°C 1min, 54°C 1min and 72°C 1min

## Similarity Searches

DNA and protein similarity searches were carried out using the BLAST program (http://www.ncbi.nlm.nih.gov/blast/blast.cgi?Jform=0).

**Frame analysis**

Frame Plot 2.3 from the *Actinomyces* resource centre (http://www.nih.go.jp/~khotta/saj/) which predicts the most probable translation direction for a sequence.

# Chapter 8 (*S. citricolor*).

# Results and discussion

## Introduction

The aim of this work was to isolate a protein the gene of which was situated within the aristeromycin biosynthetic operon. To achieve this goal a protein needs to be isolated which either catalyses a reaction on the biosynthetic pathway, or is part of a resistance mechanism. To accomplish this, we firstly needed to achieve reproducible growth of *S. citricolor* and production of aristeromycin.

Analysis of the aristeromycin biosynthetic pathway fig 6.8 (Jenkins & Turner 1995), revealed various target enzymes, an obvious candidate is the enzyme which converts neplanocin A to aristeromycin as some enzymological work has already been done by Parry (Parry & Jiang 1994). Parry reported that the conversion of neplanocin A to aristeromycin is an NADPH-dependent enzymatic reaction, and the reaction could be followed by UV/Vis spectroscopy. This method was followed a cell free extract was produced from an aristeromycin producing culture. The reaction was followed by the addition of neplanocin A and NADPH the activity was monitored by the aborbance change of NADPH. The cell free extract was separate by FplC and the reaction monitored through the fractions. A enzyme was isolated which had NADPH activity dependent on the presence of neplanocin A. However, when the reaction was analysed by HPLC there was no conversion from neplanocin A to aristeromycin. This procedure has not been described in the material and method section. Another entry to the biosynthetic pathway would be to isolate an enzyme which activates the tetrol compound by phosphorylation, see fig 6.8 (Jenkins & Turner 1995). Though this is only a proposed step on the biosynthetic pathway, it should be possible to follow the reaction using 32-[γ]–P-ATP as a substrate, as the tetrol would incorporate the 32-[γ]–P, this method was not pursued. The route that was followed was the isolation of a possible aristeromycin resistance protein

## Results

### Growth of *S. citricolor*

Growth of wild type *S. citricolor* (cc2779) was achieved in GAM6:6 medium, with the production of aristeromycin ≥ 0.2mg/ml. The production of aristeromycin was found to be very dependent on the aeration of the growing cells. If the cells were resuspended into fresh medium the production of aristeromycin ceased. Fig 8.1 shows aristeromycin production curve for *S. citricolor* grown in GAM 6:6, the production of aristeromycin was monitored by HPLC. Unfortunately it was not possible to determine the growth curve of *S. citricolor*, because the media contains particulate materials which decrease as *S. citricolor* grows and which make it very difficult to monitor the optical density or to measure the dry weight of cells produced.

**Fig 8.1 Aristeromycin production by *S. citricolor* in GAM 6:6 medium measured by HPLC**

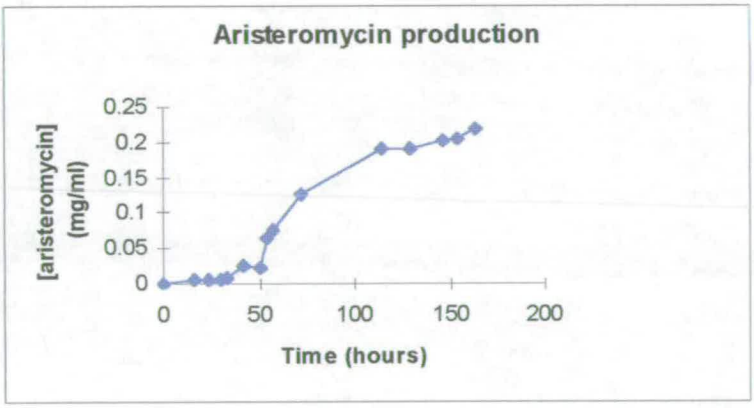


*S. citricolor* was grown in a variety of other media including GNY and GAC 1, but no production of aristeromycin was observed. Rapid cell growth was observed in GNY media.

### Expression of an aristeromycin inducible protein (AIP)

*Streptomyces citricolor* was grown in GNY media with the addition of varying amounts of aristeromycin (10µg/ml-500µg/ml), and the protein content of the cells was determined by SDS PAGE. At aristeromycin concentrations of between 50-

100μg/ml the overexpression of two additional proteins at 27kDa and 42kDa was observed. These proteins were not observed when there was no aristeromycin present. When *S. citricolor* was grown with varying concentrations of neplanocin A (10μg/ml-500μg/ml) the 42kDa protein was observed but the 27kDa absent.

As a control experiment, to determine whether these proteins were expressed as a result of general antibiotic stress, *S. citricolor* was grown in GNY media with a variety of other antibiotics; ampicillin, kanamycin and chloramphenicol at varying concentrations (10μg/ml-500μg/ml). *S. citricolor* did not grow in the presence of chloramphenicol, and it had limited growth in the presence of ampicillian and kanamycin. Examination of the cellular extracts showed that there was no expression of either the 27kDa or the 42kDa proteins. *S. citricolor* was also grown in the presence of adenine and adenosine (10μg/ml-500μg/ml) and here again the 27kDa and 42kDa band were not observed. To determine if this was a species specific response, *Streptomyces lividans* was grown in the presence of aristeromycin and neplanocin A (10μg/ml-500μg/ml), but neither the 27kDa and 42kDa bands were observed.

## Purification & N-terminal sequence of the 27kDa aristeromycin induced protein (AIP)

The 27kDa protein which was only induced by the presence of aristeromycin was more strongly expressed than the 42kDa protein, and was therefore the obvious target for isolation. The 27kDa protein was purified by two ion exchange chromtaography steps, using Q-Sepharose and RESOURCE Q leading to an extract containing the 27kDa protein which was pure enough to obtain an N-terminal sequence, see fig 8.2.

**Fig 8.2 SDS-PAGE of the purification stages of the AIP 27kDa protein**

The growth of *S. citricolor* and the purification of the AIP 27 kDa protein is described in chapter 7 *Materials & Methods*. Lane 1 Standard 94 67 43 30 20.1 14.4kDa, Lane 2 CFE of *S. citricolor* no aristeromycin, Lane 3 CFE of *S. citricolor* 100ug/ml aristeromycin, Lane 4 CFE of *S. citricolor* 100ug/ml aristeromycin after Q-Sepharose, Lane 5 CFE of *S. citricolor* 100ug/ml aristeromycin after RESOURCE Q

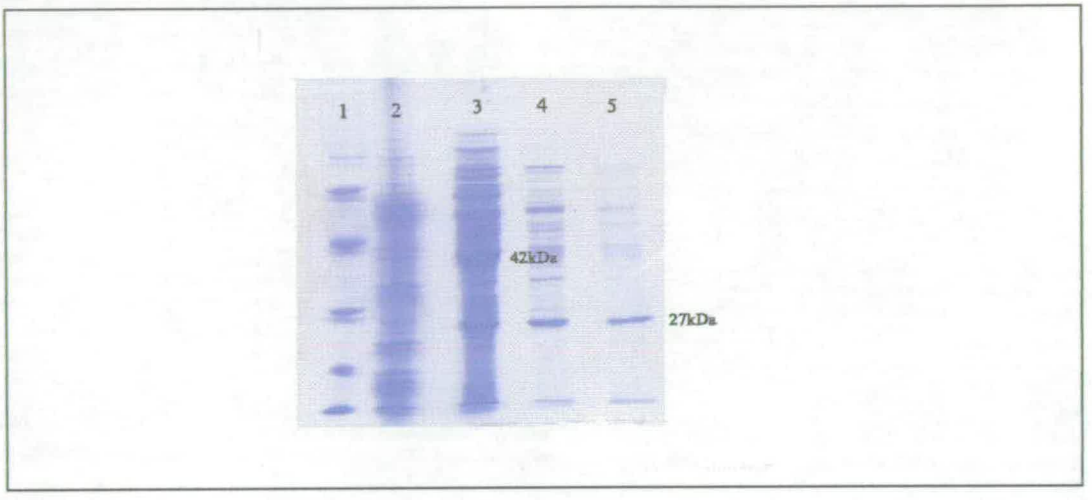


After the final purification step on a RESOURCE Q column the 27kDa protein was transferred to a nitrocellulose membrane (western blot), and its N-terminal sequence was determined by the Edman degradation method, see fig 8.3.

**Fig 8.3 The N-terminal sequence of 27kDa AIP**

| 1 | 2 | 3 | 4 | 5 | 6 | 7 | 8 | 9 | 10 | 11 | 12 |
|---|---|---|---|---|---|---|---|---|---|---|---|
| ? | S | F | Q | L | P | P | L | L | Y<br>P<br>G | D<br>E | Y |

| 13 | 14 | 15 | 16 |
|---|---|---|---|
| D | E<br>G | E<br>L<br>L | S<br>E |

From this N-terminal sequence three DNA probes were designed. The codon choice was determined using the *Streptomyces* preferential codon usage (ref hhttp ://www .nih.go.jp /~jun/act /codon /104.gcg). AIP 1 probe was based on the first eight amino acids and was non-degenerate, the sequence was based on the most preferred codon

usage for *Streptomyces*. AIP 2 was again based on the first eight amino acids but was degenerate, incorporating all possible codon *Streptomycetes* usage of *S. citricol*or. AIP3 was similar to AIP 2 but incorporated the next two amino acids in the N-terminal sequence.

**Table 8.1 Probes designed from the N-terminal sequence of the AIP protein**

Amino acids are represented in blue and the codons are represented in pink.

B = T + C +G, V = A+ C + G, S = C + G

| | | | | | | | | |
|---|---|---|---|---|---|---|---|---|
| AIP 1 | S<br>TCC | F<br>TTC | Q<br>CAG | L<br>CTG | P<br>CCG | P<br>CCG | L<br>CTG | L<br>CTG |
| AIP 2 | S<br>TCS | F<br>TTC | Q<br>CAG | L<br>CTS | P<br>CCS | P<br>CCS | L<br>CTS | L<br>CTS |
| AIP 3 | AIP 2 + Y/P/G<br>BVS | | | D/E<br>GAS | | | | |

## Isolation of 1000bp fragment of *S. citricolor* DNA

*S. citricolor* chromosomal DNA which had been prepared by Dr. Gareth Roberts was cut with the restriction endonucleases *Sma* I, *Sac* I and *Pst* I, and the DNA was size separated on an agarose gel. The DNA was transferred to a nitrocellulose membrane, and hybridised against the probes. Hybridisation was attempted using AIP 1, AIP 2 and AIP3 at various temperatures and washing conditions. The aim was to achieve a single hit, where a single band lit up on the autoradiograph. This was eventually achieved under the following conditions:

| | |
|---|---|
| Probe | AIP 3 |
| Hybridization temperature | 62°C |

Washing conditions

| | [Buffer] | Temperature | Time (mins) |
|---|---|---|---|
| 1 | 2 × SSC | RT | 2 |
| 2 | 2 × SSC | 62°C | 5 |
| 3 | 1 × SSC | 62°C | 5 |
| 4 | 0.5 × SSC | 62°C | 5 |
| 5 | 0.2 × SSC | 62°C | 5 |
| 6 | 0.2 × SSC | 62°C | 5 |
| 7 | 0.1 × SSC | 62°C | 5 |

A band at 1000bp on chromosomal DNA which had been cut with *Sma* I showed on the radiograph, see fig 8.4

**Fig 8.4 Autoradiograph of *S. citricolor* chromosomal DNA cut with restriction endonucleases and probed with AIP 3**

Lane 1, *S. citricolor* chromosomal DNA cut with *Pst* I, Lane 2 *S. citricolor* chromosomal DNA cut with Sma I, Lane 3 PCR standards 2000bp, 1500bp, 1000bp, 900bp, 800bp, 700bp, 600bp,

*S. citricolor* chromosomal DNA was cut with *Sma* I and size seperated on an agarose gel. A band at 1000bp was cut out and gel eluted from the agarose gel, see fig8.5.

**Fig 8.5.a** Lane 1, λ Hind III standards 23 130, 9 460, 6557, 4361, 2311, 2027, 564, 124bp, Lane 2 PCR markers 2000, 1500, 1000, 900, 800, 700, 600, 500., Lane 3 *S. citricolor* chromosomal DNA cut with *Sma* I

**Fig 8.5 b** Lane 1, λ Hind III standards 23 130, 9 460, 6557, 4361, 2311, 2027, 564, 124bp, Lane 2 PCR markers 2000, 1500, 1000, 900, 800, 700, 600, 500., Lane 3 *S. citricolor* chromosomal DNA cut with *Sma* I, with 1000bp band cut

**Fig 8.5 a** **Fig 8.5 b**

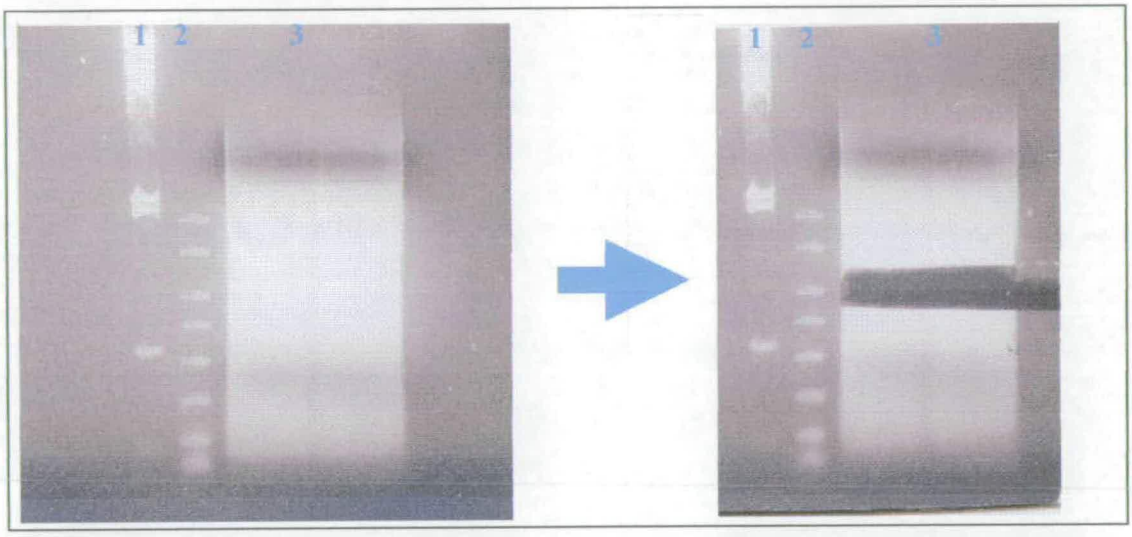


The 1000bp fragment of *S. citricolor* DNA cut with *Sma* I was ligated with pUC 18 cut with *Sma* I (Yanisch-Perron *et al.* 1985). The *E. coli* strain TOP10 One Shot™ was used for transformation of the ligation mixes. Ten plates were obtained from the pUC18/1000bp clones. The DNA from these colonies were transferred to a nitrocellulose membrane and a hybridisation with AIP 3 was carried out using the same conditions as those used to previously isolate the single 1000bp band of *S. citricolor* chromosomal DNA cut with *Sma* I. The autoradiograph showed numerous positive spots, and which were then correlated with the original colonies on the plate. The colonies which matched the spots on the autoradiograph were picked, and the plasmids contained in these colonies were isolated. The isolated plasmids were then cut with *Sma* I and separated on an 0.8% agarose gel and transferred to a

nitrocellulose membrane. Hybrisation was carried out with AIP 3 using conditions established previously. This step was repeated numerous times until a plasmid was isolated containing the 1000bp fragment which gave a positive hit on the autoradigraph.

## Characterisation of the 1000bp DNA fragment

The isolated positive clone was then cut with *Sma* I, showing two DNA fragments at ~900bp and ~1000bp. This plasmid was transformed into Top 10 One Shot™ cells. Ten of the resulting colonies were picked and the plasmid DNA prepared and again cut with *Sma* I and separated on a 0.8% agarose gel, see fig 8.6.

**Fig 8.6 Plasmid DNA cut with *Sma* I from transformed positive colonies**

Lane 1 λ Hind III standards 23 130, 9 460, 6557, 4361, 2311, 2027, 564, 124bp, Lane 2 clone 1, Lane 3 clone 2, Lane 4 clone 3, Lane 5 clone 4, Lane 6 clone 5, Lane 7 clone 6, Lane 8 clone 7, Lane 9 clone 8, Lane 10 clone 9, Lane 11, clone 10, Lane 12 PCR markers 1000, 900, 800, 700, 600, 500.

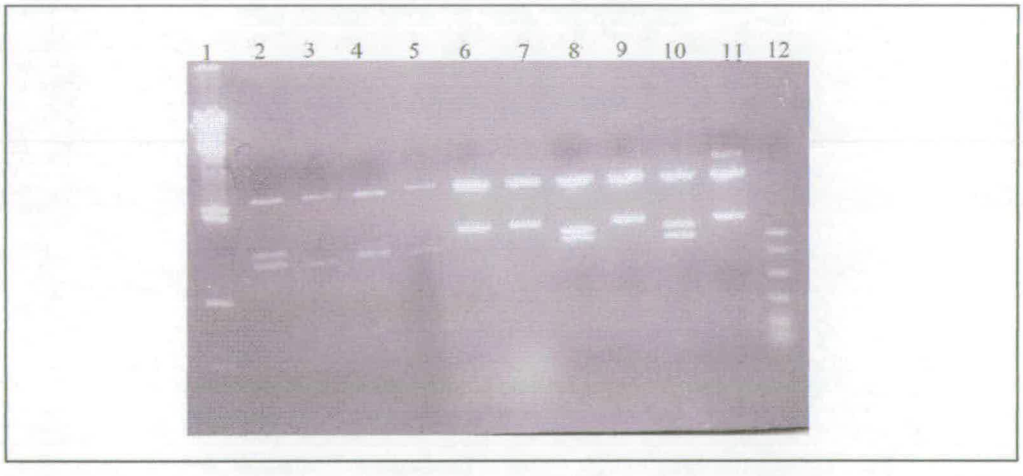


The plasmids prepared proved to be a mixture of clones which contained either a single insert or double insert, see fig 8.6. The DNA was transferred to a nitrocellulose membrane, and hybridisation was carried out. Clone 9 (fig 8.6 lane 10), showed a positive result, this clone was cut with *Sma* I it showed a double insert. This clone obviously needed further investigation. Southern blotting procedure was inconclusive and it was difficult to determine which clone corresponded to the positive band. The clones in lane 9 and lane 11, clones 8 and 10 respectively, were

sequenced by Sanger dideoxy chain termination method. The frame which the DNA was translated into was analysed by Frame Plot 2.3 from the *Actinomyces* resource centre (http://www.nih.go.jp/~khotta/saj/). The resulting protein sequence showed similarity to glutathione reductase proteins from various organisms. The N-terminal sequence was not present in the translated DNA sequence or the DNA sequence.

Clone 9 was cut with *Eco* RI and *Hind* III whose sites on pUC18 are situated either side of the *Sma* I site. Therefore these will lift out the whole insert. The DNA was size separated on an agarose gel, and a band at 2kbp was observed. This band was cut out of the agarose gel and gel eluted. The resulting DNA was then cut with *Sma* I, two fragments resulted at ~900bp and ~1000bp. Clone 9 was then cut with *Sma* I and the resulting fragments were separated on an agarose gel, both the ~900bp and ~1000bp fragments were cut out of the agarose gel and gel eluted. Each fragment was cloned into pUC 18, some of the resulting colonies were isolated and the plasmid DNA prepared and cut with *Sma* I. The cut DNA was transferred to a nitrocellulose membrane and hybridisation was carried out using the established conditions. The 1000bp fragment gave a positive result. This fragment was then sequenced by the Sanger dideoxy chain termination method. A PCR reaction was carried out using AIP 3 (5′ TCSTTCCAGCTSCCSCCSCTSCTSBVSGAS 3′) oligonucleotide as a primer in two separate reactions with the pUC 18 forward (NR 5′ CGC CAG GGT TTT CCC AGT CAC G 3′) and reverse primers (M13 5′ GTT GTG TGG AAT TGT GAG CGG 3′). A band at 300 bp was observed, see fig 8.7.

**Fig 8.7 Gel of amplified positive 1000bp fragment by AIP3 pUC 18 forward primer (NR)**

Lane 1 Amplified fragment using the primer NR & AIP 3, Lane 2 PCR markers 1000bp, 900bp, 800bp, 700bp, 600bp, 500bp, 400bp, 300bp, 200bp

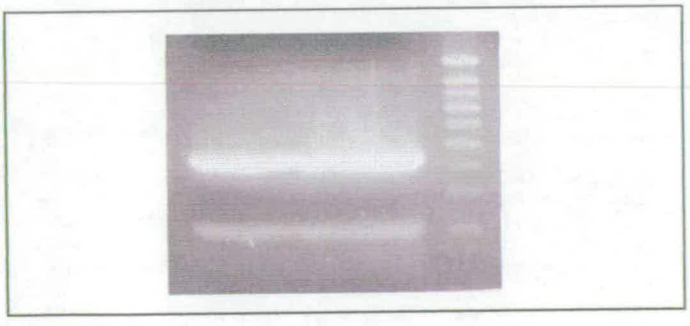

The sequence was determined by the Sanger dideoxy chain termination method. The position of the oligonucleotide sequence of AIP 3 is at 300bp into the sequence, and has 64% identity with the determined sequence, see fig 8.8. However, it does not translate to the N-terminal sequence, which was determined for the aristeromycin induced protein. The sequence was determined to translate in the 3`-5` direction by Frame Plot 2.3 from the *Actinomyces* resource centre (http://www.nih.go.jp/~khotta/saj/), which predicts the most probable translation direction for a sequence. The sequence does not contain an open reading frame, but when translated in the 3`-5` direction it gave a sequence of amino acids with no stop codons. Conversely, when translated into the other five frames the sequence was littered with stop codons and very improbable sequences. Sequence alignment studies were carried out, and the translated sequence corresponds to various AMP binding proteins. There is also similarity to some proteins in the database of unspecified functions.

**Fig 8.8 Diagramatic representation of 1000bp fragment of DNA isolated**

The blue line represents the positive 1000bp fragment of isolated *S. citricolor* DNA; the fragment is cloned into the vector pUC18 which is not shown here. The red arrows represent the pUC 18 forward primer (NR) and the reverse primer (M13). The red line represents the AIP 3 probe, showing where it anneals to *S. citricolor* positive DNA fragment. The pink arrow represents the direction of translation.

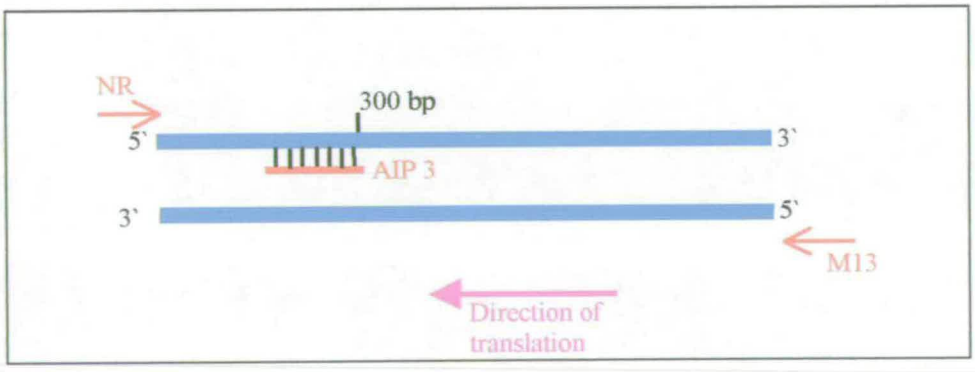

## Discussion

The aim of this project was to isolate a protein whose gene would be situated on the aristeromycin biosynthetic operon. This is a difficult task as there is not a common probe for the aristeromycin biosynthetic pathway unlike the polyketide pathways, which could be used to probe *S. citricolor* chromosomal DNA. Many polyketide biosynthetic operons have been isolated and many of the genes present in these operons are similar. Therefore a common enzyme involved in polyketide biosynthesis can be used to probe the chromosomal DNA of another species which produce a different polyketide, and so can provide an entry into the biosynthetic pathway. For example the rapamycin biosynthetic genes were identified by hybridisation using DNA from the polyketide synthase genes from *Saccharopolyspora erthraea* that govern the biosynthesis of polyketide erythromycin A (Schwecke *et al.* 1995, Cortes *et al.* 1990, Donadio *et al.* 1991).

In the initial phase of this study Dr. G. Roberts adopted this approach of using a gene of an enzyme from another organism which may be present on the pathway. He used the gene of adenine phosphoribosyl transferase from *Streptomyces ceolicolor* (Chakraburtty *et al.* 1996), which catalyses the reaction of 5-phosphoribosyl-1-pyrophosphate with adenine to form adenosine monophosphate, as a probe for the aristeromycin biosynthetic operon. There is a proposed carbocyclic equivalent reaction at step 3 of the aristeromycin biosynthetic pathway (fig 6.8). The tetrol is activated as the pyrophosphate and is then converted to the carbocyclic analogue of adenine monophosphate. This is the same reaction as catalysed by adenosine phosphoribosyl transferase but using the carbocyclic analogue of ribosyl-1-pyrophosphate. When G. Roberts probed *S. citricolor* chromosomal DNA, he found that a number of bands were giving a positive hit, and one band in particular was very strong. He then probed the *S. citricolor* cosmid library which we had constructed. When the positive cosmids were isolated and sequenced they were found to have 80% similarity with *S. coelicolor* adenine phosphoribosyl transferase, and it seems likely that the gene identified is that of the *S. citricolor* adenine phosphoribosyl transferase. However, there were other fainter bands which were showing a positive result on the autoradiograph, when the *S. citrcolor* chromosomal

DNA was probed with adenine phosphoribosyl transferase gene. One these may contain the gene or fragment of the gene for enzyme which catalyses the conversion of tetrol-pyrophosphate to neplanocin A. Work is currently underway to identify which of these cosmids may contain the gene, and hence the aristeromycin biosynthetic pathway.

Of course a more specific approach would be to isolate an enzyme whose gene is present on the aristeromycin biosynthetic operon. Various targets were defined in aristeromycin biosynthetic pathway, and the initial target was to isolate the enzyme which converts neplanocin A to aristeromycin. Parry (Parry & Jiang 1994) had already carried out initial studies on this stage of the pathway, and made the observation that the reaction was NADPH dependant. However, Parry did not isolate the enzyme. We attempted to isolate this enzyme using an NADPH $\rightarrow$ $NADP^+$ assay in the presence of neplanocin A. An enzyme which oxidised NADPH in the presence of neplanocin A was partially purified. However, when the reaction products were analysed by HPLC no conversion of neplanocin A to aristeromycin was observed. The only conclusion that can be reached is that the enzyme was NADPH dependant and requires neplanocin A as an allosteric activator. However, we were unable to identify the substrate or product(s), and there is no evidence that this activity is related to the biosynthetic pathway. Consequently this approach was abandoned.

Other targets enzymes on the biosynthetic pathway were considered such as the proposed step where the tetrol is phosphorylated to form the tetrol pyrophosphate. A radioactive assay was considered using the tetrol compound and 32-[γ]–P ATP. However, this assay was never fully developed, due to the shortage of the synthetic tetrol. Another stage in the pathway which was considered was the isolation of the enzyme which converts the tetrol pyrophosphate to neplanocin A. Again this assay was not developed due to the lack of tetrol pyrophosphate. Work on the chemical synthesis of potential intermediates on the biosynthetic pathway is however at an advanced stage, new compounds may lead to new targets for the isolation of enzymes on the biosynthetic pathway.

Since isolation of an enzyme did not appear straightforward (or possible in the short term) another approach was conceived. This was to identify a aristeromycin resistance enzyme from *S. citricolor*. As aristeromycin is an antibiotic it is likely that *S. citricolor* would have a mechanism of resistance to it. The genes for resistance mechanism are often situated on the biosynthetic operon of the antibiotic (Cundliff 1984). The usual method for isolating the resistance enzyme is usually done directly at the DNA level. The *S. citricolor* cosmid library would be transformed into cells which are sensitive to aristeromycin. The cells are then grown on a plate containing aristeromycin, any colonies which grow must contain the cosmid which encodes the mechanism of resistance to aristeromycin. This cosmid could then be isolated, and sequenced in the hope that it may contain part or the whole of the aristeromycin biosynthetic operon. Unfortunately no suitable cell lines were sensitive to aristeromycin, therefore this method could not be pursued. It was found that *S. citricolor* only produced aristeromycin in the complex media GAM 6:6. When grown in defined media such as GNY, a high cell mass was achieved but no aristeromycin production was observed. *S. citricolor* was grown in the presence of varying amounts of aristeromycin in GNY media, and the expression of two proteins at 27kDa and 42kDa was observed. These were not presents when there was no aristeromycin. *S. citricolor* was then grown in the presence of varying amounts of neplanocin A in GNY media and only the 42kDa protein was observed. This suggested that the 27kDa protein may be a fragment of the 42kDa protein. To ascertain whether this response was a general antibiotic stress response, *S. citricolor* was grown with various other antibiotics, but neither of these proteins were expressed. This protein may not necessarily be an aristeromycin resistance enzyme. However, the protein is not induced by the presence of adenosine or adenine, which suggests that it is not part of the purine pathways.

There are relatively few investigations into the biological activity of antibiotics apart from the obvious antibiotic function. However, alternative biological activities such as triggers of gene expression (Murakami *et al.* 1989), differentiation (Sarkar & Paulus 1972) and sporulation (Ozcengiz & Alaeddinoglu 1991, Ristow *et al.* 1975)

have been suggested. The mechanism by which these antibiotics elicit these alternative responses or influence the metabolism of producing or resistant organisms is only partly understood (Demain 1995, Luckner 1990). These alternative biological activities can be rationalised by the idea that antibiotics represent "molecular fossils" that exert their biological activities through ancient conserved sites in macromolecules (Davies 1992). One particular response which is of interest is the trigger of gene expression which has occurred when aristeromycin is added to a non-producing strain of *S. citricolor*.

One study which has been carried out on the induction gene expression by an antibiotic, is using the antibiotic thiostrepton (Murakami *et al.* 1989). Thiostrepton is produced by *Streptomyces azureseus* and its mechanism of action is the prevention of the binding of translational initiation, elongation, and termination factors to the ribosome (Cundliffe 1980). *Streptomyces azureseus* contains ribosomes which are resistant to the antibiotic, and the *tsr* gene encodes for this mechanism of resistance. (Cundliffe 1978, Thompson *et al.* 1982). The *tsr* gene is commonly used as selective marker for the construction of *Streptomycetes* cloning vectors. It was found that, when thiostrepton was added to a *Streptomyces lividans* strain containing the *tsr* gene, it induced the expression of four proteins (Murakami *et al.* 1988). The gene encoding the most strongly expressed protein (*tipA*) was cloned and sequenced, it revealed no similarity to proteins in the databases. The sequence was found to contain a thiostrepton inducible promotor. This was cloned into a separate vector and is now a valuable tool in the study of gene expression *Streptomycetes*. Further studies have been carried out on the other proteins that thiostrepton induces in *Streptomyces lividans* including TipAL and TipAS (Chiu *et al.* 1996, Holmes *et al.* 1993). A protein was purified which was found to be a thiostrepton induced transcriptional activator TipAL. Thiostrepton enhanced binding of TipAL to the promotor catalysed the specific transcription *in vitro* of TipAS. A second gene product of the same open reading frame, consisting of the C-terminal domain of TipAL, is apparently translated using its own in frame initiation site. However, there is no record of what effect thiostrepton has on its producing organism *Streptomyces azureus*.

In an attempt to isolate the 27kDa aristeromycin induced protein, its N-terminal sequence was determined, and used to probe *S. citricolor* chromosomal DNA. When southern blots are performed, it is difficult to determine which positive on the hybridisation film corresponds to which DNA on the membrane. Two clones were sequenced which were in the area of the positive band on the film. The first clone which was sequenced when it was translated into the correct frame had high identity to glutathione reductase from various species. The N-terminal sequence of the 27kDa aristeromycin induced protein was not present in any of the translated frames of the protein, and no similarity to the DNA sequence of the AIP 3 probe was found. The conclusion was reached that the other clone was the positive one. The other clone was sequenced, and the N-terminal sequence of the 27kDa aristeromycin induced protein was again not present in the translated sequence. However a sequence at three hundred base pairs into the DNA was found to have 68% identity to the AIP 3 probe. This was also confirmed by PCR, a reaction was carried out using the AIP 3 probe as a primer and a pUC 18 primer, an amplified fragment of 300 bp was observed.

In conclusion the fragment of *S. citricolor* DNA which was isolated is unrelated to the aristeromycin biosynthetic operon. The probe was too degenerate, with eighteen out of thirty base pairs degenerate. There are over 300 000 possible sequences of the probe. A more specific probe will have to be used, such as the AIP1 probe, because it is non-degenerate and is based on the most frequent codon usage in Streptomycetes. The N-terminal sequence has to be repeated, as there is some doubt as to what certain residues are. This is a relatively new project and there are many potential target enzymes on the aristeromycin biosynthetic pathway which could be isolated and N-terminal sequenced. Probes could then be designed based on these sequences. Cross hybridisation experiments could then be carried out using multiple probes which would give a higher probability of isolating the aristeromycin biosynthetic pathway.

## References

Beck, J., Ripka, S., Sienger, A., Schiltz, E. & Schweizer, E. (1990). The multifunctional 6-methylsalicylic acid synthase gene of penicillium-patulum- its gene structure relative to that of other polyketide synthases. *European Journal of Biochemistry* **192**, 487--498.

Bennett, L. L., Allan, P. W. & Hill, D. L. (1968). Metabolic studies with carbocyclic analogs of purine nucleosides. *Molecular Pharmacology* **4**, 208-217.

Bennett, L. L., Brockman, R. W., Rose, L. M., Allan, P. W., Shaddix, S. C., Shealy, Y. F. & Clayton, J. D. (1985). Inhibition of utilisation of hypoxanthine and guanine in cells treated with the carbocyclic analog of adenosine. *Molecular Pharmacology* **27**, 666-675.

Bennett, L. L., Bowdon, B. J., Allan, P. W. & Rose, L. M. (1986). Evidence that the carbocyclic analog of adenosine has different mechanisms of cytotoxicity to calls with adenosine kinase activity and to cells lacking this enzyme. *Biochemical Parmacology* **35**(22), 4106-4109.

Chakraburtty, R., White, J., Takano, E. & Bibb, M. J. (1996). Cloning, characterisation and disruption of a (p)ppGp synthase gene (relA) of *Streptomyces coelicolor* A3(2). *Molecular Microbiology* **19**, 357-368.

Chiu, M. L., Folcher, M., Griffin, P., Holt, T., Klatt, T. & Thompson, C. J. (1996). Characterisation of the covalent binding of thiostrepton to a thiostrepton-induced protein from *Streptomyces lividans*. *Biochemistry* **35**, 2332-2341.

Cortes, J., Haydock, S. F., Roberts, G. A., Bevitt, D. J. & Leadlay, P. F. (1990). An unusually large multifunctional polypeptide in erthromycin-producing polyketide synthase of *Saccharopolyspora erythraea*. *Nature* **348**, 176-178.

Cundliffe, E. (1978). Mechanism of resistance to thiostrepton in producing organism

*Streptomyces azureus*. *Nature* **272**, 792-795.

Cundliffe, E. (1980). *Ribosomes: structure, function and genetics*, University Park Press, Baltimore.

Cundliffe, E. (1984). Self defence in antibiotic-producing organisms. *Medical Bulletin* **40**(1), 66-67.

Davies, J. (1992). *Molecular Microbiology* **4**, 1227-1232

De-Clercq, E. (1987). S-Adenosylhomocysteine hydrolase inhibitors as broad spectrum antiviral agents. *Biochemical Pharmacology* **26**(15), 2567-2575.

Deiman, A. L. (1995). *Fifty years of antimicrobial: past perspectives and future trends*. Society for general microbiology (Hunter, P. A., Darby, G. K. & Russell, N. J., Eds.), 53, Cambridge University Press, Cambridge.

Donadio, S., Staver, M. J., McAlpine, J. B., Swanson, S. J. & Katz, L. (1991). Modular organisation of genes required for complex polyketide biosynthesis. *Science* **252**, 675-679.

Fernandez-Moreno, M. A., Martinez, E., Boto, L., Hopwood, D. A. & Malpartida, F. (1992). Nucleotide sequence and deduced functions of a set of cotranscribed gene Streptomyces coelicolor A3 (2) including the polyketide synthase for the antibiotic actinorodin. *Journal of biological Chemistry* **267**, 19278-19290.

Hayashi, M., Yaginuma, S., Yoshioka, H. & Nakatsu, K. (1981). Studies on neplanocin A , new antitumour antibiotic producing organism, isolation and characterisation. *Journal of Antibiotics* **34**, 675.

Hayes, J. D., Kerr, L. A. & Cronshaw, A. D. (1989). Evidence that glutathionine S-tranferases-β1β1 and S-transferase-β2β2 are the products of separate genes and that their expression in human liver is subject to inter-individual variation-molecular relationship between the β1-subunit and β2-subunit and other alpha class glutathione sSD transferase. *Biochemistry Journal* **264**, 437-445.

Hill, D. L., Straight, S., Allan, P. W. & Bennett, L. L. (1971). Inhibition of guanine metabolism of mammalian tumour cells by carbocyclic analogue of adenosine. *Molecular Pharmacology* **7**, 375-380.

Holmes, D. J., Caso, J. L. & Thompson, C. J. (1993). Autogenous transcriptional activation of a thiostrepton-induced gene in *Streptomyces lividans*. *EMBO* **12**, 3183-3191.

Jenkins, G. N. & Turner, N. J. (1995). The biosynthesis of carbocyclic nucleosides. *Chemical Society Reviews*, 169-176.

Khosla, C. & Zawada, R. J. X. (1996). Generation of polyketide libraries via combinatorial biosynthesis. *Tibtech* **14**, 335-341.

Kim, C. G., Yu, T. W., Fryhle, C. B., Handa, S. & Floss, H. G. (1998). 3-Amino-5-hydroxybenzoic acid synthase, the terminal enzyme in the formation of the precursor of mC7N units in rifamycin and related antibiotics. *Journal of Biological Chemistry* **273**, 6030-6040.

Kusaka, T., Yamomoto, H., Shibata, M., Muroi, M., Kishi, T. & Mizuno, K. (1967). *Journal of Antibiotics* **21**, 255.

Luckner, M. (1990). *Secondary metabolism in microorganisms, plants and animals*, Springer, Berlin.

Maniatis, S., Fritsch. (1989). *Molecular Cloning, A Laboratory Manual.*

Mao, Y., Varoglu, M. & Sherman, D. H. (1999). Molecular characterisation and analysis of the biosynthetic gene cluster for the antitumor antibiotic mitomycin C from Streptomyces lavendulae NRRL 2564. *Chemistry & Biology* **6**, 251-263.

Murakami, T., Holt, T. G. & Thompson, C. J. (1989). Thiostrepton-induced gene expression in Streptomyces lividans. *Journal of Bacteriology* **171**, 1459-1466.

Murray, A. W. (1966). *Journal of Biochemistry* **100**, 671-674.

Nilsson, D. & Hove-Jensen, B. (1987). Phosporibosylpyrophosphate synthetase of *Bacillus subtilis*. Cloning, characterisation and chromosomal mapping of the *prs* gene. *Gene* **53**, 247-255.

Ozcengiz, G. & Alaeddinoglu, N. G. (1991). Bacilysin production and sporulation in *Bacillus subtilis*. *Current Microbiology* **23**, 61-64.

Paisley, S. D., Wolfe, M. S. & Borchardt, R. T. (1989). Oxidation of neplanocin A to the corresponding 3`-keto derivative by S-adenosylhomocysteine hydrolase. *Journal of Medicinal Chemistry* **32**(7), 1415-1418.

Palmer, J. L. & Abeles, R. H. (1979). Mechanism of action of S-adenosylhomocysteinase. *Journal of Biological Chemistry* **254**(4), 1217-1226.

Parry, R. J. & Borenemann, V. (1985). Biosynthesis of aristeromycin -elucidation of the origin of the adenine and cyclopentane rings. *Journal of the American Chemical Society* **107**, 6402.

Parry, R. J., Bornemann, V. & Subramanian, R. (1987). The biosynthesis of aristeromycin. *Abstracts Paper American Chemical Society* **194**, 14.

Parry, R. J., Bornemann, V. & Subramanian, R. (1989). Biosynthesis of the nucleoside antibiotic aristeromycin. *Journal of American Chemical Society* **111**, 5819-5824.

Parry, R. J. & Jiang, Y. (1994). The biosynthesis of aristeromycin. Conversion of neplanocin A to aristeromycin by a novel enzymatic reduction. *Tetrahedron Letters* **35**(52), 9665-9668.

Parry, R. J., Burns, M. R., Skae, P. N., Hoyt, J. C. & Pal, B. (1996). Carbocyclic analogues of $_{D}$-ribose-5-phosphate: Synthesis and behaviour with 5-phosphribosyl a-1-pyrophosphate synthetases. *Bioorganic and medicinal chemistry* **4**(7), 1077-1088.

Ransohoff, R. M., Narayan, P., Ayres, D. F., Rottman, F. M. & Nilsen, T. W. (1987). Priming of influenza mRNA transcription is inhibited in CHO cells treated with methylation inhibitor, neplanocin A. *Antiviral Res.* **7**, 317-327.

Ristow, H., Schazschneider, B. & Kleinkauf, H. (1975). Effects of the peptide antibiotic truadine and linear gramicidin on RNA synthesis and sporulation of *Bacillius brevis*. *Biochemical Biophysical Research Communication* **63**, 1085-1092.

Roessner, C. A. & Scott, A. I. (1996). Achieving natural product synthesis and diversity via catalytic networking *ex vivo*. *Chemistry & Biology* **3**, 325-330.

Sakar, N. & Paulus, H. (1972). Function of peptide antibiotics in sporulation. *Nature, New Biology* **239**, 228-230.

Schweke, T., Aparicio, J. F., Molnar, I., Konig, A., Khaw, L. E., Haydock, S. F., Oliynyk, M., caffrey, P., Cortes, J., Lester, J. B., Bohm, G. A., Staunton, J. & Leadlay,

P. F. (1995). The biosynthetic gene cluster for the polyketide immunosuppressant rapamycin. *Proceeding National Academy of Science* **92**, 7839-7843.

Shealy, Y. F. & Clayton, J. D. (1966). *Journal of American Chemical Society* **111**, 5819.

Southern, E. M. (1975). Detection of specific sequence among DNA fragments detected by gel electrophoresis. *Journal of Molecular Biology* **98**, 503-517.

Thompson, C. J., Skinner, R. H., Thompson, J., Ward, J. M., Hopwood, D. A. & Cundliffe, E. (1982). Biochemical characterisation of resistance determinants cloned from antibiotic-producing *Streptomycetes*. *Journal of Bacteriology* **151**, 678-685.

Wolfe, M. S., Lee, Y., Bartlett, W. J., Borcherding, D. R. & Borchardt, R. T. (1992). 4`-modified analogs of aristeromycin and neplanocin A synthesis and inhibitory activity towards S-adenosyl-L-homocysteine hydrolase. *Journal of Medicinal Chemistry* **35**(16), 1782-1789.

Wong, C. H., McCurry, S. D. & Whitesides, G. M. (1980). Practical enzymatic syntheses of ribulose-1,5-bisphosphate and ribose 5-phosphate. *Journal of American Chemical Society* **102**, 7938-7939.

Yaginuma, S., Muto, N., Tsujino, M., Sudate, Y., Hayashi, M. & Otani, M. (1981). Studies on neplanocin A, new antitumor antibiotic producing organism isolation and characterisation. *Journal of Antibiotics* **34**, 359.

Yanisch-Perron, C., Vieira, J. & Messing, J. (1985). Improved M13 phage cloning vectors and host strains: Nucleotide sequences of M13mp18 and pUC19 vectors. *Gene* **33**, 103-119.

## Lectures & conferences attended

### 1996-1997

Departmental Organic Seminars (1996-1997) Oral presentation given
Departmental Colloquia (1996-1997)
ECPT Seminars (1996-1997)
European Peptide Symposium
Romanes Lecture
Walker Memorial Lecture
Ames Symposium
25th Royal Society of Chemistry - Perkin Division (Edinburgh 12.96)
Royal Society of Chemistry (Perkin division) Bio-organic Group –Liverpool

### 1997-1998

Departmental Organic Seminars (1997-1998)
Departmental Colloquia (1997-1998)
ECPT Seminars (1997-1998)
26th Royal Society of Chemistry - Perkin Division (Strathclyde 12.97)
Walker Memorial Lecture
Ames Symposium
SET Mentoring Programme
Radiation Protection course
Technical Writing Workshop
Royal Society of Chemistry (Perkin division) Bio-organic Group –Cardiff Oral Presentation given

### 1998-1999

Departmental Organic Seminars (1998-1999). Oral presentation given
Departmental Colloquia (1998-1999)
ECPT Seminars (1998-1999)
Walker Memorial Lecture
Thesis writing workshop
Biochemistry Society Meeting, Leicester, poster presented
Biochemistry & Molecular Biology 1999 (American Society for Biochemistry & Molecular Biology), San Francisco, poster presented

# Appendix

Eur. J. Biochem. 257, 577–585 (1998)


# Characterisation of flavodoxin NADP$^+$ oxidoreductase and flavodoxin; key components of electron transfer in *Escherichia coli*

Lisa McIVER, Claire LEADBEATER, Dominic J. CAMPOPIANO, Robert L. BAXTER, Simon N. DAFF, Stephen K. CHAPMAN and Andrew W. MUNRO

Department of Chemistry, Joseph Black Building, The University of Edinburgh, The King's Buildings, West Mains Road, Edinburgh, UK

(Received 19 May/19 June 1998) – EJB 98 0680/4

The genes encoding the *Escherichia coli* flavodoxin NADP$^+$ oxidoreductase (FLDR) and flavodoxin (FLD) have been overexpressed in *E. coli* as the major cell proteins (at least 13.5% and 11.4% of total soluble protein, respectively) and the gene products purified to homogeneity. The FLDR reduces potassium ferricyanide with a $k_{cat}$ of 1610.3 min$^{-1}$ and a $K_m$ of 23.6 μM, and cytochrome *c* with a $k_{cat}$ of 141.3 min$^{-1}$ and a $K_m$ of 17.6 μM. The cytochrome *c* reductase rate is increased sixfold by addition of FLD and an apparent $K_m$ of 6.84 μM was measured for the affinity of the two flavoproteins. The molecular masses of FLDR and FLD apoproteins were determined as 27648 Da and 19606 Da and the isolectric points as 4.8 and 3.5, respectively. The mass of the FLDR is precisely that predicted from the atomic structure and indicates that residue 126 is arginine, not glutamine as predicted from the gene sequence. FLDR and FLD were covalently crosslinked using 1-ethyl-3(dimethylamino-propyl) carbodiimide to generate a catalytically active heterodimer. The midpoint reduction potentials of the oxidised/semiquinone and semiquinone/hydroquinone couples of both FLDR (−308 mV and −268 mV, respectively) and FLD (−254 mV and −433 mV, respectively) were measured using redox potentiometry. This confirms the electron-transfer route as NADPH→FLDR→FLD. Binding of 2′ adenosine monophosphate increases the midpoint reduction potentials for both FLDR couples. These data highlight the strong stabilisation of the flavodoxin semiquinone (absorption coefficient calculated as 4933 M$^{-1}$ cm$^{-1}$ at 583 nm) with respect to the hydroquinone state and indicate that FLD must act as a single electron shuttle from the semiquinone form in its support of cellular functions, and to facilitate catalytic activity of microsomal cytochromes *P*-450 heterologously expressed in *E. coli*. Kinetic studies of electron transfer from FLDR/FLD to the fatty acid oxidase *P*-450 BM3 support this conclusion, indicating a ping-pong mechanism. This is the first report of the potentiometric analysis of the full *E. coli* NAD(P)H/FLDR/FLD electron-transfer chain: a complex critical to the function of a large number of *E. coli* redox systems.

*Keywords:* flavodoxin; flavodoxin NADP$^+$ oxidoreductase; redox potentiometry; enzyme kinetics; cytochrome *P*-450.

The *Escherichia coli* flavodoxin NADP$^+$ oxidoreductase (FLDR or flavodoxin reductase) and flavodoxin (FLD) are the two flavin-containing components of a short electron-transfer chain from NADPH, which provides electrons for the function of the biotin synthase [1] and cobalamin-dependent methionine synthase systems [2]. The enzymes are also required during anaerobic growth of the organism, participating in the pyruvate formate/lyase system of *E. coli* – a crucial mechanism for the anaerobic generation of pyruvate for glycolysis [3] and in the generation of deoxyribonucleotides through the enzyme anaerobic ribonucleotide reductase [4]. Recently, the FLDR/FLD system has also been recognised as the *E. coli* 'reductase', which can support the function of heterologously expressed eukaryotic cytochromes *P*-450 [5], even though no endogenous *P*-450s have yet been identified in the bacterium.

*Correspondence to* A. W. Munro, Department of Chemistry, Joseph Black Building, The University of Edinburgh, The King's Buildings, West Mains Road, Edinburgh, EH9 3JJ, UK

*Fax:* +44 131 650 4760.

*E-mail:* Andrew.Munro@ed.ac.uk

*Abbreviations.* CPR, cytochrome *P*-450 reductase; FLD, *E. coli* flavodoxin; FLDR, *E. coli* flavodoxin NADP$^+$ oxidoreductase; IPTG, isopropyl-β, D-thiogalactopyranoside; P-450, cytochrome *P*-450 monooxygenase.

We have overexpressed and purified the FLDR and FLD proteins in order to investigate their function in biotin synthesis and cytochrome *P*-450 reduction. Of particular interest was the analysis of the interactions of the FLDR and FLD proteins and the redox characteristics of these enzymes, since it is known that the cytochromes *P*-450 require two successive single-electron transfers to perform their activation of molecular oxygen. While the flavodoxins have been considered to function as single-electron donors by cycling between the hydroquinone and semiquinone states [6], it is by no means certain that the hydroquinone is a physiologically relevant species in electron-transport chains using NAD(P)H, FLDR and FLD, since the midpoint reduction potential of NAD(P)H (−320 mV) is likely to be considerably higher (more positive) than that of the FLD semiquinone/hydroquinone couple. Indeed, there is evidence to support the utilisation of the flavodoxin semiquinone as the electron donor for methionine synthetase [2, 7]. It is known that flavodoxins, in general, stabilise a semiquinone-1-electron-reduced form as opposed to the 2-electron-reduced hydroquinone. In fact, potentiometric studies on non-recombinant *E. coli* FLD, purified from large-scale cultures, indicated that this enzyme stabilises a blue neutral semiquinone form of FMN [8].

In this paper, we report the results of biophysical studies of the *E. coli* FLDR and FLD, analysing the interactions between

these two proteins and determining the redox properties of the flavin cofactors. These data allow clearer understanding of the energetics of electron distribution between the two flavoproteins and of their capacity to participate in multiple *E. coli* redox systems, as well as their function as a cytochrome *P*-450 reductase system.

## EXPERIMENTAL PROCEDURES

***E. coli* strains and plasmid vectors.** *E. coli* strain HMS174 (DE3) ($F^-$, *rec*A, *hsd*R [$r_{K12}^-m_{K12}^-$] Rif$^r$) [9] was used for overexpression of the flavodoxin NADP$^+$ reductase (*fldr*) gene. Strain JM101 (F′, *tra*D36, *lacI*$^q$ Δ(*lac*Z) M15, *pro*A$^+$B$^+$/*sup*E, *thi*, Δ(*lac-pro*AB) [10] was used for overexpression of the flavodoxin (*fld*A) gene. Plasmid pCL21 was used for production of FLDR and was constructed by amplification of the structural gene from plasmid pEE1010 (a gift from Dr Elizabeth Haggård-Ljungquist, Department of Chemistry, Karolinska Institute, Stockholm, Sweden) [11] using primers 'RED FOR' (5′ CAGGAGAATTCCATGGCTGATTGGGTAACAGGC 3′) and 'RED REV' (5′ ATAAGGATCCGCTTACCAGTAATGCTCCGCTGTCAT 3′). 'RED FOR' contains a *Nco*I site (bold) encompassing the start codon (underlined) of the *fldr* gene. 'RED REV' contains a *Bam*HI site (bold) encompassing the stop codon (underlined) of *fldr*. The PCR product was cleaved with *Nco*I and *Bam*HI and the digested product was ligated into plasmid pET16b (Novagen Inc.) under the control of a T7*lac* promoter to produce plasmid pCL21. Plasmid pDH1 (a gift from Dr Rowena Matthews, Division of Biological Chemistry, University of Michigan) was used for production of FLD [12].

**Enzyme preparations.** *E. coli flavodoxin NADP$^+$ oxidoreductase.* Transformant HMS174 (DE3)/pCL21 was grown in 2–10 l of Luria-Bertani media containing ampicillin (100 μg/ml) to an $A_{600}$ = 1.0 and production of FLDR was induced by the addition of 1 mM isopropyl-β, D-thiogalactopyranoside (IPTG). Thereafter, growth was continued for 3 h and the cells (≈2.5 g/l wet mass) were then harvested by centrifugation (5000 *g* for 10 min, 4°C), washed by resuspension in ice-cold buffer A (10 mM sodium phosphate, pH 7.5) and lysed by intermittent sonication (30 s on, 30 s off) for 5 min. Cellular debris was removed by centrifugation (15000 *g* for 30 min, 4°C) and the supernatant was loaded directly on a Q-Sepharose 26/10 Hi-Load anion exchange column (Pharmacia) which had been washed in buffer A. Protein was eluted with a gradient (0–1 M) of sodium chloride in buffer A. Yellow FLDR-containing fractions were collected from 130–150 mM NaCl. These were combined and loaded on a 2′,5′-ADP Sepharose column (1 cm×20 cm), equilibrated with buffer A containing 150 mM NaCl. Pure FLDR was eluted using buffer A containing 500 mM NaCl. The purified enzyme was dialysed against buffer A, concentrated by ultrafiltration (Amicon, 10000 Da cut-off) to a concentration of ≈5 mg/ml and stored frozen at −20°C. PMSF (0.1 mM) was added to all buffers to minimise proteolysis.

*E. coli flavodoxin.* Transformant JM101/pDH1 was grown and induced in similar fashion to HMS174 (DE3)/pCL21, except that cells were harvested 6 h after induction with IPTG (100 μM), and riboflavin (5 mg/l) was also added to the culture at the time of induction. Cells (≈1.5 g/l wet mass) were washed by resuspension in ice-cold buffer B (50 mM Tris/HCl, pH 7.5), broken by sonication and the cell lysate collected after centrifugation as previously. Protamine sulfate was added to a final concentration of 0.1% (mass/vol.) to the extract and the mixture centrifuged (15000 *g* for 30 min, 4°C). The supernatant was loaded directly on a Q-Sepharose 26/10 Hi-Load anion exchange column (Pharmacia), which had been washed in buffer C (100 mM sodium actetate, pH 5.0) and FLD was eluted from the column in a gradient of NaCl (0–1 M) in buffer C, between 375 mM and 425 mM NaCl. The pH of the bright-orange FLD-containing fractions was increased to pH 7.5 immediately following elution by dialysis against buffer B. This single-step procedure resulted in a fraction in which >90% of the protein was FLD. Further purification was achieved by a second anion-exchange-chromatography step using a Resource Q column (Pharmacia). Protein was loaded in buffer B and eluted using a linear gradient of 0–1 M NaCl in buffer B. Pure FLD was eluted between 350 mM and 400 mM NaCl. The final FLD fraction was dialysed against buffer B, concentrated by ultrafiltration (Amicon, 10000 Da cut-off) to a concentration of ≈5 mg/ml and stored frozen at −20°C. $PhMeSO_2F$ (0.1 mM) was added to all buffers.

**Potentiometric titrations.** All redox titrations were conducted within a Belle Technology glove box under a $N_2$ atmosphere, with $O_2$ maintained at less than 5 ppm. Degassed, concentrated enzyme samples were passed through an anaerobic Sephadex G25 column (1×20 cm) (Sigma) immediately on admission to the glove box to remove all traces of $O_2$. The column was equilibrated and proteins were eluted with 100 mM sodium phosphate, pH 7.0, which was used throughout the experimental procedures. Protein solutions were titrated electrochemically according to the method of Dutton [13] using sodium dithionite as reductant and potassium ferricyanide as oxidant. Mediators were introduced prior to titration; typically 2-hydroxy-1,4-napthaquinone (5 μM), benzyl viologen (1 μM) and methyl viologen (1 μM) within sample volumes of 5–10 ml. After 10–15 min equilibration following each reductive/oxidative addition, spectra were recorded on a Shimadzu 1201 ultraviolet/visible spectrophotometer (typically between 350 nm and 800 nm) contained within the anaerobic environment. The electrochemical potential of the sample solutions were monitored using a CD740 meter (WPA) coupled to either Pt/calomel or Pt/Ag–AgCl combination electrodes (Russell pH Ltd) at 25±2°C. The electrodes were calibrated using the $Fe^{III}/Fe^{II}$ EDTA couple as a standard (+108 mV). The calomel and Ag–AgCl electrodes were corrected by +244±2 mV and +198±3 mV, respectively, both relative to the normal hydrogen electrode. For experiments involving FLDR, ultraviolet/visible spectra were affected by the slow formation of a protein precipitate, which resulted in a small increase in baseline absorbance with time. This was corrected for by transforming each spectrum with a $1/\lambda$ subtraction calculated to return the absorbance at 800 nm back to zero (at this wavelength chromophore absorbance is minimal). All data manipulations and non-linear least-squares curve fitting of electrochemistry data were conducted using Origin (Microcal).

**Enzyme assays.** Steady-state kinetic parameters for FLDR and FLD were measured at 30°C in 100 mM sodium phosphate, pH 7.5, on a Shimadzu 2101 ultraviolet/visible spectrophotometer. Reduction of cytochrome *c* (horse heart, type 1) was monitored by the absorbance increase at 550 nm, using a Δ absorbance coefficient of 22 640 $M^{-1}$ $cm^{-1}$. Reduction of potassium ferricyanide was measured by the absorbance decrease at 420 nm, using a coefficient of 1010 $M^{-1}$ $cm^{-1}$.

Measurements of *P*-450 BM3 haem-domain-catalysed fatty acid (arachidonic acid) oxidation [14] supported by FLDR and FLD were performed as described previously for the catalysis of pregnenolone oxidation by *P*-450 c17 [5]. To determine the mechanistic nature of the FLDR/FLD/*P*-450 interactions, a series of oxidation-rate measurements were performed in the presence of saturating (1 mM) NADPH – with FLD maintained constant at 25 μM, FLDR varied from 0.25 μM to 10 μM and *P*-450 BM3 haem-domain maintained constant (in three different experimental sets) at 0.76 μM, 2.54 μM and 3.81 μM. Re-

tion rates were determined at 30°C in 100 mM sodium phosate, pH 7.5, and the reciprocals of the data plotted against the ciprocals of the [FLDR] for each concentration of *P*-450 used.

Stopped-flow measurements of transient absorbance changes sociated with reduction of FLDR and FLD flavins (decrease absorbance at 456 nm and increase at 583 nm, respectively), oxidation of the flavins (same wavelengths) and reduction of tochrome *c* (550 nm) were made using an Applied Photophys- SF.17 MV stopped-flow kinetics spectrophotometer. Reacns were performed at 30°C in 100 mM sodium phosphate, 7.5 (unless otherwise stated). Rates of FLDR−FLD electron nsfer were measured after enzyme and buffer solutions had en degassed and bubbled for 15 min with $O_2$-free $N_2$. Traces $O_2$ were subsequently removed from the enzyme solutions by ssing the concentrated stock solutions of enzyme down a G25 -filtration column (1×20 cm) within the anaerobic environnt of a glove box (Belle Technology). The enzyme solutions re then diluted to the required concentrations, transferred to stopped-flow syringes and sealed within the glove box be- transferring to the stopped-flow apparatus.

Analysis of stopped-flow data was performed using the .17 MV software and Origin (Microcal), both of which use n-linear least-squares regression analysis. The reduction of DR by NADPH was measured by rapid mixing of NADPH μM−2 mM) with FLDR (40 μM) and monitored at 456 nm tal flavin reduction). The electron transfer from FLDR to FLD s monitored at 583 nm (formation of FLD blue semiquinone) er mixing of 40 μM FLDR (reduced with 2 mM NADPH or lium dithionite) with FLD (20 μM). When sodium dithionite s used, FLDR was reduced completely in an anaerobic envinment with excess reductant, then separated from the dithioe by gel filtration under anaerobic conditions. Reoxidation of DR was measured after mixing of enzyme (80 μM) with a -stoichiometric quantity of reductant (40 μM NADPH) and nitoring the absorbance increase at 456 nm. Reoxidation of FLD semiquinone (absorbance decrease at 583 nm) was asured after anaerobic reduction of the enzyme with excess lium dithionite, isolation of the reduced enzyme by gel filtran and dilution of reduced FLDR into aerobic buffer. Reducn of cytochrome *c* was measured at 550 nm after reaction reduced FLDR (10−50 μM enzyme + 2 mM NADPH) with ochrome *c* (horse heart, type 1; 4 μM).

**Chemical crosslinking of FLDR and FLD.** Purified FLD μM) and FLDR (8 μM) were covalently and specifically sslinked using 1-ethyl-3-(dimethylamino-propyl) carbodide (EDC) (10 mM) in 10 mM Hepes buffer (2 ml, pH 7.0) at m temperature [15]. 10-ml aliquots were withdrawn from the ction at 15-min intervals to assess the progress of the reaction SDS/PAGE. After 1 h, the reaction was stopped by the addin of ammonium acetate (100 mM) and the protein mixture ncentrated to approximately 0.5 ml by ultrafiltration [using a 000 Da cut-off Centricon concentrator (Amicon)]. The crossed complex was separated from the FLDR and FLD proteins gel filtration on FPLC (Superdex 75 column, 1.6×60 cm) in mM Tris/HCl, pH 7.5, containing 50 mM KCl.

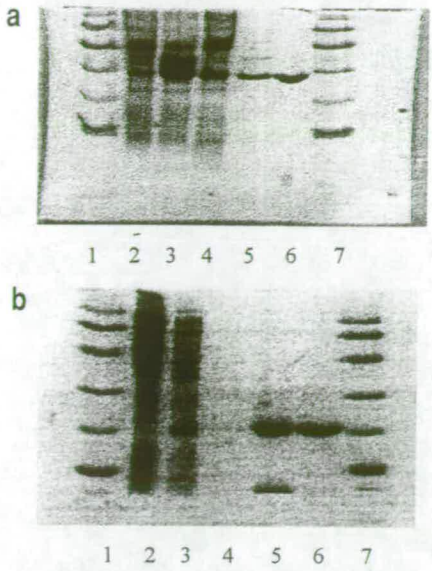


**Fig. 1. (a) SDS/PAGE of *E. coli* flavodoxin NADP⁺ oxidoreductase (FLDR) purification steps.** Lane 1, low molecular mass standards (94000, 67000, 43000, 30000, 20 100, 14 400 Da); lane 2, uninduced cells; lane 3, induced cells; lane 4, cell lysate; lane 5, Q-Sepharose; lane 6, 2′, 5′-ADP Sepharose; lane 7, low molecular mass standards (as lane 1). (b) SDS/PAGE of *E. coli* flavodoxin (FLD) purification steps. Lane 1, low molecular mass standards (94000, 67000, 43000, 30000, 20 100, 14 400 Da); lane 2, uninduced cell lysate; lane 3, induced cell lysate; lane 4, empty; lane 5, Q-Sepharose; lane 6, Resource-Q; lane 7, low molecular mass standards (as lane 1).

## RESULTS

**Protein characterisation.** *Flavodoxin NADP⁺ oxidoreductase.* FLDR is a monomeric (247 amino acids, $M_r$ 27620 Da) enzyme which contains FAD. *E. coli* HMS174 (DE3)/pCL21 was used to overexpress FLDR. The protein was purified by sequential chromatography steps on Q-Sepharose and 2′,5′-ADP Sepharose (Table 1). Samples were analysed at all steps by SDS/PAGE (Fig. 1a) and ultraviolet-visible spectroscopy. The molecular mass of the expressed FLDR apoprotein was determined as 27648 Da by electrospray mass spectroscopy. This is 28 Da higher than the predicted molecular mass of 27620 Da, calculated from the amino acid sequence derived from the database gene sequence [16] (less the N-terminal methionine). However, the recent solution of the atomic structure of the *E. coli* FLDR indicates that an arginine is present at position 126, as opposed to a glutamine predicted from the gene sequence [17]. The difference in molecular mass of these two residues is exactly 28 Da, corresponding to the apparent discrepancy. The isoelectric point of FLDR was measured as 4.8 by isolelectric focusing; rather more acidic than the theoretical value of 6.19 (SwissProt).

FLDR is bright yellow in its oxidised form and it is converted to a neutral blue semiquinone by the addition of one reducing equivalent. FLDR has an absorption coefficient of

**le 1. Purification table for *E. coli* NADP⁺ flavodoxin oxidoreductase (FLDR).** Total protein was estimated by absorbance at 280 nm. FLDR estimated by measurement of absorbance (Abs) at the peak of the longer wavelength flavin band (456 nm).

| ification step | Total volume (V) | Total protein | Total FLDR | $Abs_{456}/Abs_{280}$ | Purification |
|---|---|---|---|---|---|
| | ml | $V \times Abs_{280}$ | $V \times Abs_{456}$ | | -fold |
| ate | 55 | 833.9 | 18.26 | 0.0207 | 1 |
| epharose | 80 | 119.1 | 9.28 | 0.0779 | 3.77 |
| -ADP Sepharose | 35 | 37.5 | 5.74 | 0.1531 | 7.41 |

7100 $M^{-1}$ $cm^{-1}$ at 456 nm [5]. The oxidised FLDR had flavin absorbance maxima at 456 nm and 400 nm, with a shoulder on the longer wavelength band at 483 nm. Based on the 7.41-fold purification value calculated using flavin absorbance at this wavelength, the overexpressed FLDR comprises 13.5% of the total soluble protein in the *E. coli* extract.

FLDR used for kinetic and potentiometric studies was obtained from transformants of pCL21 in strain HMS174 (DE3), which yielded approximately 23 mg pure FLDR/l of cells. The re-cloning of the *fldr* gene into vector pET16b (to generate pCL21) along with an improved purification scheme (two steps rather than four) allowed significantly higher levels of recovery of FLDR compared with the original clone in pEE1010 (≈3.5 mg/l) [16]. Transformants of pCL21 in strain BL21 (DE3) resulted in even higher expression of *fldr* (≈35 mg/l); but the specific activity of the purified FLDR was considerably lower than that purified from the HMS174 (DE3) strain.

*Flavodoxin.* FLD is a small (177 amino acids, $M_r$ 19606 Da) acidic flavoprotein, which contains FMN as its prosthetic group. FLD was produced from *E. coli* transformant JM101/pDH1 and the purification was followed by a combination of SDS/PAGE and spectroscopic characterisation on FLD-containing fractions (Table 2). SDS/PAGE analysis of the purified protein showed a single species which migrated at $m$ = 20 kDa (Fig. 1b). The molecular mass was confirmed by electrospray mass spectrometry as 19606 Da, precisely the mass predicted from the amino acid sequence (less the N-terminal methionine). The isoelectric point of FLD was measured as 3.5; slightly more acidic than the theoretical value of 4.21 (SwissProt). Fractions containing the protein had the distinct bright-orange colour expected for flavodoxin in its oxidised state. Pure FLD has an absorption coefficient of 8250 $M^{-1}$ $cm^{-1}$ at 466 nm [2] and a ratio of $A_{274}/A_{466}$ of 5.8 [12]. Oxidised pure FLD had flavin absorbance maxima at 466 nm and 372 nm, with a distinct shoulder on the longer wavelength band at ≈495 nm and a less obvious shoulder at ≈438 nm. Total recovery was estimated at 37% based on the purity of the flavodoxin at the end of the short purification scheme and the assumption that the absorbance at 466 nm is specific for the overexpressed protein. Clearly, other *E. coli* flavin-containing proteins (as well as those containing, for example, haem or iron-sulfur centres) will have absorbance in this region; so this figure is likely to be a small underestimate. Based on an 8.8-fold purification value, the overexpressed flavodoxin comprised 11.4% of the total soluble protein in the *E. coli* extract.

In JM101/pDH1 transformants, flavodoxin was overexpressed to a level of approximately 19.5 mg/l.

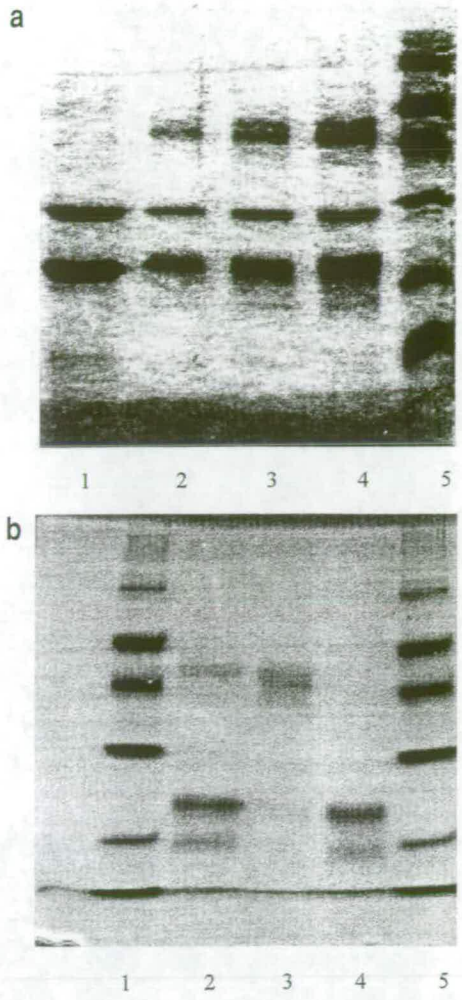


**Fig. 2. (a) SDS/PAGE gel of formation of EDC-linked FLDR/FL complex as described in the Experimental Procedures section.** La 1, pure FLDR and FLD proteins, no EDC added; lane 2, 15 min af addition of 10 mM EDC; lane 3, 30 min after addition of EDC; lane 1 h after addition of EDC; lane 5, molecular mass standards (940 67000, 43000, 30000, 20 100, 14 400 Da). (b) SDS/PAGE gel showi purification of EDC-linked FLDR/FLD complex using FPLC (Superd 75). Lane 1, molecular mass standards (94000, 67000, 43000, 300 20 100, 14 400 Da); lane 2, complex/FLDR/FLD mixture prior to g filtration; lane 3, FPLC fraction containing complex; lane 4, FPLC fra tion containing FLDR/FLD; lane 5, as lane 1.

**FLDR/FLD crosslinked complex.** The FLDR/FLD complex was generated using EDC as a crosslinking agent, as indicated in Experimental Procedures. The time course of the production of the complex is shown in Fig. 2a. The complex was purified from unreacted FLDR/FLD using gel filtration on FPLC (Superdex 75) (Fig. 2b). It appears that only a single species was produced in the reaction with an apparent molecular mass (by SDS/PAGE) of 47 kDa. The complex was analysed by electrospr mass spectrometry and a molecular mass of 47430 Da was o tained − close to the value of 47360 Da predicted for a 1 EDC-linked complex of FLDR/FLD. There was no evidence f self-complexation of FLDR or FLD after EDC treatment, su gesting that the interactions between FLDR and FLD a stronger than those between FLD and FLD or FLDR and FLD

**Table 2. Purification table for *E. coli* flavodoxin (FLD).** Total protein was estimated by absorbance (Abs) at 280 nm. FLD was estimated measurement of absorbance at the peak of the longer-wavelength flavin band (466 nm).

| Purification step | Total volume (V) | Total protein | Total flavodoxin | $Abs_{466}/Abs_{280}$ | Purificatio |
|---|---|---|---|---|---|
| | ml | $V \times Abs_{280}$ | $V \times Abs_{466}$ | | -fold |
| Cell lysate | 23 | 1166.1 | 21.62 | 0.0185 | 1 |
| Q-Sepharose | 120 | 62.52 | 7.68 | 0.123 | 6.65 |
| Resource-Q | 4.8 | 46.5 | 7.54 | 0.162 | 8.76 |

**ble 3. Steady-state kinetic parameters for FLDR.** Rates of reduc- n of artificial electron acceptors were measured at 550 nm for cyto- ome *c* (22 640 $M^{-1}$ $cm^{-1}$) and 420 nm for potassium ferricyanide 010 $M^{-1}$ $cm^{-1}$). Rates were measured at 30°C in 100 mM sodium osphate, pH 7.5, with saturating (200 μM) NADPH. The $K_m$ for ADPH was determined under conditions of saturating cytochrome *c* 50 μM). The $K_m$ for the FLD was determined under conditions of satu- ng cytochrome *c* and NADPH, with the FLDR at 16.65 nM.

| ostrate | $k_{cat}$ | $K_m$ |
|---|---|---|
| | $min^{-1}$ | μM |
| tassium ferricyanide | 1610.3 ± 50.1 | 23.6 ± 3.2 |
| tochrome *c* | 141.3 ± 5.3 | 17.6 ± 2.15 |
| ADPH | – | 3.85 ± 0.5 |
| D | – | 6.84 ± 0.68 |

**ble 4. Steady-state kinetic parameters for the EDC-linked com- x of FLDR/FLD.** Experiments were performed as described above.

| ostrate | $k_{cat}$ | $K_m$ |
|---|---|---|
| | $min^{-1}$ | μM |
| tassium ferricyanide | 782.0 ± 35 | 33.2 ± 6.4 |
| tochrome *c* | 109.2 ± 4.5 | 87.4 ± 8.2 |

sible spectra of the complex showed absorbance maxima at 9.5 nm and 462 nm, with shoulders at ≈487 nm and 404 nm. ese absorbance characteristics are different from those of the dividual FLDR and FLD – with absorbance maxima located tween the peaks of the isolated flavoproteins. Addition of ADPH was seen to induce a decrease in the intensity of the vin spectrum, but not to induce the formation of a species sorbing in the 550–600 nm region, suggesting that there was formation of the neutral blue semiquinone form expected for e FMN in FLD.

**nzyme activities.** Purified FLDR has NADPH-dependent ductase activity towards a variety of electron acceptors able 3). Using cytochrome *c* (horse heart, Sigma) as the accep- , a $k_{cat}$ of 141.3 ± 5.3 $min^{-1}$ and a $K_m$ of 17.6 ± 2.15 μM were easured using homogeneous FLDR at 30°C in 100 mM so- um phosphate, pH 7.5. With saturating cytochrome *c*, the $K_m$ NADPH was estimated at 3.85 ± 0.5 μM. Under similar con- ions, potassium ferricyanide was reduced, with a $K_m$ of .6 ± 3.2 μM and a $k_{cat}$ of 1610.3 ± 50.1 $min^{-1}$. Purified FLD ts as a single electron shuttle and is able to stimulate the rate FLDR-dependent cytochrome *c* reduction approximately six- ld under the above conditions. With saturating cytochrome *c* 00 μM) and FLDR at 16.65 nM, a Michaelis curve was ob- ned for the stimulation of cytochrome *c* reductase activity by LD, indicating an apparent $V_{max}$ of 272 ± 11.5 $min^{-1}$ and an parent $K_m$ of the FLD for the FLDR of 6.84 ± 0.68 μM.

The purified EDC-linked complex of FLDR/FLD was also talytically active (Table 4). With cytochrome *c* as the acceptor, $k_{cat}$ of 109 ± 5 $min^{-1}$ and a $K_m$ of 87 ± 8 μM were measured th the complex at 30°C in 100 mM sodium phosphate, pH 7.5. ith potassium ferricyanide, a $k_{cat}$ of 782 ± 4 $min^{-1}$ and a $K_m$ of ± 6 μM were measured. Both the rate of reduction and the finity of these substrates for the complex were lower than ose for FLDR on its own (Tables 3 and 4).

**opped-flow characterisation.** Investigations of the rates of duction of FLDR (40 μM) with NADPH (4 μM–2 mM) were performed with measurement of the rate of decrease in absorbance at 456 nm, the oxidised FLDR absorbance maximum. The rate observed was 15 ± 2 $s^{-1}$, regardless of the concentration of NADPH. A similar value was obtained when the concentration of FLDR was altered.

Attempts to measure the rate of electron transfer between NADPH-reduced FLDR and FLD (following the formation of FLD semiquinone at 583 nm) proved difficult under aerobic conditions due to the slow rate of this process and the relatively rapid reoxidation of the FLDR. To solve this problem, solutions were degassed and made up anaerobically (as described in the Experimental Procedures section) prior to performing the stopped-flow experiments. The rate of formation of FLD semiquinone was seen to be very slow when reduced FLDR (40 μM) was mixed with FLD (20 μM), regardless of whether NADPH (500 μM–2 mM) or sodium dithionite was used as the reductant. Over the first 60 s, a single exponential rate of only (3.4 ± 0.2)×$10^{-2}$ $s^{-1}$ was recorded in the presence of 2 mM NADPH.

To compare the reduction of an artificial electron acceptor on stopped flow/steady-state time scales, the reduction of cytochrome *c* by FLDR was investigated. NADPH (2 mM)–reduced FLDR (10–50 μM) was mixed with cytochrome *c* (4 μM) and absorbance monitored at 550 nm. A $k_{cat}$ of 29 ± 2 $s^{-1}$ and a $K_m$ of 12.58 ± 1.1 μM were calculated by fitting the first-order rate data against [cytochrome *c*] to a rectangular hyperbola on Origin software. All stopped-flow data is tabulated (Table 5).

To measure the rate of reoxidation of the reduced FLDR, the enzyme was reduced aerobically in the stopped-flow apparatus by mixing with a sub-stoichiometric quantity of NADPH and recording the increase in absorbance at 456 nm. At 30°C, FLDR (80 μM) was observed to reoxidise after rapid mixing with NADPH (60 μM) with a rate of (5.44 ± 0.5)×$10^{-2}$ $s^{-1}$ (3.26 $min^{-1}$). To measure reoxidation of the FLD semiquinone, we initially attempted the same experiment as used for FLDR, employing 80 μM FLD and 60 μM sodium dithionite as the reductant. However, it was found that reduction of FLD by the dithionite was very slow, with the semiquinone taking several minutes to form completely. Instead, the FLD was reduced with an excess of dithionite under anaerobic conditions, until the semiquinone formation was seen to be complete (maximal absorbance at 583 nm). Thereafter, excess dithionite was removed from the FLD by gel filtration (G25) within the anaerobic glove box and the reduced FLD removed from the anaerobic environment. The reduced FLD was then diluted to 30 μM in oxygenated buffer, the buffer bubbled with air for 2 min and the rate of reoxidation of the semiquinone measured at 583 nm under steady-state conditions. The semiquinone was seen to be air sta-

**Table 5. Stopped-flow parameters for oxidation/reduction reactions involving FLDR and FLD.** Reaction rates were determined at 30°C in 100 mM sodium phosphate, pH 7.5, as described in the Experimental Procedures section. Measurement of FLDR reduction was made at 456 nm, FLD reduction to its semiquinone at 583 nm and cytochrome *c* reduction at 550 nm. Reoxidation of FLDR and FLD were monitored at the same wavelengths used to measure their reduction.

| Stopped-flow rate | *k* |
|---|---|
| | $s^{-1}$ |
| FLDR reduction (by NADPH) | 15 ± 2 (900 $min^{-1}$) |
| FLDR oxidation | (5.44 ± 0.5)×$10^{-2}$ (≈3.3 $min^{-1}$) |
| FLD reduction (by FLDR) | (3.4 ± 0.2)×$10^{-2}$ (≈2.0 $min^{-1}$) |
| FLD oxidation | (1.07 ± 0.03)×$10^{-3}$ (3.85 $h^{-1}$) |
| Cytochrome *c* reduction (by FLDR) | 29.0 ± 2.0 (1740 $min^{-1}$) |

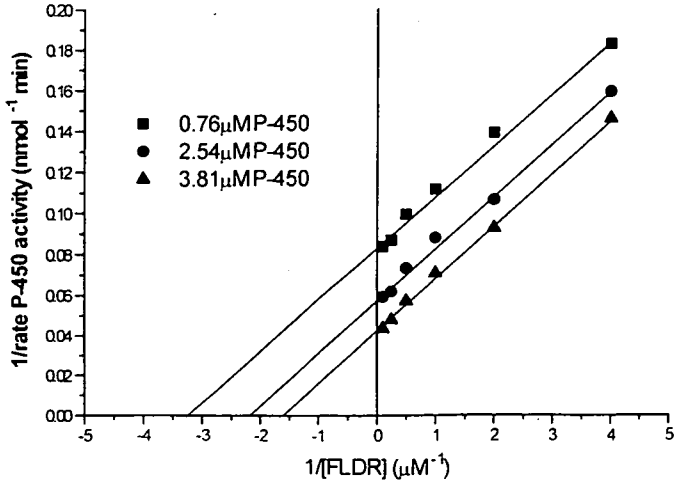


**Fig. 3. Reciprocal plot of *P*-450 BM3 haem-domain catalysed arachidonic acid oxidation versus concentration of FLDR.** The three experimental data sets shown were perfomed as described in the Experimental Procedures section, with *P*-450 BM3 haem-domain maintained constant at 0.76 μM, 2.54 μM or 3.81 μM; FLD maintained at 25 μM throughout and FLDR varied between 0.25 μM and 10 μM. The parallel data plots indicate that a ping-pong mechanism for FLDR/FLD-supported *P*-450 reduction is likely.

ble, taking several hours to reoxidise completely. The reoxidation trace at 583 nm fitted accurately to a single exponential curve, with a rate of $3.85 \pm 0.11\ h^{-1}$ ($0.642\ min^{-1}$).

**Cytochrome *P*-450 reduction.** To analyse the nature and kinetics of the reduction of cytochrome *P*-450 by the FLDR/FLD system, we examined the ability of these flavoproteins to support the oxidation of arachidonic acid by the haem-domain of flavocytochrome *P*-450 BM3 [18]. The FLDR/FLD system proved able to transfer electrons to the *P*-450. At concentrations of 0.762 μM *P*-450, 0.25 μM FLDR and 25 μM FLD, a rate of $5.48 \pm 0.95$ mol arachidonic acid oxidised/min was measured. Data were collected from three sets of fatty acid-oxidation assays, in which the *P*-450 was maintained at one of three different concentrations (0.76 μM, 2.54 μM or 3.81 μM), FLD was kept constant at 25 μM (fourfold in excess of its apparent $K_m$ for FLDR) and FLDR was varied between 0.25 μM and 10 μM. The plots of the reciprocal rates of these data versus the reciprocals of the [FLDR] were used to generate the graph shown in Fig. 3. The fact that the lines plotted are parallel (not convergent) indicates that the *P*-450 reduction mechanism is ping-pong in nature, rather than involving a ternary complex between the *P*-450, FLDR and FLD.

**Potentiometric titrations.** *Flavodoxin NADP⁺ oxidoreductase.* Fig. 4a shows the redox titration of the *E. coli* FLDR at ≈72 μM monitored by ultraviolet/visible spectrophotometry between 350 nm and 800 nm. Fig. 4b plots the proportion of FLDR oxidised based on the sum of the absorbance values between 440 nm and 480 nm against the potential of the enzyme solution. The first electron reduction of FLDR does not result in the accumulation of a stable semiquinone intermediate with long-wavelength absorbance. Thus, potentiometric data for both first and second electron reductions are determined from the continuous decrease in absorbance between 440 nm and 480 nm.

The absorbance versus potential data is fitted in Fig. 4b to an equation (Eqn 1) comprising the sum of two 1-electron redox function designed to model the absorbance of a flavin passing through three different oxidation states.

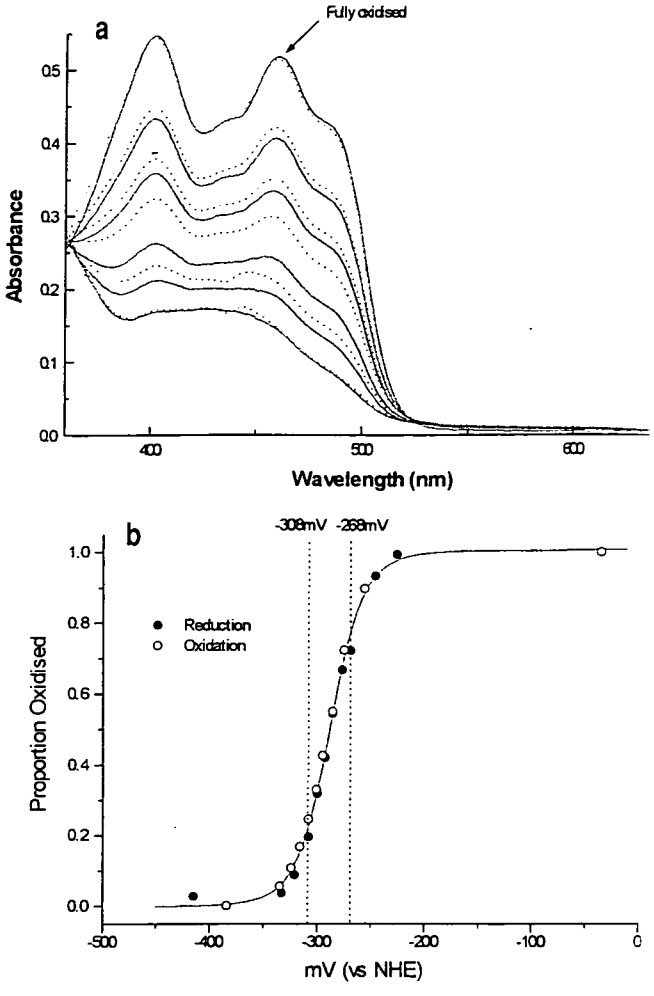


**Fig. 4. (a) Ultraviolet-visible spectra of *E. coli* FLDR (72 μM) dur redox titration.** Reductive (sodium dithionite) and oxidative (potassi ferricyanide) titrations were performed anaerobically as described in Experimental Procedures section. The spectra shown in solid lines from the reductive titration and the flavin signals become less inte on reduction. The dotted spectra are from reoxidation of the redu FLDR and become more intense with successive additions of potassi ferricyanide until the original spectrum of oxidised FLDR returns. Plot of proportion FLDR oxidised versus reduction potential (E', m during reductive and oxidative titrations, using absorbance betwe 440 nm and 480 nm fitted to Eqn. 1, as described in Results. From th data $E'_1$ (oxidised/semiquinone) = $-308 \pm 4$ mV and $E'_2$ (semiquino reduced) = $-268 \pm 4$ mV.

$$\text{Flavin absorbance} = \frac{a10^{(E-E'_1)/59} + b + c10^{(E'_2-E)/59}}{1 + 10^{(E-E'_1)/59} + 10^{(E'_2-E)/59}} \quad (1$$

where a, b, c = absorbance coefficients for oxidised, semiqu none and reduced flavin, respectively; E = electrode potenti and $E'_1$, $E'_2$ = midpoint potentials for the oxidised/semiquino couple and the semiquinone/reduced couple, respectively.

In a subsequent experiment, the redox titration of FLDR w repeated in the presence of a saturating concentration (5 mM) 2′ adenosine monophosphate (2′ AMP) in order to investig the effects of binding of a nucleotide analogue to the NADP site on the redox properties of the FAD in FLDR. 2′ AMP non-redox active and, thus, can be used in redox titrations mimic the effects of binding of $NADP^+$ on the FAD redox pro erties. In preliminary experiments, the affinity of 2′ AMP f FLDR was estimated by measurement of its $IC_{50}$ (≈1 mM) f FLDR-mediated cytochrome *c* reduction. The concentration

**Table 6. Midpoint reduction potentials (E′ in mV) for the flavin cofactors in purified *E. coli* FLDR (NADP⁺ flavodoxin oxidoreductase) and FLD (flavodoxin).** Values were calculated from electrode potential versus absorbance data as described in the Results section and in Figs 2 and 3. $E'_{1_2}$ refers to the midpoint potential for the 2-electron reduction of the flavins in each protein, while $E'_1$ and $E'_2$ refer to the midpoint reduction potentials for the oxidised/semiquinone and semiquinone/hydroquinone couples, respectively, for FLD and FLDR. The values are compared with those of the FAD and FMN cofactors in the reductase domain of flavocytochrome *P*-450 BM3 from *Bacillus megaterium* (BM3) [29] and mammalian *P*-450 reductase (CPR) [30], and with the values for free FAD/FMN [31, 32].

| | $E'_{1_2}$ | $E'_1$ | $E'_2$ |
|---|---|---|---|
| FLDR FAD | −288 ± 4 | −308 ± 4 | −268 ± 4 |
| FLDR FAD (+2′ AMP) | −261 ± 6 | −293 ± 6 | −230 ± 7 |
| FLD FMN | −343 ± 6 | −254 ± 5 | −433 ± 6 |
| BM3 FAD | −332 ± 4 | −292 ± 4 | −372 ± 4 |
| BM3 FMN | −203 ± 6 | −213 ± 5 | −193 ± 6 |
| CPR FAD | −327 | −290 | −365 |
| CPR FMN | −190 | −110 | −270 |
| FREE FAD | −207 | – | – |
| FREE FMN | −205 | −172 | −238 |

mM used in the titration was based on this result. An increase in the reduction potentials of both the oxidised/semiquinone ($E'_1$ elevated by 15 mV to −293 ± 6 mV) and semiquinone/reduced ($E'_2$ elevated by 38 mV to −230 ± 7 mV) couples of FLDR was observed in the presence of 2′ AMP (Table 6).

*E. coli flavodoxin.* Fig. 5a shows the redox titration of the *E. coli* FLD at ≈80 μM monitored by visible spectrophotometry between 400 nm and 800 nm. Fig. 5b plots the sum of absorbance values between 600 nm and 650 nm against the potential of the enzyme solution. The increase and decrease in absorbance in this region reflects the build up (0−1 electron reduced) and loss (1−2 electron reduced), respectively, of the flavodoxin neutral-blue semiquinone. The FLD data was also fitted to Eqn (1). In this case, $E'_1$ represents the oxidised/semiquinone couple of FLD and $E'_2$ the semiquinone/reduced couple.

Values for the reduction potentials of the FLDR and FLD flavins are collated in Table 6. Although the potentials for the two 1-electron couples of the FLD are very well separated (179 mV), this is clearly not so for the FLDR. For the FLDR, the first couple (oxidized/semiquinone − $E'_1$) is calculated to be more negative than the second (semiquinone/reduced − $E'_2$) by 0 mV. In FLDR, the two 1-electron-reduction processes appear to occur simultaneously and the data can be represented reasonably accurately by a 2-electron function. The midpoint reduction values in Table 6 are compared with those from the homologous domains of flavocytochrome *P*-450 BM3 and eukaryotic *P*-450 reductase, and with the potentials of free FAD and FMN.

Analysis of the later data sets for the FLDR was complicated by the tendency of this enzyme to form a precipitate (very slowly) over the course of the experiment. For this reason, the quality of these data is not as high as those obtained for FLD. However, correction of these data by subtraction of $1/\lambda$ from each spectrum (to compensate for the small increases in turbidity) results in values that fit well to the 2-electron Nernst function used to derive the flavin reduction potentials for FLDR.

Based on the wide separation of the midpoint reduction potentials of the oxidised/semiquinone and semiquinone/hydroquinone couples of the FLD; we calculate that a maximum of 94% blue semiquinone can be formed during the reductive titration of this protein. As shown in Fig. 5a, the strongly absorbing semiquinone has a peak at approximately 583 nm. The maximum absorbance reached by the semiquinone is 56.2% of that of the oxidised flavin band at 466 nm. Based on this proportion and the known coefficient of 8250 $M^{-1}$ $cm^{-1}$ for the 466-nm band [2], we calculate a coefficient of 4933 $M^{-1}$ $cm^{-1}$ for 100% of the semiquinone.

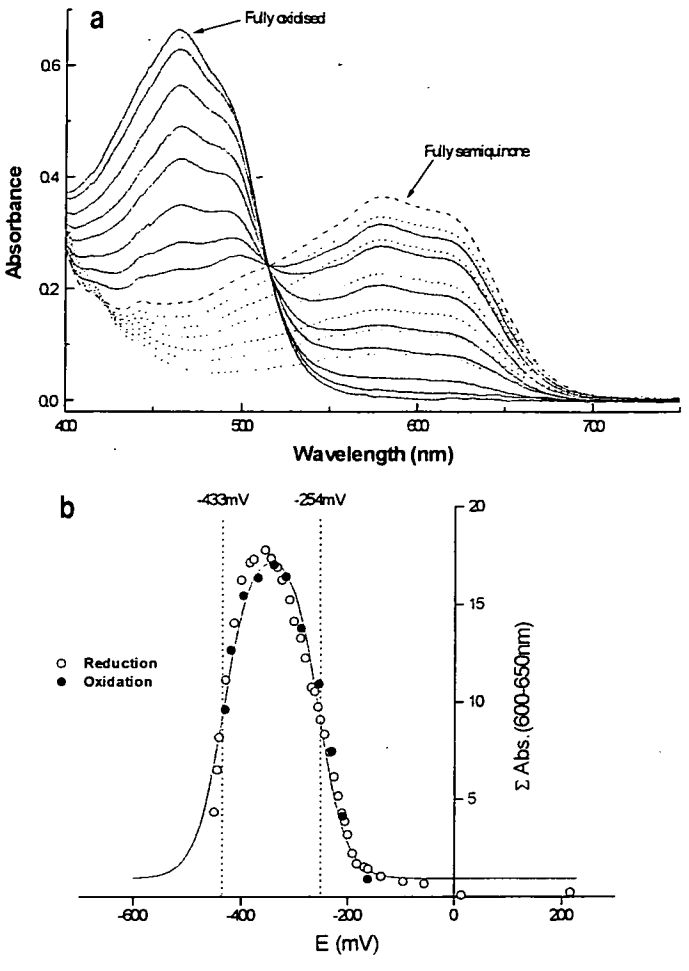


**Fig. 5. (a) Ultraviolet-visible spectra of *E. coli* FLD (80 μM) during redox titration.** Reductive (sodium dithionite) titrations were performed anaerobically as described in the Experimental Procedures section. The spectra shown by solid lines are those representing the conversion from the oxidised to the semiquinone form; with decreasing absorbance in the 450-nm region and increasing absorbance in the 600-nm region (semiquinone region). The dashed line shows the spectrum of the maximal semiquinone species (absorbance maximum at 583 nm). Spectra shown by dotted lines are those representing the conversion from the semiquinone to the hydroquinone (fully reduced) form; with decreasing absorbance in the 600-nm region. Oxidative titrations with potassium ferricyanide give essentially identical results to the reductive titrations. (b) Plot of the sum of absorbance between 600 nm and 650 nm against electrode potential (E′, mV) during reductive and oxidative titrations, fitted to Eqn. 1, as described in Results. From these data, $E'_1$ (oxidised/semiquinone) = −254 ± 5 mV and $E'_2$ (semiquinone/reduced) = −433 ± 6 mV.

## DISCUSSION

This is the first report of the determination of all of the reduction potentials for the flavins in the FLDR and FLD system, the flavoprotein electron-transfer chain of the *E. coli* biotin (vitamin H)-synthase system, which also supports the function of heterologously expressed cytochrome *P*-450 in *E. coli* [5]. The knowledge of these values is central to our understanding of the roles of these flavoproteins in electron transfer to these en-

zymes; and to the multiple other redox enzymes with which FLDR/FLD communicate, such as cobalamin-dependent methionine synthase and anaerobic ribonucleotide reductase.

The quantities of pure FLDR and FLD recovered are considerably higher than those reported previously [5, 16]. The high levels of expression achievable with the T7 polymerase/promoter system, coupled with efficient purification regimes (including a 2′,5′-ADP Sepharose affinity step for FLDR) facilitate good recovery. Protein purification data indicate that the FLDR and FLD proteins can be overexpressed to at least 10% of total cell protein without notable detrimental effects on cell growth. However, it was noted that transformants of the *fldr* gene in the faster growing BL21 (DE3) strain yielded protein with considerably lower specific activity than that from HMS174 (DE3). This is possibly due to failure of the cells to match FAD synthesis and/or incorporation to the production of FLDR apoenzyme with strong induction under the faster growth conditions.

It is worthy of note that *E. coli* FLDR is capable of reduction of cytochrome *c* in the absence of flavodoxin or alternative protein mediators (e.g. ferredoxin); this has not been reported previously. However, the rate is considerably elevated by the presence of *E. coli* FLD. In a recent publication, Jenkins and coworkers [19] reported the kinetics of cytochrome *c* reduction with the *Anabaena variabilis* flavodoxin $NADP^+$ reductase/flavodoxin system. In this system, there is negligible flavodoxin-independent cytochrome *c* reduction by the *Anabaena* FLDR. However, the cytochrome *c* turnover number of 1200 $min^{-1}$ for the *Anabaena* FLDR/FLD system is much higher than that of its *E. coli* homologue reported here. From stopped-flow studies, the first reduction of cytochrome *c* by reduced FLDR can occur at up to 29 $s^{-1}$ (1740 $min^{-1}$) compared with only 141.3 $min^{-1}$ during steady state. Clearly, the reduction of cytochrome *c* by FLDR is rate-limited by processes other than its binding and the transfer of an electron to the ferric haem.

The value determined from mass spectrometry of FLD is exactly that predicted from the amino acid sequence translated from the sequenced DNA [12]. However, the mass of the FLDR shows a discrepancy of 28 Da from that predicted by translation of the determined nucleotide sequence [16]. The recently determined atomic structure of FLDR [17] indicated the presence of an arginine as opposed to a glutamine residue at position 126. The difference in mass between these two residues is precisely 28 Da; thus, our data indicate that the discrepancy is in the DNA sequence and not the atomic structure, and that residue 126 is an arginine. It is worthy of note, also, that the masses determined for both FLD and FLDR indicate that insignificant proportions of the purified proteins retain their initiator methionine residue, and that there are no covalent modifications of either flavoprotein in the homologous host.

The potentiometric data demonstrate clearly that the *E. coli* flavodoxin stabilises a neutral-blue semiquinone form of FMN and that the FLD hydroquinone cannot be postulated as a realistic electron transferase to the biotin synthase enzyme or cytochrome *P*-450; since the midpoint reduction potential for the semiquinone/hydroquinone couple is some 100 mV more negative than that of the NADPH/$NADP^+$ couple (and 165 mV and 125 mV more negative than those of the FLDR oxidised/semiquinone and semiquinone/hydroquinone couples, respectively). The midpoint reduction-potential values for the FLD (−254 mV [oxidised/semiquinone] and −433 mV [semiquinone/reduced]) are similar to those obtained from non-recombinant *E. coli* FLD and flavodoxins from other species [20]. Repeats of the FLDR titration in the presence of a saturating concentration of 2′ AMP indicated that the midpoint potentials of both the oxidised/semiquinone and semiquinone/reduced couples are elevated by binding this nucleotide analogue and that $E'_{12}$ is increased by 27 mV from −288 ± 4 mV to −261 ± 6 mV. The effect of bound nu otide analogue is similar to that observed previously for the mologous FAD-containing enzymes adrenodoxin reductase and cytochrome $b_5$ reductase [22] and indicates that the bin of $NADP^+$ to FLDR may exert an important controlling in ence on the catalytic properties of the enzyme. The elevation both of the reduction potentials of FLDR places them e closer to that of the oxidised/semiquinone couple of FLD decreases further the driving force for electron transfer to FLD. This may at least partially explain the very slow rates electron transfer measured between FLDR and FLD us stopped-flow spectrophotometry.

The potentiometric data have important implications relat to the mechanism of the reduction of cytochromes *P*-450 (a other enzyme systems). They indicate that (unless there is a v large increase in the FLD semiquinone/hydroquinone cou caused by binding of FLD to *P*-450), the two electrons requir for *P*-450 catalysis must be delivered through two consecuti single electron transfers from FLD semiquinone; as opposed the first FMN-haem electron transfer being mediated by FM hydroquinone and the second by FMN semiquinone. This rais the question as to whether these transfers occur in a ternary co plex of FLDR/FLD/*P*-450 or through a ping-pong mechani in which the FLD may interact firstly with the FLDR and s ondly with the *P*-450. The fact that the flavins in both prote are relatively exposed suggests that electron transfer betwe them is likely to be through close approach of the isoalloxazi rings, as opposed to involving a protein pathway [16, 23]. T atomic structure of a eukaryotic *P*-450 reductase also indica that the edges of the FAD and FMN ring systems in this prot are only 0.4 nm apart and that inter-flavin electron transfer m occur without mediation by any amino acid side chains [2- Thus, it appeared most likely that reduced FLDR and FL would dock, an electron would be transferred to form the FL semiquinone and the FLD would then dissociate from the FLD and associate with a *P*-450 to reduce this enzyme, again via exposed FMN. The ping-pong kinetic properties of the FLD FLD/*P*-450 BM3 haem-domain system (Fig. 3) are consiste with this model, suggesting that the FLD acts as a shuttle b tween FLDR and the *P*-450, as opposed to the three protei forming a ternary complex for electron transfer.

The data presented here clearly define the electron-transf route through this system as NADPH→FLDR (FAD)→FL (FMN) and then onto other enzyme partners. This is a simil flavin electron-transfer path as that described previously for t *E. coli* sulfite reductase and for the diflavin reductases of cyt chromes *P*-450 (*P*-450 reductase or CPR) and nitric oxide sy thase [25]. In fact, the FLDR and FLD proteins show structur homology to the FAD and FMN domains of CPR [26], and the domains have been expressed independently for both a eukar otic *P*-450 reductase and the reductase of flavocytochrom *P*-450 BM3 − a natural CPR/*P*-450 fatty-acid hydroxylase f sion protein [27, 28]. However, it is of particular interest to no here that the FAD and FMN domains of *P*-450 BM3 show ve different redox characteristics to FLDR and FLD, with the bl semiquinone being found on the FAD domain of *P*-450 BM [29] (Table 6). In *P*-450 BM3, the FAD hydroquinone thermodynamically unfavourable, while it is the FMN of FL in the *E. coli* system. In all three systems, the high and lo potential flavins are the FMN and FAD, respectively. Howeve both the $E'_{12}$ and $E'_2$ values for FLDR are considerably less neg tive than those for the related reductases. Also, the oxidise semiquinone and semiquinone/reduced couples for FLD are bo more negative than those for the *P*-450 BM3 [29] and CPR [3 systems. Indeed, the semiquinone/reduced couple of FLD has very negative potential (−433 mV) which makes electr

nsfer via a NADPH-driven system virtually impossible. The sults indicate that the overall driving force, i.e. the difference reduction potential, for single electron transfer from NADPH-duced FLDR to oxidised FLD is considerably less than that r CPR and *P*-450 BM3. In addition, the binding of nucleotide $ADP^+$) to FLDR may result in further increase in the flavin duction potentials (as we have shown with 2′ AMP) and crease further the driving force for electron transfer to FLD. ur stopped-flow data are consistent with these findings. The te of reduction of FLDR (15 $s^{-1}$) is markedly slower than that en in the *P*-450 BM3 system (> 700 $s^{-1}$) and the reduction of LD by reduced FLDR is also very slow (0.034 $s^{-1}$).

The authors acknowledge support from the University of Edinburgh M), the Edinburgh Centre for Protein Technology (CL) and the Bio-hnology and Biological Sciences Research Council (DJC and SND). VM and SKC wish to thank the Royal Society of Edinburgh and Cale-nian Research Foundation (Caledonian Research Foundation/Royal ciety of Edinburgh Fellowship to AWM and SOEID Fellowship to C).

## EFERENCES


Sanyal, I., Cohen, G. & Flint, D. H. (1994) Biotin synthase – purification, characterization as a [2Fe-2S] cluster protein, and *in vitro* activity of the *Escherichia coli* BioB gene product, *Biochemistry 33*, 3625–3631.

Fujii, K. & Huennekens, F. M. (1974) Activation of methionine synthase by a reduced triphosphopyridine nucleotide-dependent flavoprotein system, *J. Biol. Chem. 249*, 6745–6750.

Blaschkowski, H. P., Neuer, G., Ludwig-Festl, M. & Knappe, J. (1982) Routes of flavodoxin and ferredoxin reduction in *Escherichia coli* coA acylating pyruvate – flavodoxin and NADPH-flavodoxin oxidoreductases participating in the activation of the pyruvate-formate lyase, *Eur. J. Biochem. 123*, 563–569.

Reichard, P. (1993) The anaerobic ribonucleotide reductase from *Escherichia coli*, *J. Biol. Chem. 268*, 8383–8386.

Jenkins, C. M. & Waterman, M. R. (1994) Flavodoxin and NADPH-flavodoxin reductase from *Escherichia coli* support bovine cytochrome P450 c17 hydroxylase activities, *J. Biol. Chem. 269*, 27401–27408.

Mayhew, S. G. & Tollin, G. (1993) General properties of flavodoxins, in *Chemistry and biochemistry of flavoenzymes* (Müller, F., ed.) pp. 389–426, CRC Press, Boca Raton, Florida.

Fujii, K., Galivan, J. H. & Huennekens, F. M. (1977) Activation of methionine synthase: further characterization of the flavoprotein system, *Arch. Biochem. Biophys. 178*, 662–666.

Vetter, H. & Knappe, J. (1971) Flavodoxin and ferredoxin of *Escherichia coli*, *Hoppe-Seylers Physiol. Chem. 352*, 433–436.

Studier, F. W. & Moffat, B. A. (1986) Use of bacteriophage T7 RNA polymerase to direct selective high-level expression of cloned genes, *J. Mol. Biol. 189*, 113–130.

Yanisch-Perron, C., Viera, J. & Messing, J. (1985) Improved M13 phage cloning vectors and host strains: nucleotide sequences of the M13mp18 and pUC19 vectors, *Gene 33*, 103–108.

Bianchi, V., Reichard, P., Eliasson, R., Pontis, E., Krook, M., Jornvall, H. & Haggård-Ljungquist, E. (1993) *Escherichia coli* ferredoxin-$NADP^+$ reductase: activation of *Escherichia coli* anaerobic ribonucleotide reduction, cloning of the gene (*FPR*) and overexpression of the protein, *J. Bacteriol. 175*, 1590–1595.

Bianchi, V., Eliasson, R., Fontecave, M., Mulliez, E., Hoover, D. M., Matthews, R. & Reichard, P. (1993) Flavodoxin is required for the activation of the anaerobic ribonucleotide reductase, *Biochem. Biophys. Res. Commun. 197*, 792–797.

Dutton, P. L. (1978) Redox potentiometry: determination of midpoint potentials of oxidation-reduction components of biological electron transfer systems, *Methods Enzymol. 54*, 411–435.

Munro, A. W., Malarkey, K., McKnight, J., Thomson, A. J., Kelly, S. M., Price, N. C., Lindsay, J. G., Coggins, J. R. & Miles, J. S. (1994) The role of tryptophan 97 of cytochrome P-450 BM3 from *Bacillus megaterium* in catalytic function, *Biochem. J. 303*, 423–428.

Pirola, M. C., Monti, F., Alverti, A. & Zanetti, G. (1994) A functional heterologous electron-transfer protein complex, *Desulfovibrio vulgaris* flavodoxin covalently linked to spinach ferredoxin-$NADP^+$ reductase, *Arch. Biochem. Biophys. 311*, 480–486.

Bianchi, V., Haggård-Ljungquist, E., Pontis, E. & Reichard, P. (1995) Interruption of the ferredoxin (flavodoxin) $NADP^+$ oxidoreductase gene of *Escherichia coli* does not affect anaerobic growth but increases sensitivity to paraquat, *J. Bacteriol. 177*, 4528–4531.

Ingelman, M., Bianchi, V. & Eklund, H. (1997) The 3-dimensional structure of flavodoxin reductase at 1.7 Angstrom resolution, *J. Mol. Biol. 268*, 147–157.

Miles, J. S., Munro, A. W., Rospendowski, B. N., Smith, W. E., McKnight, J. & Thomson, A. J. (1992) Domains of the catalytically self-sufficient cytochrome P-450 BM3: genetic construction, overexpression, purification and spectroscopic characterization, *Biochem. J. 288*, 503–509.

Jenkins, C. M., Genzor, C. G., Fillat, M. F., Waterman, M. R. & Gomez Moreno, C. (1997) Negatively charged *Anabaena* flavodoxin residues [Asp (144) and Glu (145)] are important for reconstitution of cytochrome P450c17 alpha-hydroxylase, *J. Biol. Chem. 272*, 22509–22513.

Sykes, G. A. & Rogers, L. J. (1984) Redox potentials of algal and cyanobacterial flavodoxins, *Biochem. J. 217*, 845–850.

Lambeth, J. D. & Kamin, H. (1976) Adrenodoxin reductase: properties of the complexes of reduced enzyme with $NADP^+$ and NADPH, *J. Biol. Chem. 251*, 4299–4306.

Iyanagi, T. (1977) Redox properties of microsomal reduced nicotinamide adenine dinucleotide-cytochrome $b_5$ reductase and cytochrome $b_5$, *Biochemistry 16*, 2725–2730.

Hoover, D. M. & Ludwig, M. L. (1997) A flavodoxin that is required for enzyme activation: the structure of oxidized flavodoxin from *E. coli* at 1.8 Å resolution, *Protein Sci. 6*, 2525–2537.

Wang, M., Roberts, D. L., Paschke, R., Shea, T. M., Masters, B. S. S. & Kim, J.-J. P. (1997) Three dimensional structure of NADPH-cytochrome P-450 reductase: prototype for FMN- and FAD-containing enzymes, *Proc. Natl Acad. Sci. USA 94*, 8411–8416.

Abu-Soud, H. M., Feldman, P. L., Clark, P. & Stuehr, D. J. (1994) Electron transfer in the nitric oxide synthases: characterization of L-arginine analogs that block heme iron reduction, *J. Biol. Chem. 269*, 32318–32326.

Porter, T. D. (1991) An unusual, yet strongly conserved flavoprotein reductase in bacteria and mammals, *Trends Biochem. Sci. 16*, 154–158.

Smith, G. C. M., Tew, D. G. & Wolf, C. R. (1994) Dissection of NADPH-cytochrome P450 oxidoreductase into distinct functional domains, *Proc. Natl Acad. Sci. USA 91*, 8710–8714.

Govindaraj, S. & Poulos, T. L. (1997) The domain architecture of cytochrome P450 BM3, *J. Biol. Chem. 272*, 7915–7921.

Daff, S. N., Chapman, S. K., Turner, K. L., Holt, R. A., Govindaraj, S., Poulos, T. L. & Munro, A. W. (1997) Redox control of the catalytic cycle of cytochrome P-450 BM3, *Biochemistry 36*, 13816–13823.

Iyanagi, T., Makino, N. & Mason, H. S. (1974) Redox properties of the reduced nicotinamide adenine dinucleotide phosphate-cytochrome P450 and reduced nicotinamide adenine dinucleotide-cytochrome $b_5$ reductase, *Biochemistry 13*, 1701–1710.

Massey, V. (1991) A simple method for the determination of redox potentials, in *Flavins and flavoproteins 1990* (Curti, B., Ronchi, S. & Zanetti, G., eds) pp. 59–66, Walter de Gruyter, New York.

Draper, R. D. & Ingraham, L. L. (1968) A potentiometric study of the flavin semiquinone equilibrium, *Arch. Biochem. Biophys. 125*, 802–808.